

THE APPLICATION OF GEOCHEMICAL METHODS
TO GEOTHERMAL EXPLORATION

by

J. N. Moore
M. C. Adams
D. Foley

Earth Science Laboratory
University of Utah Research Institute
391 Chipeta Way, Suite C
Salt Lake City, Utah 84108

Prepared for

LAW ENGINEERING IBERICA, S.A.
Corazon de Maria, 2
28002-Madrid

January, 1985

CONTENTS

EXECUTIVE SUMMARY

- I. GEOLOGIC OCCURRENCE OF GEOTHERMAL RESOURCES
 - Characteristics of Geothermal Processes
 - Overview of Geothermal Resource Types
 - References
- II. THE ROLE OF GEOCHEMISTRY IN GEOTHERMAL EXPLORATION AND DEVELOPMENT
 - Principal Literature Sources
 - References
- III. CHARACTERISTICS OF THE GEOTHERMAL RESOURCES OF SPAIN
 - Geothermal Characteristics of Basins
 - Fluid Characteristics
 - Hydrologic Characteristics
 - Thermal Regimes
 - Conclusions
 - References
- IV. CHEMICAL CHARACTERISTICS OF GEOTHERMAL FLUIDS
 - Classification
 - Compositions
 - Processes Affecting Fluid Chemistry
 - Mixing of Fluid Types
 - Boiling
 - Relationships to Rock Type, Temperature and Origin of the Thermal Fluids
 - References
- V. GEOCHEMICAL METHODS APPLIED TO FLUID CHEMISTRY
 - Overview of Geothermometry
 - Quantitative Fluid Geothermometers
 - Cation Geothermometers
 - Geothermometry of Mixed and Boiled Waters
 - Qualitative Geothermometers
 - Geothermometers Based on Mineral Saturations
 - Interpretation of Geothermometer Temperatures
 - Applications Limitations
 - References
- VI. CHEMISTRY OF GEOTHERMAL GASES AND STABLE ISOTOPES
 - Compositions of Geothermal Gases
 - Application of Gas Data to Exploration and Geothermometry
 - Stable Isotopes in Geothermal Systems
 - Application of Stable Isotopes to Exploration and Geothermometry
 - References
- VII. SUMMARY OF BOILING AND MIXING

- VIII. ANALYTICAL METHODS
 - Aqueous Species
 - Gases
 - Isotopes
 - Determination of Analytical Quality
 - References
- IX. OTHER GEOCHEMICAL OBSERVATIONS
 - Alteration Minerals
 - Trace Element Distributions
 - Soil Geochemistry
 - Summary of Geochemical Observations
 - Applications Limitations and Cost Effectiveness
 - References
- X. METHODS OF DATA PRESENTATION
 - Introduction
 - Ion Concentration Diagrams
 - Statistical Interpretation of Geochemical Data
 - References
- XI. REVIEW OF SPANISH GEOCHEMICAL SURVEYS
 - Gran Canaria Island
 - El Pirineo (Lerida)
 - Cordilleras Costero-Catalanas, Barcelona
 - Galicia
 - La Cuenca Central y Extremadura
 - Ciudad Real
 - References
- XII. EXPLORATION STRATEGY FOR SPANISH RESOURCES
 - Introduction
 - Role of the Earth Sciences in Geothermal Exploration
 - Geology
 - Geophysics
 - Hydrology
 - Geothermal Exploration - General Considerations
 - Exploration Strategy
 - The Conceptual Geologic Model
 - Recommended Exploration Strategy - Sedimentary Basins in Spain
 - Recommended Exploration Strategy - Igneous/Fault Resources in Spain
 - Recommended Exploration Strategy - Volcanic Areas in Spain
- XIII. ADDITIONAL READING
- XIV. APPENDIX 5A - Application of Water Geochemistry to Geothermal Exploration and Reservoir Engineering
- XV. APPENDIX 10A - Introduction to SPSS Statistical Program
- XVI. APPENDIX 10B - Introduction to BMDP Statistical Program

EXECUTIVE SUMMARY

Geothermal systems are found in many different geologic environments. Geothermal resources in basins are the result of the complex interaction of thermal, chemical, and hydrodynamic regimes. Thermal input is from the normal heat flux of the earth, but local changes in sedimentary units can affect temperatures and thermal gradients. Fluids in basins may be young meteoric waters, older connate waters, which may be brines, or mixtures of these. Positive thermal anomalies are often found in areas with complex geologic structures, such as anticlines or faults, which provide permeability for rising waters. Long regional flowpaths are favorable for the development of geothermal systems. Hydrodynamic relationships in immature basins are complicated by the development of overpressured zones (which may also be thermal anomalies), and the dewatering of sediments during compaction.

Geothermal fluids found in igneous and volcanic terranes may be heated during deep circulation of meteoric water or by young intrusive rocks. Hydrologic relationships in volcanic terranes are complex and several reservoirs with different fluid compositions may be present.

Geothermal fluids vary widely in composition and temperature, and are chemically distinct from cold or warm groundwaters. Their specific chemical composition depends on many factors, including temperature, rock type, origin and residence time in the reservoir. Boiling, mixing, cooling, and heating can lead to mineral deposition and may further modify the chemistry of the deep reservoir waters before they are sampled at the surface.

Qualitative fluid geothermometers are used extensively during the preliminary chemical surveys to locate zones of upwelling, determine the distribution of thermal waters and directions of groundwater flow, and to determine the lithologies of the reservoir rocks. Fluid constituents that

have proven to be particularly useful during these surveys include the soluble elements chlorine, boron, arsenic, cesium and bromine. Changes in the concentrations of these elements as the fluids migrate from depth occur mainly from dilution or boiling. The use of atomic ratios (i.e., chloride/boron) can eliminate these effects.

Chemical geothermometers are used to predict the reservoir temperature of geothermal resources. The most widely used and successful geothermometers are based on the Na-K-Ca-Mg and silica contents of geothermal waters. Chemical geothermometers have been specifically calibrated for use on basinal and oil field brines. In addition, physical processes that define the geometry of the resource, such as boiling, mixing, cooling, and heating can be elucidated by the silica- and chloride-enthalpy relationships.

Various geothermometers have been applied to chemical data reported by IGME for the Spanish geothermal resources. In general there is a high degree of concordancy among the geothermometers of the hot spring systems sampled. The results of these calculations illustrate the applicability of existing geochemical methods to the interpretation of these chemical data.

Estimates of the reservoir temperatures can also be made indirectly from the occurrence of some of the common secondary minerals found in geothermally altered rocks. Many of these minerals are stable only over relatively narrow temperature ranges. They include the clay minerals (below about 225°C) and illite, chlorite and epidote (above 225°C). Mineral geothermometers may assume particular importance during the early stages of a drilling program when exploratory wells frequently fail to produce fluids. Supplementary trace element and mercury surveys of drill chips and soils can provide complementary data on the distribution of fluid types, temperature and permeability.

Exploration strategies for geothermal resources in basin, igneous and

volcanic terrains require integrated geochemical, geological, geophysical and hydrological efforts. Basic exploration strategies for these environments are described.

1.0 GEOLOGIC OCCURRENCE OF GEOTHERMAL RESOURCES

Geothermal energy is heat energy that originates within the earth. Under suitable circumstances a small portion of this energy can be extracted and used by man. So active is the earth as a thermal engine that many of the large-scale geological processes that have helped to form the earth's surface features are powered by redistribution of internal heat as it flows from inner regions of higher temperature to outer regions of lower temperature. Such seemingly diverse phenomena as motion of the earth's crustal plates, uplifting of mountain ranges, occurrence of earthquakes, eruption of volcanoes and spouting of geysers all owe their origin to the transport of internal thermal energy.

In the United States and in many other countries, geothermal energy is used both for generation of electrical power and for direct applications such as space heating and industrial process energy. Although the technical viability of geothermal energy for such uses has been known for many years, the total amount of application today is very small compared with the potential for application. Availability of inexpensive energy from fossil fuels has suppressed use of geothermal resources. At present geothermal application is economic only at a few of the highest-grade resources. Development of new techniques and equipment to decrease costs of exploration, drilling, reservoir evaluation and extraction of the energy is needed to make the vastly more numerous lower grade resources also economic.

The objective of this chapter is to present an overview of the exploration for and exploitation of geothermal resources. The geological principles discussed have world-wide application. Geothermal resources of high temperature are found mainly in areas where a number of specific geologic processes are active today and resources of lower temperature are more widespread. A

classification for observed resource types is presented and the geology of each type briefly described.

1.1 OVERVIEW OF GEOLOGIC PROCESSES

Although the distributions with depth in the earth of density, pressure and other related physical parameters are well known, the temperature distribution is extremely uncertain. We do know that temperature within the earth increases with increasing depth (Fig. 1.1.1), at least for the first few tens of kilometers, and we hypothesize a steadily increasing temperature to the earth's center. Plastic or partially molten rock at estimated temperatures between 700°C and 1200°C is postulated to exist everywhere beneath the earth's surface at depths of 100 km, and the temperature at the earth's center, nearly 6400 km deep, may be more than 4000°C.

Because the earth is hot inside, heat flows steadily outward over the entire surface, where it is permanently lost by radiation into space. The mean value of this surface heat flow for the world is about 60×10^{-3} watts/m² (White and Williams, 1975) and since the mean surface area of the earth is about 5.1×10^{14} m², the rate of heat loss is about 32×10^{12} watts (32 million megawatts) or about 2.4×10^{20} calories/year, a very large amount indeed. At present, only a small portion of this heat, namely that concentrated in what we call geothermal resources, can be captured for man's benefit. The mean surface heat flux of 60 milliwatts/m² is about 20,000 times smaller than the heat arriving from the sun when it is directly overhead, and the earth's surface temperature is thus controlled by the sun and not by heat from the interior (Goguel, 1976).

Two ultimate sources for the earth's internal heat appear to be most important among a number of contributing alternatives: 1) heat released throughout the earth's 4.5 billion-year history by radioactive decay of

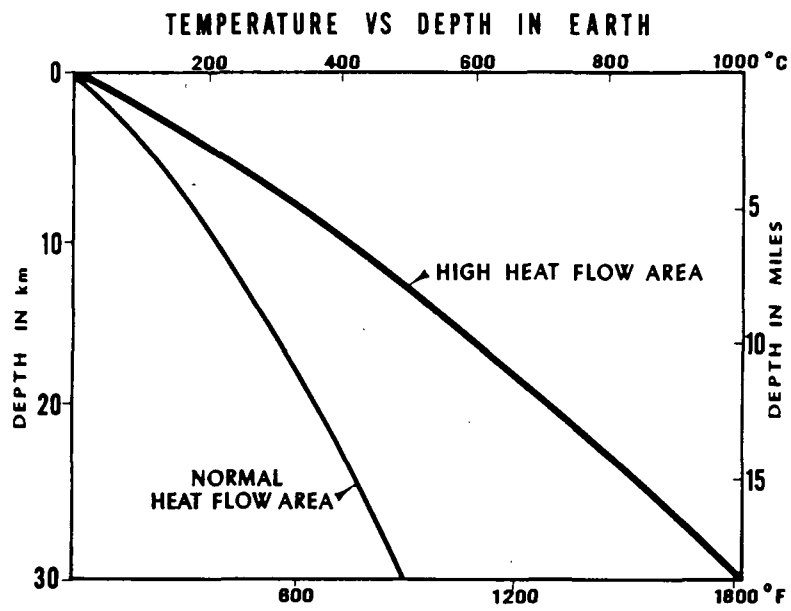


Figure 1.1.1

certain isotopes of uranium, thorium, potassium, and other elements; and 2) heat released during formation of the earth by gravitational accretion and during subsequent mass redistribution when much of the heavier material sank to form the earth's core (Fig. 1.1.2). The relative contribution to the observed surface heat flow of these two mechanisms is not yet resolved. Some theoretical models of the earth indicate that heat produced by radioactive decay can account for nearly all of the present heat flux (MacDonald, 1965). Other studies (Davis, 1980) indicate that, if the earth's core formed by sinking of the heavier metallic elements in an originally homogeneous earth, the gravitational heat released would have been sufficient to raise the temperature of the whole earth by about 2000°C. An appreciable fraction of today's observed heat flow could be accounted for by such a source. However, the distribution of radioactive elements within the earth is poorly known, as is the earth's early formational history some 4 billion years ago. We do know that the thermal conductivity of crustal rocks is low so that heat escapes from the surface slowly. The deep regions of the earth retain a substantial portion of their original heat, whatever its source, and billions of years will pass before the earth cools sufficiently to quiet the active geological processes we will discuss below. This fact helps lend order to exploration for geothermal resources once the geological processes are understood. At present our understanding of these processes is rather sketchy, but, with rapidly increasing need for use of geothermal resources as an alternative to fossil fuels, our learning rate is high.

Figure 1.1.3 shows the principal areas of known geothermal occurrences on a world map. Also indicated are areas of young volcanoes and a number of currently active fundamental geological structures. It is readily seen that many geothermal resource areas correspond with areas that now have or recently

INTERIOR OF THE EARTH

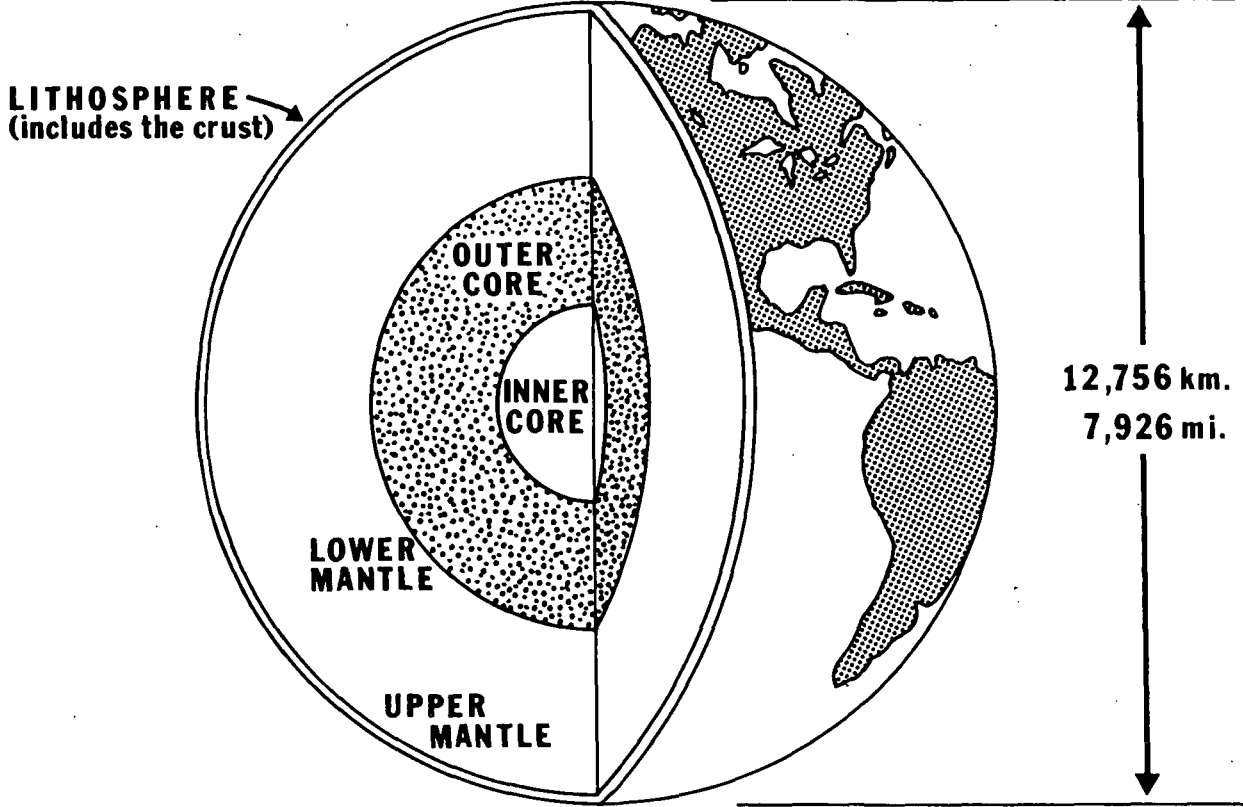
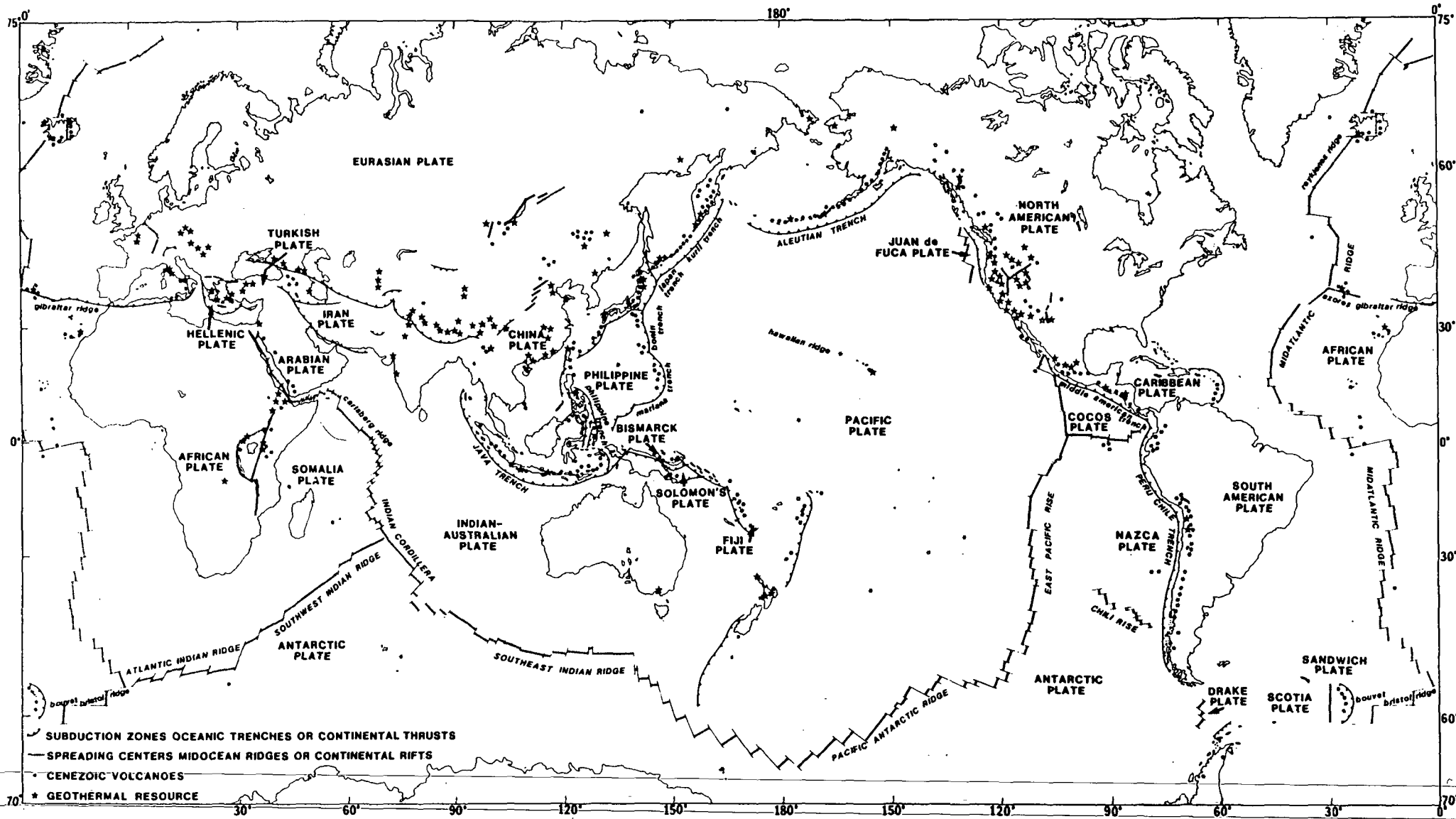


Figure 1.1.2



GEOHERMAL RESOURCES AND PLATE TECTONIC FEATURES

Figure 1.1.3

have had volcanic and other geological activity. To understand why this is true we must consider some of the geologic processes going on in the earth's interior.

A schematic cross section of the earth is shown in Figure 1.1.2. A solid layer called the lithosphere extends from the surface to a depth of about 100 km. The lithosphere is composed of an uppermost layer called the crust and of the uppermost regions of the mantle, which lie below the crust. Mantle material below the lithosphere is less solid than the overlying lithosphere and is able to flow very slowly under sustained stress. The crust and the mantle are composed of minerals whose chief building block is silica (SiO_2). The outer core is a region where material is much denser than mantle material, and it is believed to be composed of a liquid iron-nickel-copper mixture. The inner core is believed to be a solid metallic mixture.

One very important group of geological processes that cause geothermal resources is known collectively as "plate tectonics" (Wyllie, 1971). It is illustrated in Figure 1.1.4. Outward flow of heat from the deep interior is hypothesized to cause formation of convection cells in the earth's mantle in which deeper, hotter mantle material slowly rises toward the surface, spreads out parallel to the surface under the solid lithosphere as it cools and, upon cooling, descends again. The lithosphere above the upwelling portions of these convection cells cracks and spreads apart along linear or arcuate zones called "spreading centers" that are typically thousands of kilometers long and coincide, for the most part, with the world's mid-oceanic ridge or mountain system (Figs. 1.1.3 and 1.1.4). The crustal plates on each side of the crack or rift move apart at rates of a few centimeters per year, and molten mantle material rises in the crack and solidifies to form new crust. The laterally moving oceanic lithospheric plates impinge against adjacent plates, some of

CONCEPT OF PLATE TECTONICS

(NOT TO SCALE)

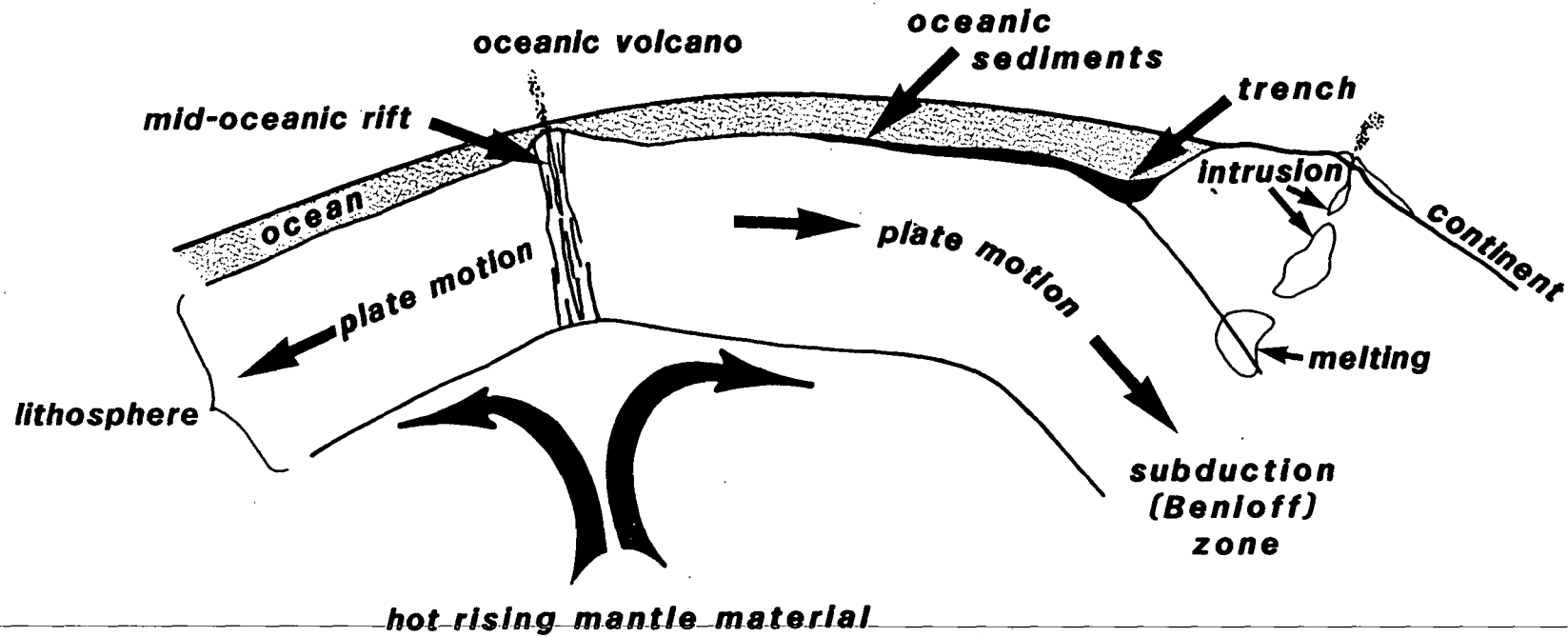


Figure 1.1.4

which contain the imbedded continental land masses, and in most locations the oceanic plates are thrust beneath the continental plates. These zones of under-thrusting, called subduction zones, are marked by the world's deep oceanic trenches which result from the crust being dragged down by the descending oceanic plate. The oceanic plate descends into regions of warmer material in the mantle and is warmed both by the surrounding warmer material and by frictional heating as it is thrust downward. At the upper boundary of the descending plate, temperatures become high enough in places to cause partial melting. The degree of melting depends upon the amount of water contained in the rocks as well as upon temperature and pressure and the upper layers of the descending plate often contain oceanic sediments rich in water. The molten or partially molten rock bodies (magmas) that result then ascend buoyantly through the crust, probably along lines of structural weakness (Fig. 1.1.5) and carry their contained heat to within 1.5 to 15 km of the surface. They give rise to volcanoes if part of the molten material escapes to the surface through faults and fractures in the upper crust.

Figure 1.1.3 shows where these processes of crustal spreading, formation of new oceanic crust from molten mantle material and subduction of oceanic plates beneath adjacent plates, are currently operating. Oceanic rises, where new crustal material is formed, occur in all of the major oceans. The East Pacific Rise, the Mid-Atlantic Ridge and the Indian ridges are examples. The ridge or rise crest is offset in places by large transform faults that result from variations in the rate of crustal spreading from place to place along the ridge. Oceanic crustal material is subducted or consumed in the trench areas. Almost all of the world's earthquakes result from these large-scale processes, and occur either at the spreading centers, the transform faults or in association with the subduction zone (Benioff zone), which dips underneath

CRUSTAL INTRUSION

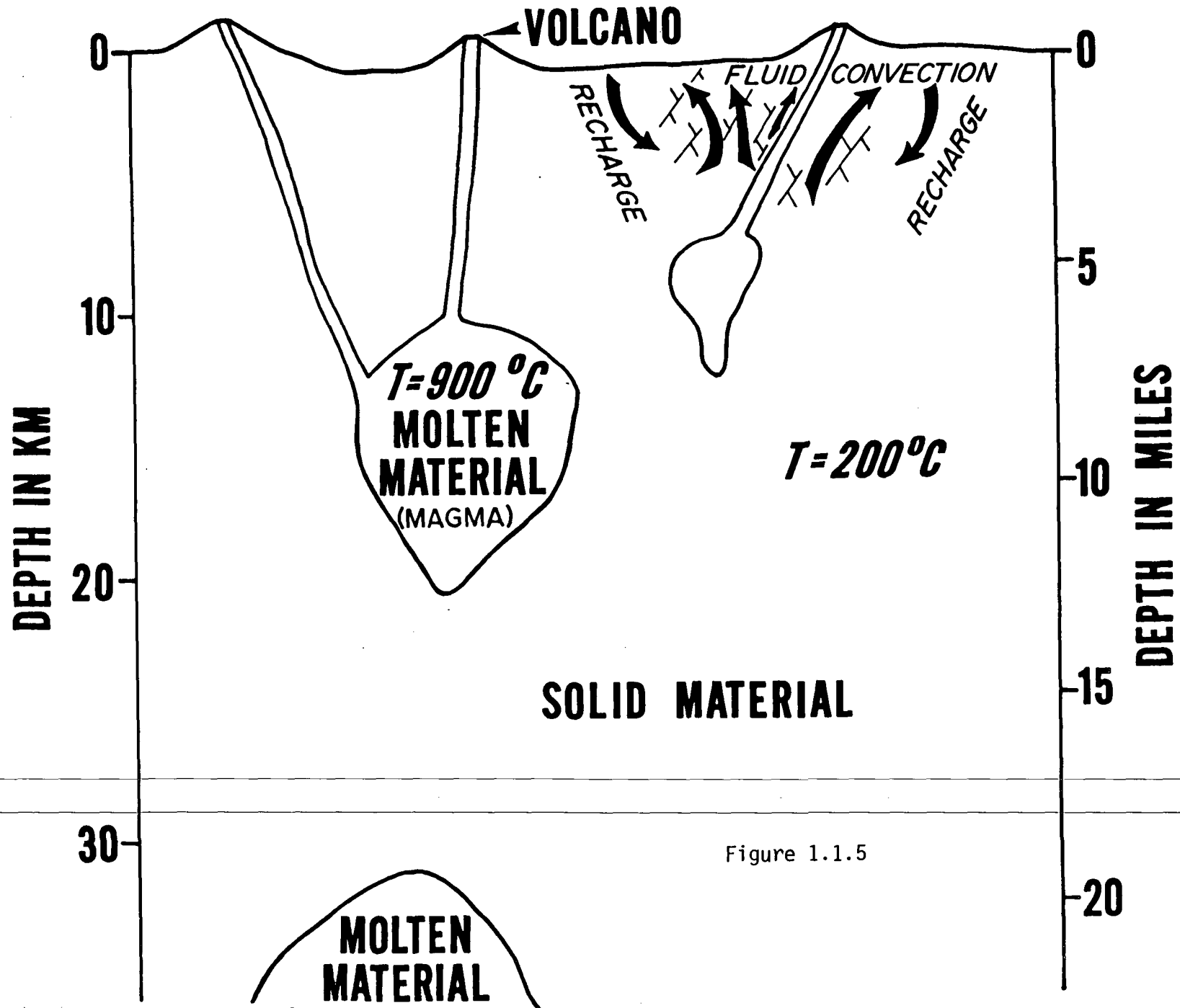


Figure 1.1.5

the continental land masses in many places. We thus see that these very active processes of plate tectonics give rise to diverse phenomena, among which is the generation of molten rock at shallow depths in the crust both at the spreading centers and above zones of subduction. These bodies of shallow molten rock provide the heat for many of the world's geothermal resources.

Before going on, let us discuss a bit more the processes of development of a crustal intrusion, illustrated in Figure 1.1.5. An ascending body of molten material may cease to rise at any level in the earth's crust and may or may not vent to the surface in volcanoes. Intrusion of molten magmas into the upper parts of the earth's crust has gone on throughout geological time. We see evidence for this in the occurrence of volcanic rocks of all ages and in the small to very large areas of crystalline, granitic rock that result when such a magma cools slowly at depth.

Volcanic rocks that have been extruded at the surface and crystalline rocks that have cooled at depth are known collectively as igneous rocks. They vary over a range of chemical and mineral composition. At one end of the range are rocks that are relatively poor in silica (SiO_2 about 50%) and relatively rich in iron ($\text{Fe}_2\text{O}_3 + \text{FeO}$ about 8%) and magnesium (MgO about 7%). The volcanic variety of this rock is basalt and an example is the black rocks of the Hawaiian Islands. The crystalline, plutonic variety of this rock that has consolidated at depth is known as gabbro. At the other end of the range are rocks that are relatively rich in silica (SiO_2 about 64%) and poor in iron ($\text{Fe}_2\text{O}_3 + \text{FeO}$ about 5%) and magnesium (MgO about 2%). The volcanic variety of this rock, rhyolite, is usually lighter in color than the black basalt and it occurs mainly on land. The plutonic variety of this rock is granite, although the term "granitic" is sometimes used for any crystalline igneous rock. Magmas that result in basalt or gabbro are termed "basic" whereas magmas that

result in rhyolite or granite are termed "acidic"; however these terms are misleading because they have nothing to do with the pH of the magma.

The upper portions of the mantle are believed to be basaltic in composition. The great outpourings of basalt seen in places like the Hawaiian Islands and on the volcanic plateaus of the Columbia and Snake rivers in the northwestern United States seem to indicate a more or less direct pipeline from the upper mantle to the surface in places. The origin of granites is a subject of some controversy. It can be shown that granitic magmas could be derived by differential segregation from basaltic magmas. However, the chemical composition of granites is much like the average composition of the continental crust, and some granites probably result from melting of crustal rocks by upwelling basaltic magmas whereas others probably result from differentiation from a basaltic magma. In any case, basaltic magmas are molten at a higher temperature than are granitic magmas (see Fig. 1.1.6) and more importantly for our discussion basaltic magmas are less viscous (more fluid) than are granitic magmas. Occurrence of rhyolitic volcanic rocks of very young age (less than 1 million years and preferably less than 50,000 years) is generally taken as a sign of good geothermal potential in an area because presumably a large body of viscous magma may be indicated at depth to provide a geothermal heat source. On the other hand, occurrence of young basaltic magma is not as encouraging because the basalt, being fairly fluid, could simply ascend along narrow conduits from the mantle directly to the surface without need for a shallow magma chamber that would provide a geothermal heat source. In many areas both basaltic and rhyolitic volcanic rocks are present and often the younger eruptions are more rhyolitic, possibly indicating progressive differentiation of an underlying basaltic magma in a chamber like those illustrated in Figure 1.1.5.

GEO THERMAL TEMPERATURES

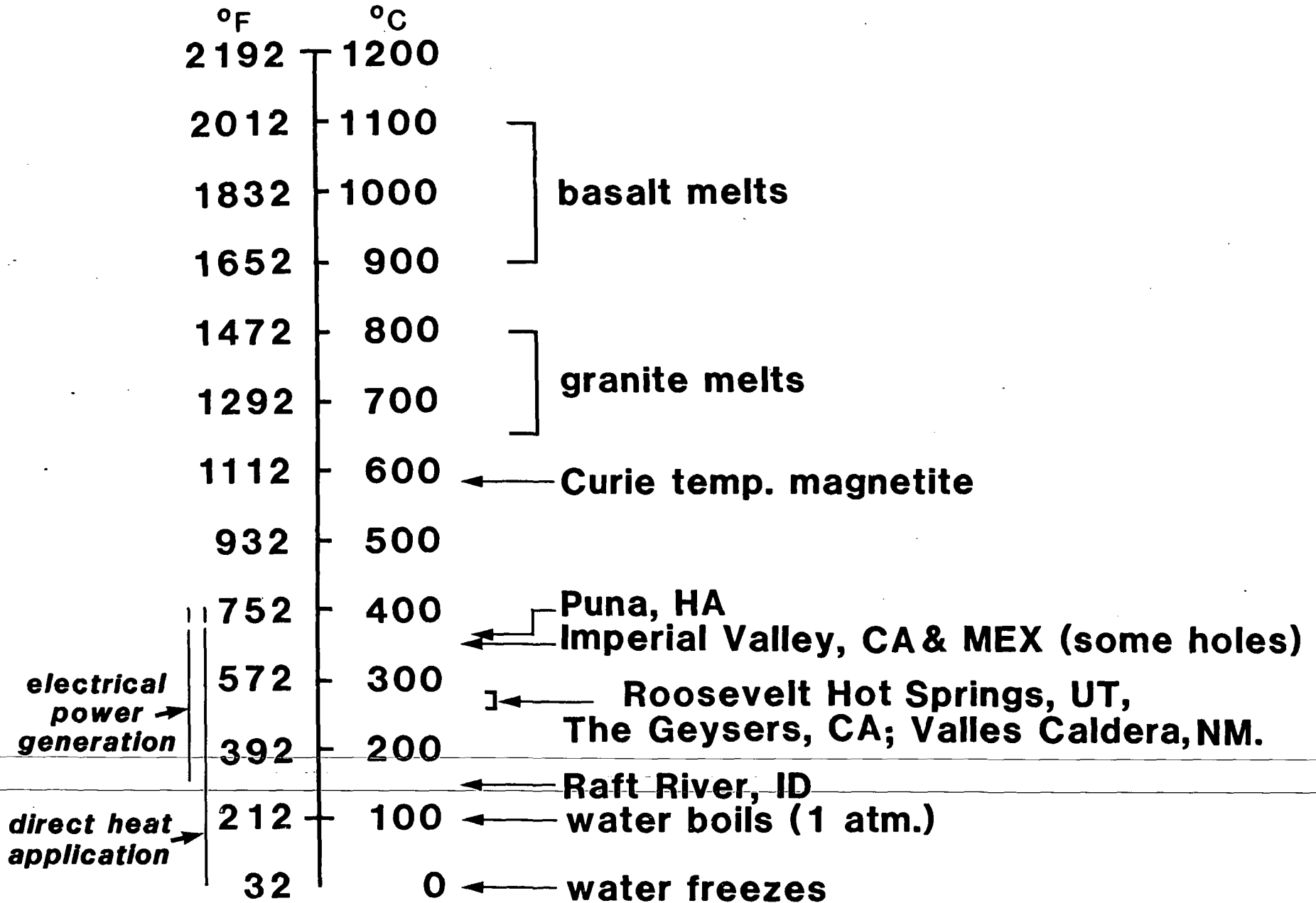


Figure 1.1.6

A second important source of volcanic rocks results from hypothesized point sources of heat in the mantle as contrasted with the rather large convection cells discussed above. It has been hypothesized that the upper mantle contains local areas of upwelling, hot material called plumes, although other origins for the hot spots have also been postulated. As crustal plates move over these local hot spots, a linear or arcuate sequence of volcanoes is developed. Young volcanic rocks occur at one end of the volcanic chain with older ones at the other end. The Hawaiian Island chain is an excellent example. Volcanic rocks on the island of Kauai at the northwest end of the chain have been dated through radioactive means at about 6 million years, whereas the volcanoes Mauna Loa and Mauna Kea on the island of Hawaii at the southeast end of the chain are in almost continual activity, at the present time having an interval between eruptions of only 11 months. In addition, geologists speculate that Yellowstone National Park, Wyoming, one of the largest geothermal areas in the world, sits over such a hot spot and that the older volcanic rocks of the eastern and western Snake River plains in Idaho are the surface trace of this mantle hot spot in the geologic past.

Not all geothermal resources are caused by near-surface intrusion of molten rock bodies. Certain areas have a higher than average rate of increase in temperature with depth (high geothermal gradient) without shallow magma being present. Much of the western United States contains areas that have an anomalously high mean heat flow (100 mwatt/m^2) and an anomalously high geothermal gradient (50°C/km). Geophysical and geological data indicate that the earth's crust is thinner than normal and that the isotherms are upwarped beneath this area. Much of the western U.S. is geologically active, as manifested by earthquakes and active or recently active volcanoes. Faulting and fracturing during earthquakes help to keep fracture systems open, and this

allows circulation of ground water to depths of 2 km to perhaps 5 km. Here the water is heated and rises buoyantly along other fractures to form geothermal resources near surface. Many of the hot springs and wells in the western United States and elsewhere owe their origin to such processes.

Geothermal Resource Types

All geothermal resources have three common components:

- 1) a heat source
- 2) permeability in the rock, and
- 3) a heat transfer fluid.

In the foregoing we have considered some of the possible heat sources, and we will discuss others presently. Let us now consider the second component, permeability.

Permeability is a measure of how easily fluids flow through rock as a result of pressure differences. Of course fluid does not flow through the rock matrix itself but rather it flows in open spaces between mineral grains and in fractures. Rocks in many, but not all, geothermal areas are very solid and tight, and have little or no interconnected pore space between mineral grains. In such rocks the only through-going pathways for fluid flow are cracks or fractures in the rock. A geothermal well must intersect one or more fractures if the well is to produce geothermal fluids in quantity, and it is generally the case that these fractures can not be located precisely by means of surface exploration. Fractures sufficient to make a well a good producer need only be a few millimeters in width, but must be connected to the general fracture network in the rock in order to carry large fluid volumes.

The purpose of the heat transfer fluid is to remove the heat from the rocks at depth and bring it to the surface. The heat transfer fluid is either water (sometimes saline) or steam. Water has a high heat capacity (amount of

heat needed to raise the temperature by 1°C) and a high heat of vaporization (amount of heat needed to convert 1 gm to steam). Thus water, which naturally pervades fractures and other open spaces in rocks, is an ideal heat transfer fluid because a given quantity of water or steam can carry a large amount of heat to the surface where it is easily removed.

Geothermal resource temperatures range upward from the mean annual ambient temperature (usually 10-30°C) to well over 350°C. Figure 1.1.6 shows the span of temperatures of interest in geothermal work.

The classifications of geothermal resource types shown in Table 1.1.1 is modeled after one given by White and Williams (1975). Each type will be described briefly. In order to describe these resource types we resort to simplified geologic models. A given model is often not acceptable to all geologists, especially at our rather primitive state of knowledge of geothermal resources today.

Hydrothermal Resources

Hydrothermal convection resources are geothermal resources in which the earth's heat is actively carried upward by the convective circulation of naturally occurring hot water or its gaseous phase, steam. Underlying some of the higher temperature hydrothermal resources is presumably a body of still molten or recently solidified rock that is very hot (300°C-1100°C). Other hydrothermal resources result simply from circulation of water along faults and fractures or within a permeable aquifer to depths where the rock temperature is elevated, with heating of the water and subsequent buoyant transport to the surface or near surface. Whether or not steam actually exists in a hydrothermal reservoir depends, among other less important variables, on temperature and pressure conditions at depth.

Figure 1.1.7 (after White et al., 1971) shows a conceptual model of a

VAPOR DOMINATED GEOTHERMAL RESERVOIR

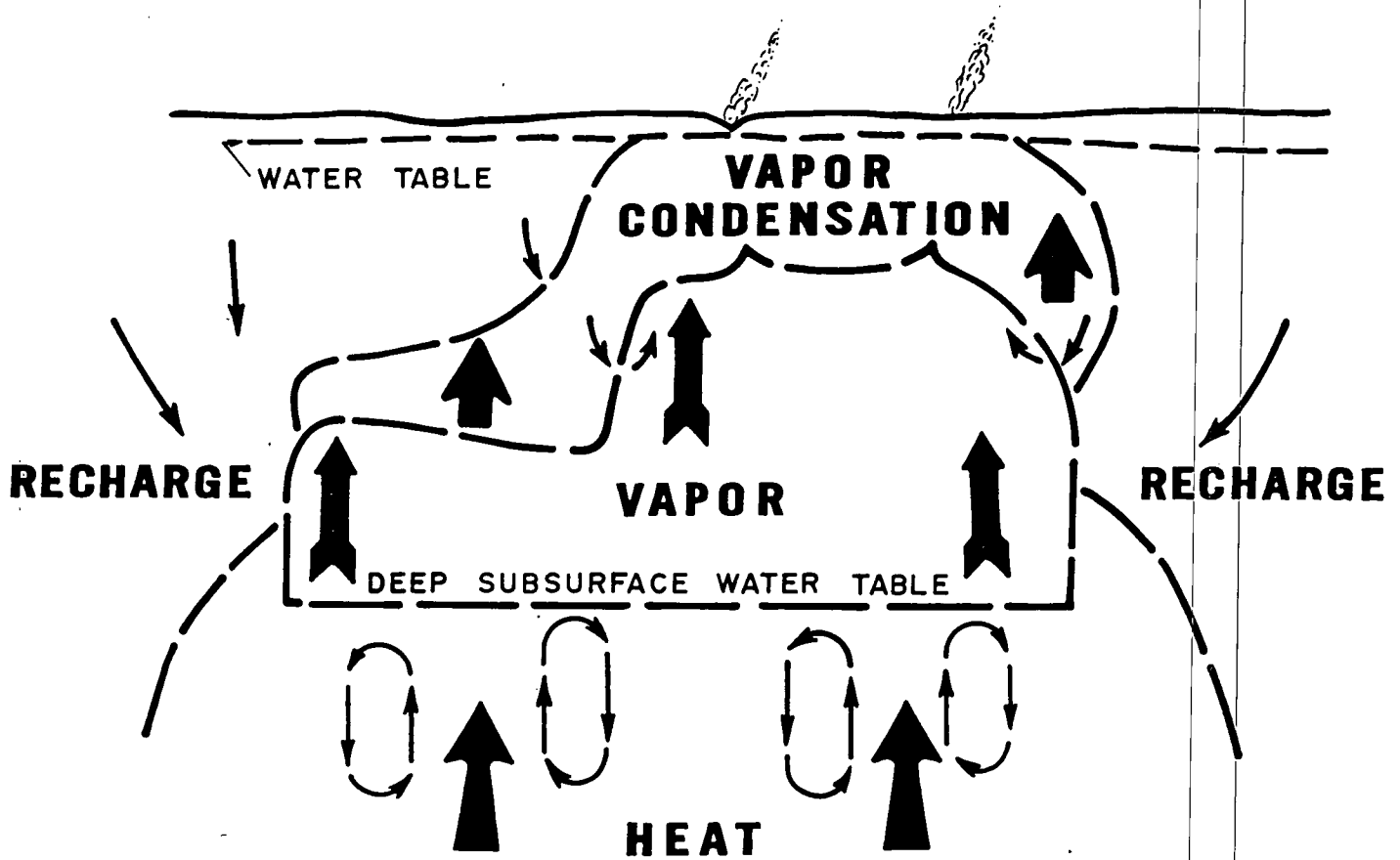


Figure 1.1.7

hydrothermal system where steam is present, a so-called vapor-dominated hydrothermal system (1a of Table 1.1.1). Convection of deep saline water brings a large amount of heat upward from depth to a level where boiling can take place under the prevailing temperature and pressure conditions. Steam moves upward through fractures in the rock and is possibly superheated further by the hot surrounding rock. Heat is lost from the vapor to the cooler, near-surface rock and condensation results, with some of the condensed water moving downward to be vaporized again. Within the entire vapor-filled part of the reservoir, temperature is nearly uniform due to rapid fluid convection. This whole convection system can be closed, so that the fluid circulates without loss, but if an open fracture penetrates to the surface, steam may vent. In this case, water lost to the system would be replaced by recharge, which takes place mainly by cool ground water moving downward and into the convection system from the margins. The pressure within the steam-filled reservoir increases much more slowly with depth than would be the case if the reservoir were filled with water under hydrostatic pressure. Because the rocks surrounding the reservoir will generally contain ground water under hydrostatic pressure, there must exist a large horizontal pressure differential between the steam in the reservoir and the water in the adjacent rocks, and a significant question revolves around why the adjacent water does not move in and inundate the reservoir. It is postulated that the rock permeability at the edges of the reservoir and probably above also, is either naturally low or has been decreased by deposition of minerals from the hydrothermal fluid in the fractures and pores to form a self-sealed zone around the reservoir. Self-sealed zones are known to occur in both vapor-dominated and water-dominated resources.

A well drilled into a vapor-dominated reservoir would produce superheated

steam. The Geysers geothermal area in California is an example of this type of resource. Steam is produced from wells whose depths are 1.5 to 3 km, and this steam is fed to turbine generators that produce electricity. The current generating capacity at The Geysers is 1454 MWe (megawatts of electrical power, where 1 megawatt = 1 million watts). This compares to the world current total from all geothermal resource types of 3790 MWe.

Other vapor-dominated resources that are currently being exploited occur at Lardarello and Monte Amiata, Italy, and at Matsukawa, Japan. The famous Yellowstone National Park in Wyoming contains many geysers, fumaroles, hot pools and thermal springs, and the Mud Volcanoes area is believed to be underlain by a dry steam field.

There are relatively few known vapor-dominated resources in the world because special geological conditions are required for their formation (White et al., 1971). However, they are eagerly sought because they are generally easier and less expensive to develop than the more common water-dominated system discussed below.

Figure 1.1.8 schematically illustrates a high-temperature, hot-water-dominated hydrothermal system (1b(i) of Table 1.1.1). The source of heat beneath many such systems is probably molten rock or rock that has solidified only in the last few tens of thousands of years, lying at a depth of perhaps 3 to 10 km. Normal ground water circulates in open fractures and removes heat from these deep, hot rocks by convection. Fluid temperatures are uniform over large volumes of the reservoir because convection is rapid. Recharge of cooler ground water takes place at the margins of the system through circulation down fractures. Escape of hot fluids at the surface is often minimized by a near-surface sealed zone or cap-rock formed by precipitation from the geothermal fluids of minerals in fractures and pore spaces. Surface manifestations

WATER DOMINATED GEOTHERMAL SYSTEM

FLOW CONTROLLED BY FRACTURES

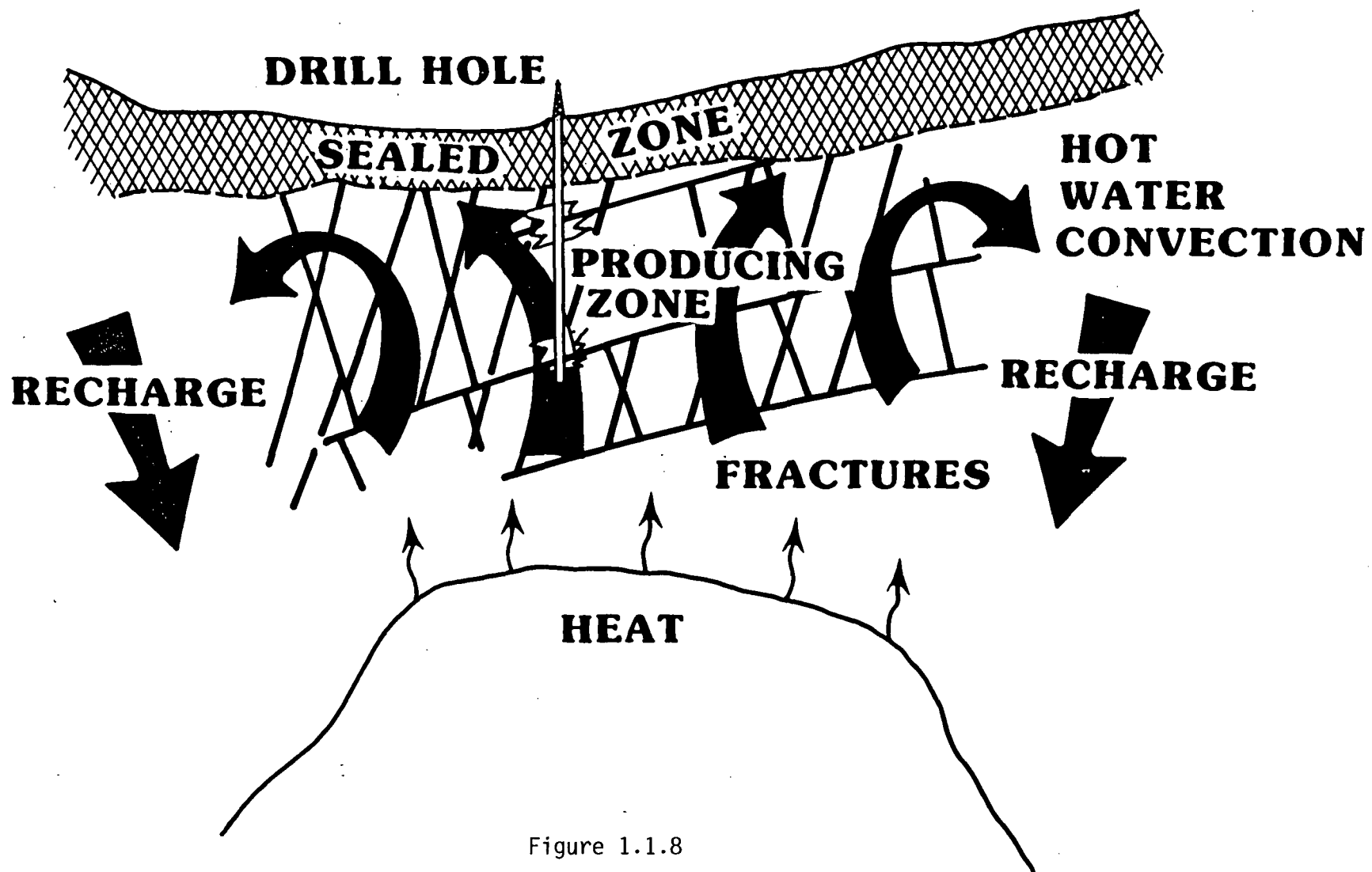


Figure 1.1.8

of such a geothermal system might include hot springs, fumaroles, geysers, thermal spring deposits, chemically altered rocks, or alternatively, no surface manifestation may occur at all. If there are no surface manifestations, discovery is much more difficult and requires sophisticated geology, geophysics, geochemistry and hydrology. A well drilled into a water-dominated geothermal system would likely encounter tight, hot rocks with hot water inflow from the rock into the well bore mainly along open fractures. Areas where different fracture sets intersect may be especially favorable for production of large volumes of hot water. For generation of electrical power a portion of the hot water produced from the well is allowed to flash to steam within the well bore or within surface equipment as pressure is reduced, and the steam is used to drive a turbine generator.

A second type of hot-water dominated system is shown in Figure 1.1.9. Here the reservoir rocks are sedimentary rocks that have intergranular permeability as well as fracture permeability. Geothermal fluids can sometimes be produced from such a reservoir without the need to intersect open fractures by a drill hole. Examples of this resource type occur in the Imperial Valley of California and Mexico. In this region the East Pacific Rise, a crustal spreading center, comes onto the North American continent. Figure 1.1.3 shows that the rise is observed to trend northward up the Gulf of California in small segments that are repeatedly offset northward by transform faults. Although its location under the continent cannot be traced very far with certainty, it is believed to occur under and be responsible for the Imperial Valley geothermal resources. The source of the heat is upwelling, very hot molten or plastic material from the earth's mantle. This hot rock heats overlying sedimentary rocks and their contained fluids and has spawned volcanoes. The locations of specific resource areas appear to be controlled

IMPERIAL VALLEY, CALIFORNIA GEOTHERMAL RESOURCE

◀ HIGH HEAT FLOW AREA ▶

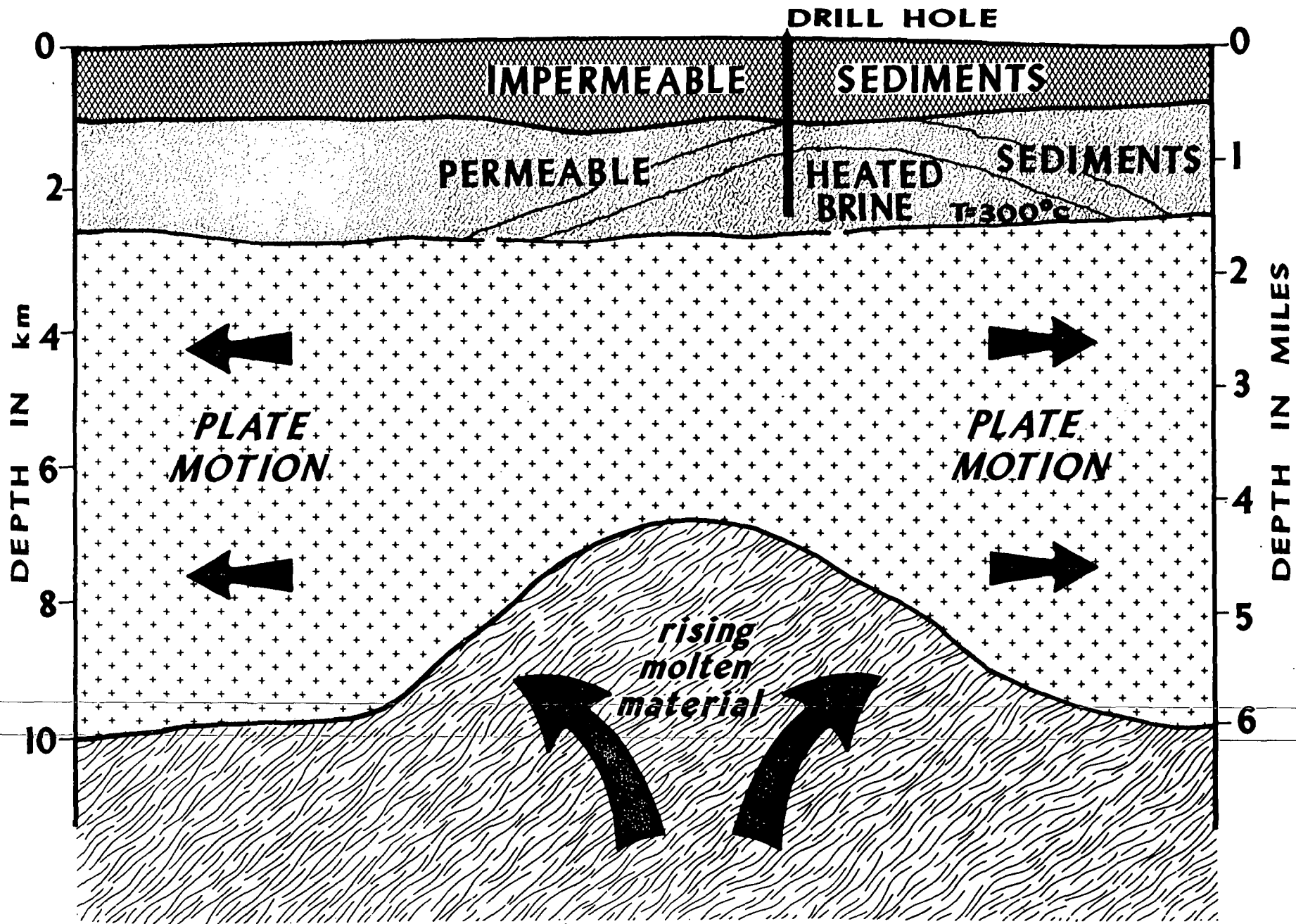


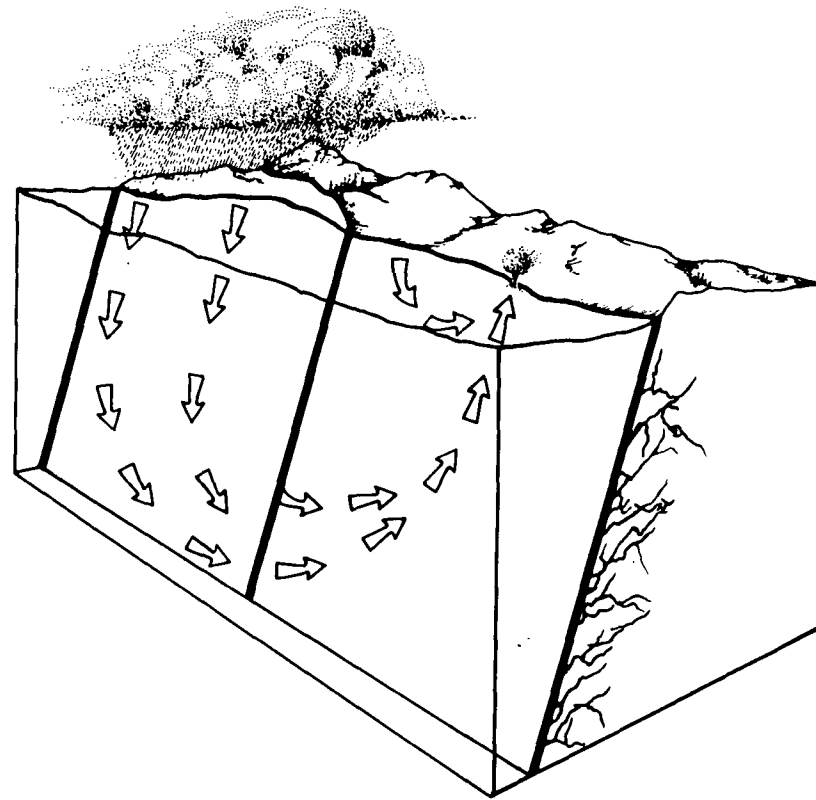
Figure 1.1.9

by faults that presumably allow deep fluid circulation to carry the heat upward to reservoir depths.

The fringe areas of high-temperature vapor- and water-dominated hydrothermal systems often produce water of low and intermediate temperature (1b(ii) and 1b(iii) of Table 1.1.1). These lower temperature fluids are suitable for direct heat applications but not for electrical power production. Low- and intermediate-temperature waters can also result from deep water circulation in areas where heat conduction and the geothermal gradient are merely average, as previously discussed. Waters circulated to depths of 1 to 5 km are warmed in the normal geothermal gradient and they return to the surface or near surface along open fractures because of their buoyancy (Fig. 1.1.10). There need be no enhanced gradient or magmatic heat source under such an area. Warm springs occur where these waters reach the surface, but if the warm waters do not reach the surface they are generally difficult to find.

Sedimentary Basins

Some basins are filled to depths of 3 km or more with sedimentary rocks that have intergranular and open-space permeability. In some of these sedimentary units, circulation of ground water can be very deep. Water may be heated in a normal or enhanced geothermal gradient and may then either return to the near-surface environment or remain trapped at depth (3a of Table 1.1.1). Figures 1.1.11a and 1.1.11b illustrate these resources. Substantial benefit is being realized in France from use of this type of resource for space heating by production of warm water contained in the Paris basin. Many other areas of occurrence of this resource type are known worldwide.



MODEL OF DEEP CIRCULATION HYDROTHERMAL RESOURCE

Figure 1.1.10

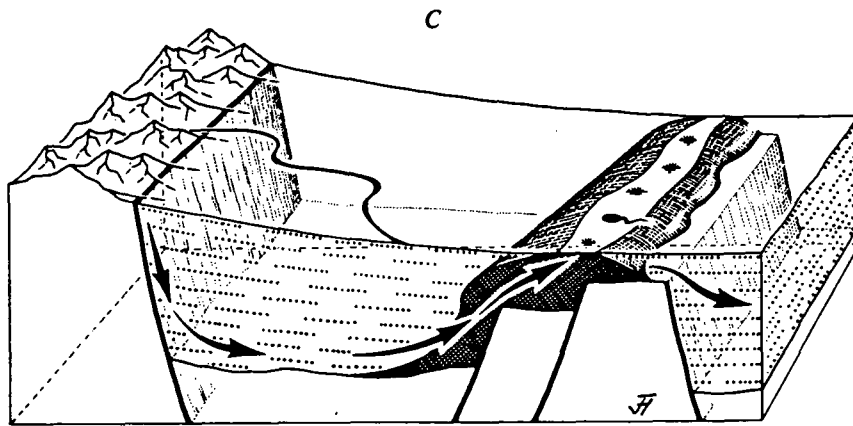
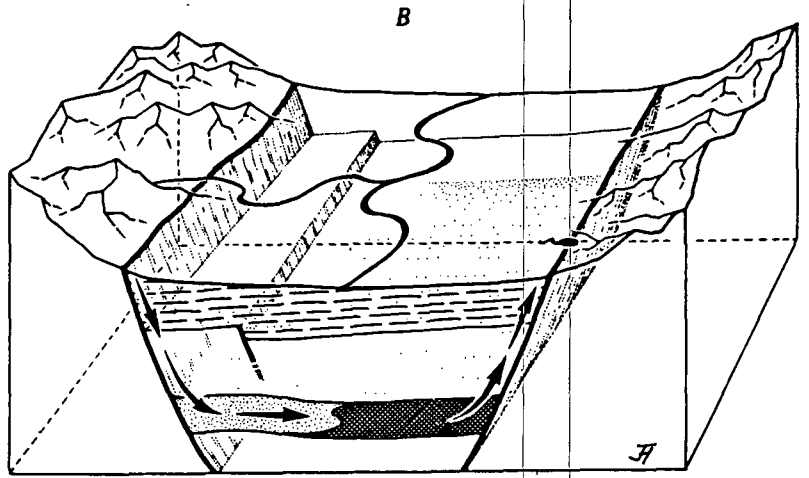
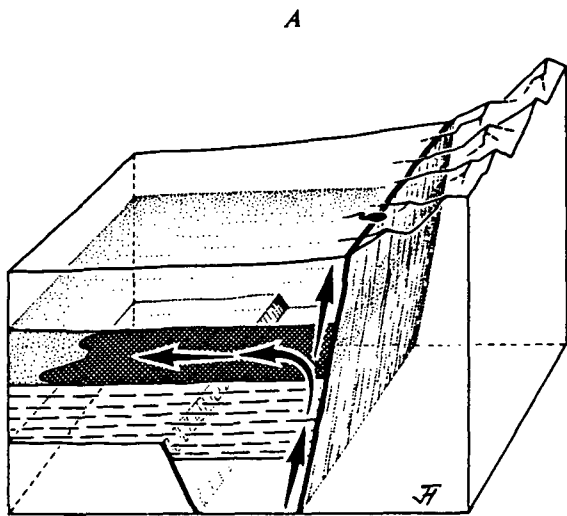


Figure 1.1.11a

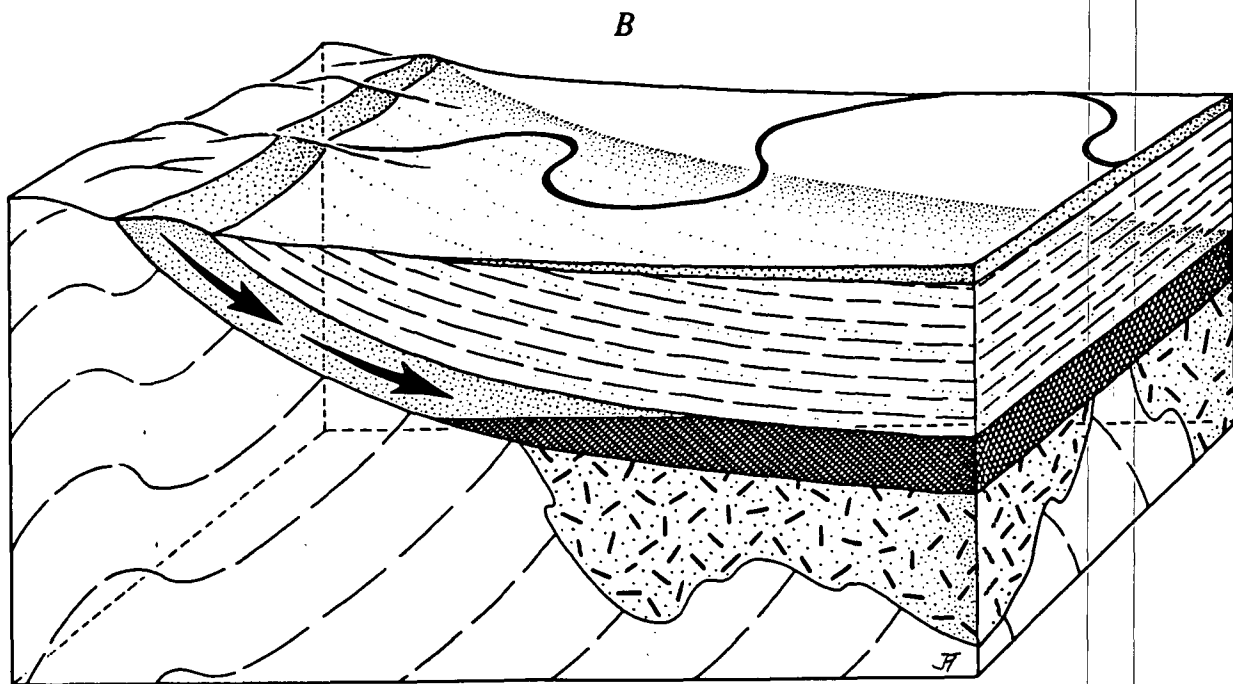
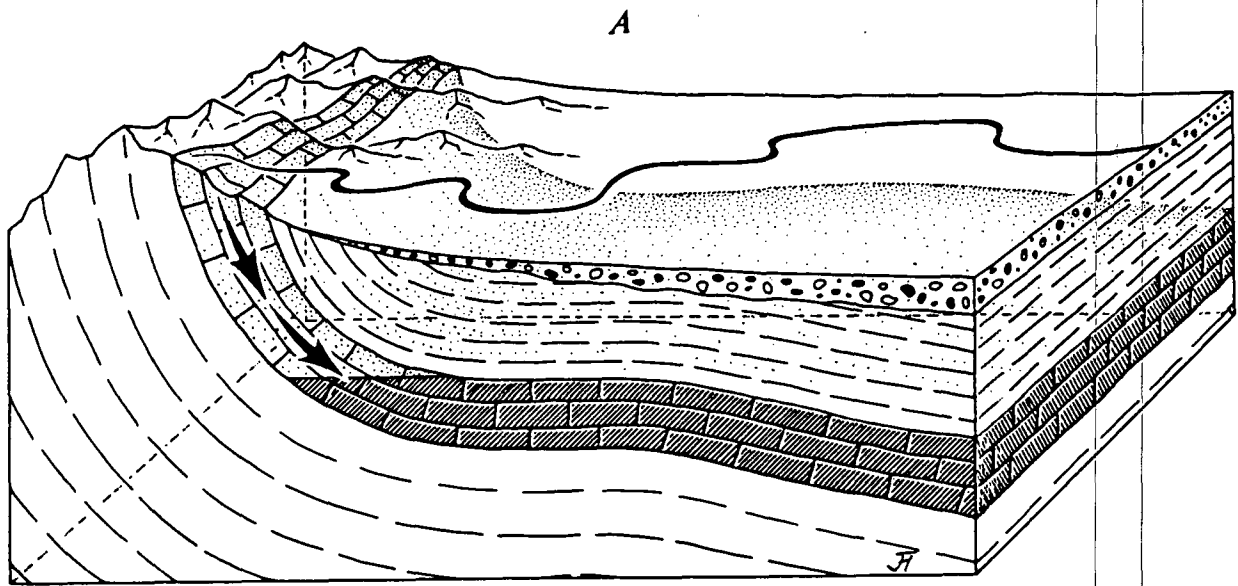


Figure 1.1.11b

Geopressured Resources

Geopressured resources (3b of Table 1.1.1) consist of deeply buried fluids contained in permeable sedimentary rocks warmed in a normal or anomalous geothermal gradient by their great burial depth. These fluids are tightly confined by surrounding impermeable rock and thus bear pressure that is much greater than hydrostatic, that is, the fluid pressure supports a portion of the weight of the overlying rock column as well as the weight of the water column. Figure 1.1.12 (from Papadopoulos, 1975) gives a few typical parameters for geopressured reservoirs and illustrates the origin of the above-normal fluid pressure. These geopressured fluids may contain dissolved methane. Therefore, three sources of energy are actually available from such resources: 1) heat, 2) mechanical energy due to the great pressure with which these waters exit the borehole, and 3) the recoverable methane.

Radiogenic Geothermal Resource

Radiogenic geothermal resources are found in places such as the eastern U.S. (3c of Table 1.1.1). The coastal plain is blanketed by a layer of thermally insulating sediments. In places beneath these sediments are intrusions having enhanced heat production due to higher content of radioactive U, Th, and K are believed to occur. Geophysical and geological methods for locating such radiogenic rocks beneath the sedimentary cover are being developed, and drill testing of the entire geothermal target concept (Fig. 1.1.13) are being completed. Success would most likely come in the form of low- to intermediate-temperature geothermal waters suitable for space heating and industrial processing.

Hot Dry Rock Resource

Hot dry rock resources (2b of Table 1.1.1) are defined as heat stored in

GEOPRESSURED GEOTHERMAL RESOURCE

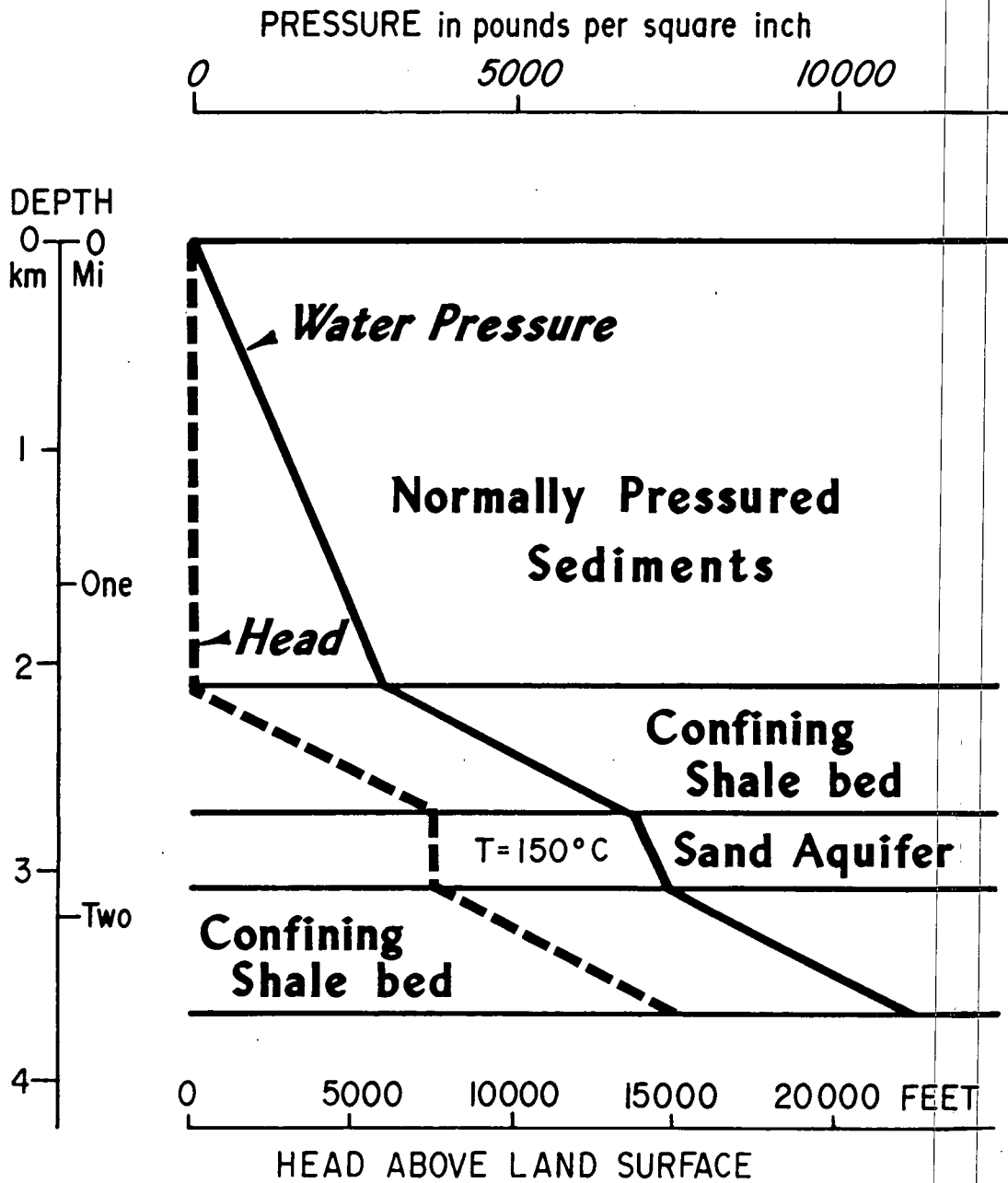


Figure 1.1.12

RADIOGENIC GEOTHERMAL RESOURCE

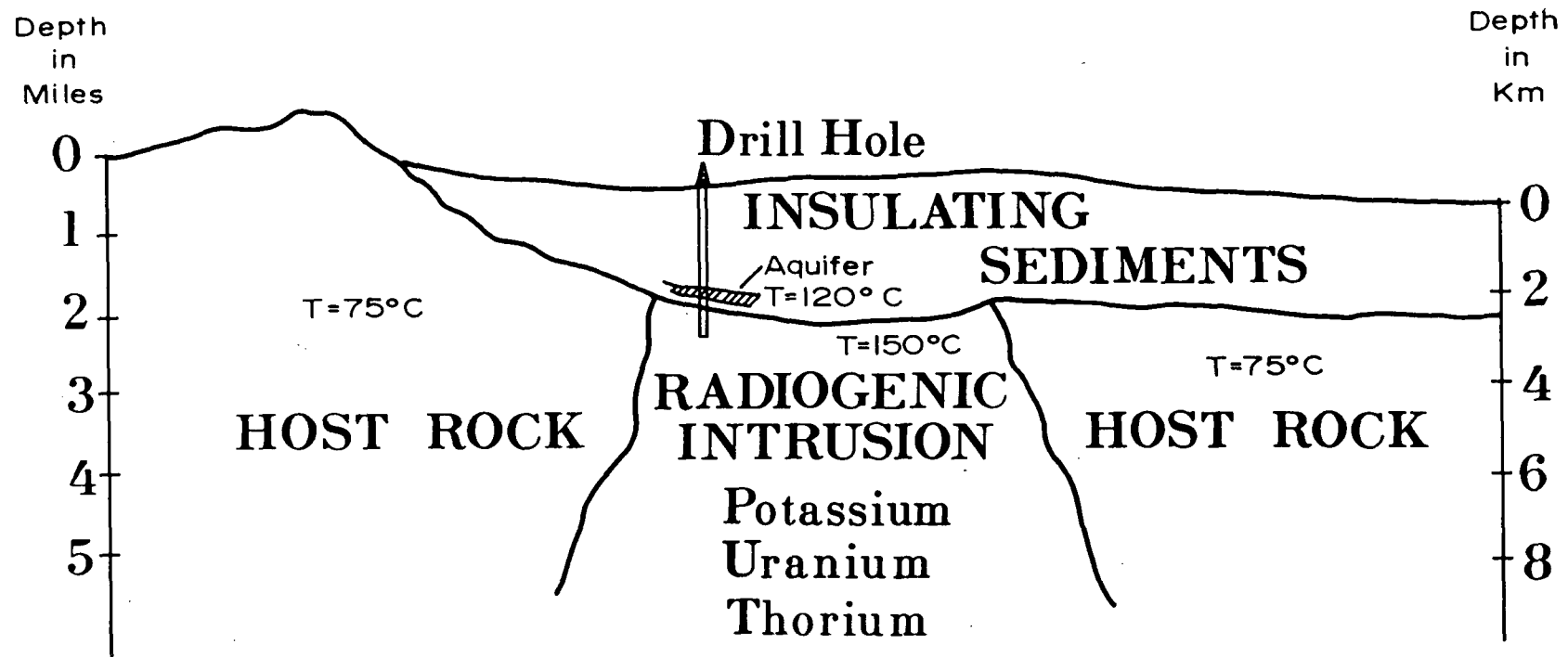
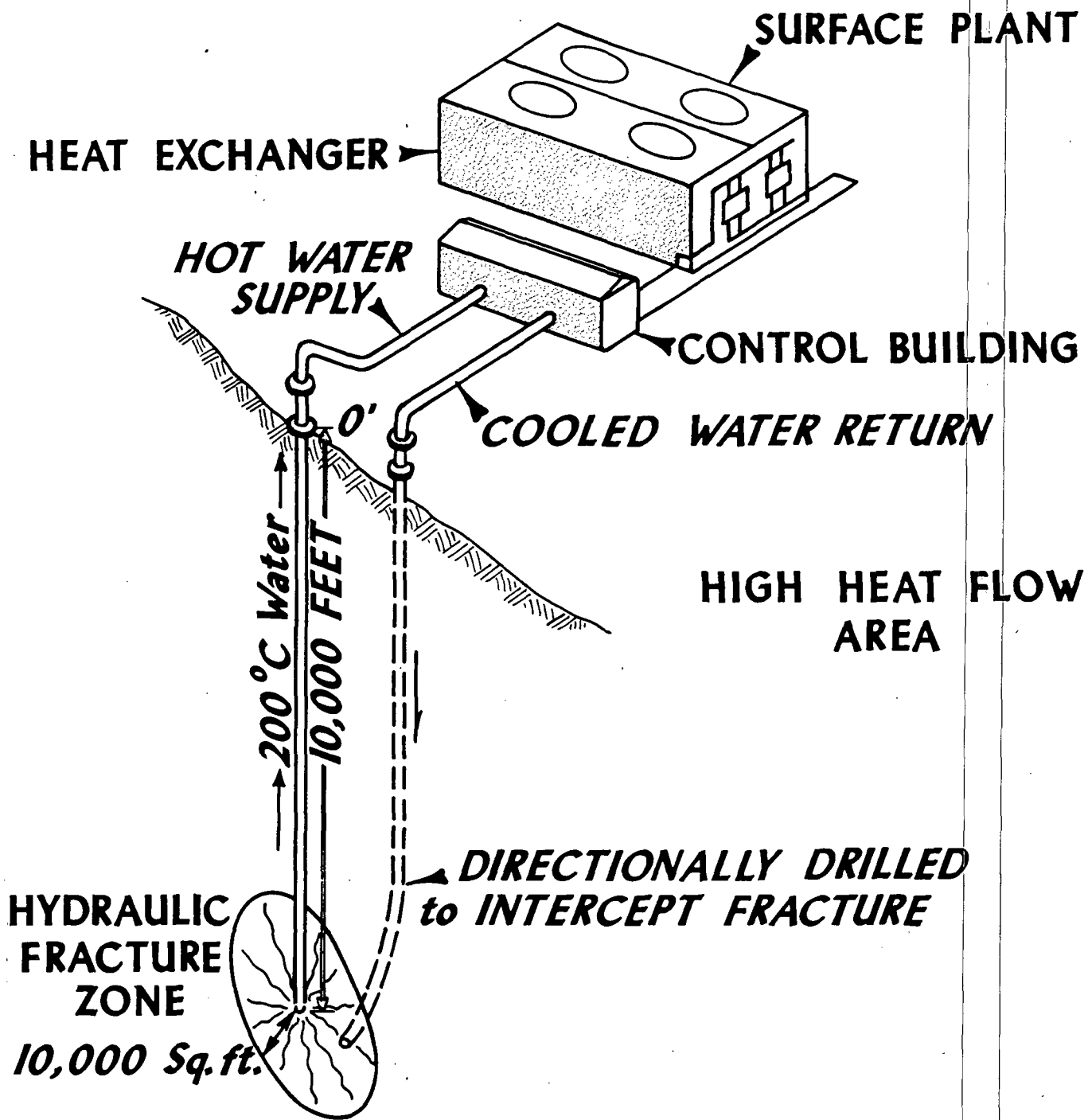


Figure 1.1.13

rocks within about 10 km of the surface from which the energy cannot be economically extracted by natural hot water or steam. These hot rocks have few pore spaces or fractures, and therefore contain little water. The feasibility and economics of extraction of heat for electrical power generation and direct uses from hot dry rocks is presently the subject of intensive research at the U.S. Department of Energy's Los Alamos National Laboratory in New Mexico (Smith et al., 1975; Tester and Albright, 1979). Their work indicates that it is technologically feasible to induce an artificial fracture system in hot, tight crystalline rocks at depths of about 3 km through hydraulic fracturing from a deep well. Water is pumped into a borehole under high pressure and is allowed access to the surrounding rock through a packed-off interval near the bottom. When the water pressure is raised sufficiently, the rock cracks to form a fracture system that usually consists of one or more vertical, planar fractures. After the fracture system is formed, its orientation and extent are mapped using geophysical techniques. A second borehole is sited and drilled in such a way that it intersects the fracture system. Water can then be circulated down the deeper hole, through the fracture system where it is heated, and up the shallower hole (Fig. 1.1.14). Fluids at temperatures of 150°C to 200°C have been produced in this way from boreholes at the Fenton Hill experimental site near the Valles Caldera, New Mexico. Much technology development remains to be done before this technique will be economically feasible.

Molten Rock Resource

Experiments are underway at the U.S. Department of Energy's Sandia National Laboratory in Albuquerque, New Mexico to learn how to extract heat energy directly from molten rock (2a of Table 1.1.1). These experiments have not indicated economic feasibility for this scheme in the near future.



HOT DRY ROCK GEOTHERMAL RESOURCE

Figure 1.1.14

Techniques for drilling into molten rock and implanting heat exchangers or direct electrical converters remain to be developed.

Hydrothermal Fluids

The processes causing many of today's high temperature geothermal resources consist of convection of aqueous solutions around a cooling intrusion. These same basic processes have operated in the past to form many of the base and precious metal ore bodies being currently exploited, although ore forming processes differ in some aspects from hydrothermal convection processes as we understand them at present. The fluids involved in geothermal resources are complex chemically and often contain elements that cause scaling and corrosion of equipment or that can be environmentally damaging if released.

Geothermal fluids contain a wide variety and concentration of dissolved constituents. Simple chemical parameters often quoted to characterize geothermal fluids are total dissolved solids (tds) in parts per million (ppm) or milligrams per liter (mg/l) and pH. Values for tds range from a few hundred to more than 300,000 mg/l. Many resources in Utah, Nevada, and New Mexico contain about 6,000 mg/l tds, whereas a portion of the Imperial Valley, California resources are toward the high end of the range. Typical pH values range from moderately alkaline (8.5) to moderately acid (5.5). A pH of 7.0 is neutral at normal ground water temperature--neither acid nor alkaline. The dissolved solids are usually composed mainly of Na, Ca, K, Cl, SiO₂, SO₄, and HCO₃. Minor constituents include a wide range of elements with Hg, F, B, and a few others of environmental concern. Dissolved gases usually include CO₂, NH₄ and H₂S, the latter being a safety hazard. Effective means have been and are still being developed to handle the scaling, corrosion and environmental problems caused by dissolved constituents in geothermal fluids.

Conclusions

Although many types of geothermal resources exist, only some of these are presently economic. Vapor- and water-dominated resources (type 1) and sedimentary basin resources (type 3a) are presently most attractive for exploitation, while hot dry rock, magma, geopressured, and radiogenic resources are further from commercial development.

Geothermal resources are found in a wide variety of geologic environments and tectonic terrains. Those characteristics relevant to Spanish resources are discussed in later chapters.

TABLE 1.1.1

GEOTHERMAL RESOURCE CLASSIFICATION
(After White and Williams, 1975)

Resource Type	Temperature Characteristics
1. <u>Hydrothermal convection resources</u> (heat carried upward from depth by convection of water or steam)	
a) Vapor dominated	about 240°C
b) Hot-water dominated	
i) High Temperature	150°C to 350°C+
ii) Intermediate	90°C to 150°C
iii) Low Temperature	less than 90°C
2. <u>Hot rock resources</u> (rock intruded in molten form from depth)	
a) Part still molten	higher than 600°C
b) Not molten (hot dry rock)	90°C to 650°C
3. <u>Other resources</u>	
a) Sedimentary basins (hot fluid in sedimentary rocks)	30°C to about 150°C
b) Geopressured (hot fluid under high pressure)	150°C to about 200°C
c) Radiogenic (heat generated by radioactive decay)	30°C to about 150°C

CHAPTER 1 REFERENCES

- Davis, G. F., 1980, Exploratory models of the earth's thermal regime during segregation of the core: *Jour. Geophys. Research*, v. 85, no. B12, p. 7108-7114.
- Goguel, J., 1976, *Geothermics*: McGraw-Hill Book Co., 200 p.
- MacDonald, B. A., 1965, Geophysical deductions from observations of heat flow: in *Terrestrial Heat Flow*; Geophys. Monograph No. 8: Amer. Geophys. Union, W. H. K. Lee, ed., 276 p.
- Papadopoulos, S. S., 1975, The energy potential of geopressured reservoirs: hydrogeologic factors, in *Proc. First Geopressured Geothermal Energy Conf.*, M. L. Dorfman and R. W. Deller, eds., Univ. of Texas, Austin.
- Smith, M. C., Aamodt, R. L., Potter, R. M., and Brown, D. W., 1976, Man-made geothermal reservoirs: *Proceedings, Second United Nations Geothermal Energy Symposium on the Development and Use of Geothermal Resources*, San Francisco, CA, May, 1975, v. 3, p. 1781-1788.
- Tester, J. W., and Albright, J. N., 1979, Hot dry rock energy extraction field test: 75 days of operation of a prototype reservoir at Fenton Hill, Segment 2, Phase I: Los Alamos Scientific Laboratory Rept. LA-7771-MS.
- White, D. E., Muffler, L. J. P., and Truesdell, A. H., 1971, Vapor-dominated hydrothermal systems compared with hot-water systems: *Economic Geology*, v. 66, no. 1, p. 75-97.
- White, D. E., and Williams, D. L., 1975, Assessment of geothermal resources of the United States - 1975: *U.S. Geol. Survey Circ.* 726, 155 p.
- Wyllie, P. J., 1971, *The Dynamic Earth: Textbook in Geosciences*: John Wiley & Sons, Inc., 416 p.

2.0. GEOCHEMICAL METHODS IN GEOTHERMAL EXPLORATION - BIBLIOGRAPHIC SEARCH

During the past decade geochemistry has played an ever increasing role in the evaluation and development of our geothermal resources. Deep drilling in many geothermal environments has provided a wealth of new data on the chemical composition, evolution, and thermal structure of geothermal reservoirs. These relationships have led to the development of quantitative geothermometers that are based on the chemical and isotopic compositions of the fluids. Concurrently investigations of the altered rocks and soils have been conducted and chemical models developed to explain the relationship between the geothermal fluids and the reservoir rocks.

Geochemical investigations can be utilized at all stages of a geothermal program. During the initial evaluation of a prospect it is common practice to collect samples from all springs and existing wells, and of possible recharge waters including samples of streams, waters, rain and snow. Chemical and isotopic analyses can at this stage be used to:

1. differentiate between vapor and liquid dominated systems;
2. determine the areal extent of the thermal system and the types of waters present;
3. estimate the reservoir temperature;
4. characterize the probable nature and types of rock present in the reservoir;
5. establish the directions of fluid movement;
6. determine if sealing during production will be a reservoir problem;
7. determine if valuable metals are contained in the reservoir fluids;
and,
8. assess possible recharge areas.

Estimates made from surface surveys can be modified as drilling or production

proceeds and deeper waters are collected.

During production, chemical analyses of the water can indicate changes in the physical and chemical state of the reservoir long before changes in production temperature or pressure become apparent.

Rocks and soils collected from geothermal deposits can also aid in estimating subsurface temperatures and delineating areas that are most directly connected to the reservoir fluids. Silica deposits (sinters) are indicative of reservoir temperatures in excess of about 180°C while calcium carbonate deposits (travertine) generally suggest lower temperatures or the presence of a lower temperature reservoir underlain by a higher temperature fluids. Soil gases, such as Hg and Rn, may show preferential enrichments along faults that extend into the reservoir.

The distribution and mineralogy of the altered rocks sampled during drilling can be used to assess temperature, permeability, fluid chemistry, rock type, pressure and time (Browne, 1978). Thus, the altered rocks contain a record of the history of the geothermal system and can be used to guide the exploration program even if fluids are not encountered. Changes in the mineralogy as a result of alteration will also affect the physical properties of the rocks. Because these changes will substantially affect the geophysical responses of the rocks at depths, estimates of the extent and character of the hydrothermal phenomena are needed to quantitatively interpret the geophysical responses.

A bibliographic search of geochemical and geothermal journals, published reports and transactions from technical meetings was undertaken in order to establish and document the application of various geochemical techniques used worldwide for the exploration of geothermal resources. Over 500 pertinent references were assembled and are listed at the end of this report. A data

base which indicates the worldwide application of various geochemical methods for geothermal exploration was created by reviewing the more significant publications within the bibliography. This data base was then used to evaluate the effectiveness of the geochemical methods within specific geologic and tectonic settings.

PRINCIPAL LITERATURE SOURCES

A computer-aided bibliographic search was conducted using the GEOREF data base of Dialog Information Services, Palo Alto, California. This search resulted in an extensive listing of technical articles which describe the application of geochemical methods for the exploration of geothermal resources around the world. A total of 302 listings was obtained which included references from technical journals, transactions and extended abstracts from technical meetings, government publications, doctoral and masters theses and geothermal texts. Approximately 211 additional references were obtained through a specific literature search, so that the total number of bibliographic references exceeds 500.

The GEOREF bibliographic entries are included in the Appendix of this report and are listed according to a GEOREF identification number which includes the year that the reference was placed in the data base. The most recently published references are generally listed first with the article title shown in boldface lettering. Unfortunately, there is no author cross-reference to aid in the search for a particular article. A bonus with this reference list is the list of key words that accompanies each reference entry. These key words provide valuable information regarding the articles. Abstracts are also included for some of the more recent listings.

The 200 additional references came from transactions of selected technical meetings, texts and technical journals. They are listed by author. There may be some duplication between the GEOREF and the supplemental reference listings.

The GEOREF bibliography was broken down into six categories. The description of the categories and the number of articles in each category found by computer search are given below.

- 1) Primary geochemical exploration techniques. These techniques are generally applicable to geothermal exploration. They are primarily semi-empirical and the papers are written for teaching one how to use these techniques. More articles of this type can be found in the reference list of each chapter. (3 articles listed)
- 2) Secondary geochemical exploration techniques. These techniques are somewhat complicated and/or site specific. They range from theoretical to empirical and are not written to teach, but to elucidate geologic relations within a specific area. (26 articles listed)
- 3) Qualitative exploration tools. These studies relate mineralogy and fluid trace element compositions to temperature. They can be used to roughly estimate temperature regimes or to study the past thermal history of a geothermal area. (74 articles listed)
- 4) Site-specific studies of geothermal areas in volcanic, igneous or metamorphic terrains. (154 articles listed)
- 5) Site-specific studies of geothermal areas in sedimentary basins. (42 articles listed)
- 6) Production and utilization of geothermal fluids. This category includes such diverse areas as excess enthalpy and aqua-culture. (3 articles listed)

PRINCIPAL LITERATURE SOURCES

A computer-aided bibliographic search was conducted using the GEOREF data base of Dialog Information Services, Palo Alto, California. This search resulted in an extensive listing of technical articles which describe the application of geochemical methods for the exploration of geothermal resources around the world. A total of 302 listings was obtained which included references from technical journals, transactions and extended abstracts from technical meetings, government publications, doctoral and masters theses and geothermal texts. Approximately 211 additional references were obtained through a specific literature search, so that the total number of bibliographic references exceeds 500.

The GEOREF bibliographic entries are included in the Appendix of this report and are listed according to a GEOREF identification number which includes the year that the reference was placed in the data base. The most recently published references are generally listed first with the article title shown in boldface lettering. Unfortunately, there is no author cross-reference to aid in the search for a particular article. A bonus with this reference list is the list of key words that accompanies each reference entry. These key words provide valuable information regarding the articles. Abstracts are also included for some of the more recent listings.

The 200 additional references came from transactions of selected technical meetings, texts and technical journals. They are listed by author. There may be some duplication between the GEOREF and the supplemental reference listings.

The GEOREF bibliography was broken down into six categories. The description of the categories and the number of articles in each category found by computer search are given below.

- 1) Primary geochemical exploration techniques. These techniques are generally applicable to geothermal exploration. They are primarily semi-empirical and the papers are written for teaching one how to use these techniques. More articles of this type can be found in the reference list of each chapter. (3 articles listed)
- 2) Secondary geochemical exploration techniques. These techniques are somewhat complicated and/or site specific. They range from theoretical to empirical and are not written to teach, but to elucidate geologic relations within a specific area. (26 articles listed)
- 3) Qualitative exploration tools. These studies relate mineralogy and fluid trace element compositions to temperature. They can be used to roughly estimate temperature regimes or to study the past thermal history of a geothermal area. (74 articles listed)
- 4) Site-specific studies of geothermal areas in volcanic, igneous or metamorphic terrains. (154 articles listed)
- 5) Site-specific studies of geothermal areas in sedimentary basins. (42 articles listed)
- 6) Production and utilization of geothermal fluids. This category includes such diverse areas as excess enthalpy and aqua-culture. (3 articles listed)

CHAPTER 2 REFERENCES

Browne, P. R. L., 1978, Hydrothermal alteration in active geothermal fields:
Ann. Rev. Earth Planet. Sci., v. 6, p. 229-250.

3.0 GEOTHERMAL CHARACTERISTICS OF BASINS

3.1 Introduction

Geothermal resources in sedimentary basins are the product of groundwater hydrodynamics, which is controlled by the stratigraphic and structural development of each basin. The presence of a geothermal resource in a basin is dependent upon complex interactions of thermal and hydrologic regimes.

In order to identify thermal conditions in a basin, it is useful to define a thermal anomaly. The U. S. Geological Survey (Reed, 1983) has defined a thermal anomaly as a site where the surface temperature of the groundwater is 10°C or more above the mean annual temperature at that site, and where the geothermal gradient is equal to or greater than 25°C per kilometer. This definition is not strictly geological, as mean annual air temperature is included to separate anomalous geologic conditions from regional solar heating. The gradient figure of 25°C per kilometer is useful on a regional basis (at least in the United States) to identify positive thermal anomalies. This thermal gradient also implies the economic constraint that the favorability of geothermal development may be controlled by the depth of drilling required to reach a resource.

The three basic parameters of any geothermal system are: a source of heat, a thermal transport mechanism (water), and permeability to transport the heat through. Thermal input to most presently economic electrical generation geothermal sites is from young volcanic activity. Thermal input in sedimentary basins is often just from the regional heat flow, as volcanic activity is often lacking. Waters in basins have complex, laterally and vertically changing chemistry. Major permeability in basins is often fractured controlled, with the distribution of these fractures dependent on structural and stratigraphic conditions. Both horizontal and vertical permeability are

often required to generate geothermal anomalies.

The dynamic nature of fluid flow within basins, coupled with the changing stratigraphic and structural environments found within units, implies that widely different geothermal systems may exist. Thermal and hydrologic stratification may exist between units in a basin. Circulation systems may be vertically distinct or vertically connected. Lateral changes in chemistry may be due to water-rock interaction or mixing of different fluids, and such changes may occur within or between beds. The thermal regime may also change over short vertical or horizontal distances as a result of fluid movement.

3.2 Fluid Characteristics of Basins

Hydrothermal systems in basins have a wide range of fluid chemistries, from dilute fresh water to highly concentrated brines. The composition of water at any place in a basin is the product of the starting composition of the water, the types of rock the water has encountered in its flowpath, and the temperatures and residence times of the chemical reactions with each rock type.

The source of waters in basins is ultimately meteoric, but water trapped at the time of deposition of the sediments, whether meteoric, seawater, brackish water, or concentrated brines, and waters that moved through the sediments immediately after deposition but prior to deep burial, may also be important. The water contained in formations is called connate (White, 1957). Geochemical modeling suggests that most connate waters can be assumed to have the composition of seawater (Hitchon and others, 1971). Table 3.2.1 shows the typical changes in basin brines that can occur as a result of water-rock interaction.

Most chemical analyses of basin waters are made to evaluate the possible presence of hydrocarbons (Collins, 1975; Hitchon and others, 1971). These

TABLE 3.2.1

COMPARISON OF SEA WATER AND VOLUME-WEIGHTED MEAN FORMATION
WATER FROM THE WESTERN CANADA SEDIMENTARY BASIN

Component	Sea water		Formation water		Formation water Sea water	Net change	
	mg/l	meq	mg/l	meq		mg/l	meq
Li	0.17	0.02	10.7	1.54	62.9	+10.53	+1.52
Na	10,760	468.06	14,340	623.88	1.3	+3580	+155.73
K	387	9.90	561	14.35	1.4	+174	+4.45
Rb	0.12	0.00	0.88	0.01	7.3	+0.76	+0.009
Mg	1290	106.09	317	26.07	0.25	-973	-80.02
Ca	413	20.61	2210	110.38	5.3	+1797	+89.67
Sr	8	0.18	108	2.46	13.5	+100	+2.28
Mn	0.002	0.00	0.32	0.01	160.0	+0.318	+0.01
Zn	0.01	0.00	0.30	0.01	30.0	+0.29	+0.01
Cl	19,350	545.67	26,920	759.06	1.4	+7570	+213.47
Br	67	0.84	114	1.42	1.7	+47	+0.59
I	0.06	0.00	9	0.07	150.0	+8.94	+0.07
HCO ₃	142	2.33	1500	24.52	10.6	+1358	+22.26
SO ₄	2710	56.42	350	7.29	0.13	-2360	-49.14
Total dissolved solids	35,100	-	46,400	-	1.3	+11,300	-

from: Hitchon and others, 1971

data are not collected specifically for geothermal studies, and thus are not an optimum data set for evaluating geothermal resources in a basin. Other chemical analyses of basin waters are usually available from shallow water wells, which are drilled for local water supply, deep water wells, which may be for industrial processes, or non-producing oil wells.

The distinction between geologically recent meteoric waters and connate waters is important in evaluating geothermal resources. One major reason for identifying the origin of the waters is to seek to find areas of upwelling (i.e. warmer) fluids from deeper in the system. Waters that are recent will have had much less residence time in the basin, both to reach chemical equilibrium with the rocks and to acquire heat. Another reason it is useful to distinguish meteoric and connate waters is to evaluate the reliability of chemical geothermometers.

It is important to note that this distinction is not always clear, as the normal evolution of meteoric water chemistry in a basin will follow the path outlined by Ottlik and others (1981) as:

The ground-water originating from precipitation starts as bicarbonate water and changes, when migrating downwards, through a sequence of bicarbonate + chloride to chloride + bicarbonate to chloride + sulphate or sulphate + chloride and finally to a predominantly chloride water approaching the composition of the sea-water.

This implies that basin brines may originally have a sea-water type composition, and that normal groundwater may also evolve toward this composition.

Isotopic analyses of waters are probably the most useful method to distinguish meteoric from connate waters (Clayton and others, 1966; Zak and Gat, 1975; Hitchon and Friedman, 1969). Meteoric waters will often plot close to the present meteoric line for an area, while connate waters will have more interaction with the rocks, and may have precipitated under different climatic conditions (and therefore have a different starting composition). In areas

where isotopic data are not available, it may be possible to distinguish these waters by relative salinities or chemical constituents that would be the product of different flowpaths (Rittenhouse, 1967).

Although the general processes of importance in the evolution of fluids within a basin are well known, the detailed evaluation of the evolution of fluid compositions remains the subject of controversy in many areas. Hitchon and others (1971), on the basis of factor analysis, identify the major processes as:

dilution by fresh water -
is common in many basins

membrane filtration -
through shales, increases in efficiency with depth,
pressure and temperature

solution of halite -
may be a major process in some basins (Land and
Prezbindowski, 1981; Manheim and Bischoff, 1969)

dolomitization -
may increase Ca and reduce Mg; where opposite occurs, may
have dedolomitization (Land and Prezbindowski, 1981)

bacterial reduction of sulfate --
possibly important in conjunction with petroleum

formation of chlorite -
also many other diagenetic reactions (Chilingarian and
Rieke, 1969)

cation exchange on clays -
dependent on type of clay, exchange sites, and type,
bonding, and activity of ions

contributions from organic matter -
may be locally important

solubility relations -
important for most elements (see extensive discussion of
geothermal waters in next section)

The Gulf Coast of Texas is one area where differences between upwelling older waters and downflowing recent waters are dramatic, and controversy

exists about the chemical processes controlling the composition of the deep brines. Table 3.2.2 presents analysis of cold downwelling waters in a carbonate reservoir, deep waters from the basin, and a possible mixed water from a sandstone reservoir.

Carpenter (1978) suggested that brines (> 100,000 ppm) in basins may be associated with evaporates in three ways: dissolving the evaporites, fluids being expelled from evaporites, and alteration of evaporite minerals. Carpenter (1985) adds the processes of dolomitization and loss of sulfate to this list to account for brine compositions in the Texas Gulf Coast.

Land and Prezbindowski (1981, 1985) feel that these processes are oversimplified. They point out the dynamic nature of Gulf Coast hydrology (Woodruff and Foley, in press), and suggest that recrystallization of halite, combination with carbon dioxide and reaction with sedimentary minerals, anorthite, K-feldspar, anhydrite and calcite to form brines.

Stoessell and Moore (1983, 1985) more closely follow the suggestions of Carpenter for the origin of brines, counting on halite-saturated brines mixing with interstitial fluids and reacting with the rocks. They also discount the importance of interstitial brines, preferring instead to generate original brines during the precipitation of the original salt beds.

In summary, the chemistry of basin waters is extremely complex. Different sources of water, reacting with different rock types, flowing along different paths, can ultimately mix to provide the fluid sampled in a well or at the surface.

3.3 Hydrologic Characteristics of Basins

The hydrologic regimes of basins are the complex products of the interaction of the stratigraphic history, structural development, and stage of maturity of each basin and its surrounding areas. Recharge, permeability,

flow rates, pressure gradients, and the nature of discharge all impact both the basinwide and local favorability for the development of geothermal systems.

Darcy's law controls the flow of fluids in geologic media:

$$Q = KA \, dH/dL$$

Q - flow per unit time

k - hydraulic conductivity of rocks

A - cross-sectional area

dH/dL - pressure gradient

This law is similar to the heat flow equation, which suggests that similar physical principles are working (Woodruff and Foley, in press). Water flow will increase with higher pressure or greater conductivity.

Two major sources of pressure gradients exist in basins. These are from downward flow of recharging waters from topographically higher regions, or upward flow caused by deep burial, compaction and dewatering of unconsolidated sediments. Secondary sources of pressure gradient include capillary activity and thermal buoyancy.

The stratigraphic history and structural development of basins can be very complex. The tectonic setting of formation, the depositional regimes of sediments, and the post-deposition modifications of the basin are important in determining the present configuration of the basin (Kingston and others, 1983). Each of these facets contributes to the present hydrothermal regime in the basin. For instance, basins in continental interiors may be cooler than basins at continental margins or rift zones, basins with thick shale sequences will retain heat better than sand- or lime-dominated areas, and basins with complex post-depositional tectonism will have more fracture and fault permeability than basins that were quiescent after sedimentation ceased.

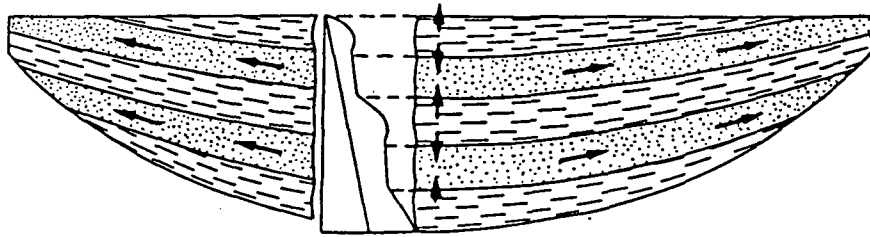
The major factor that determines the hydrologic regime in a basin is the level of maturity of the basin (Coustaou and others, 1975; Coustaou, 1977). Figure 3.3.1 is a summary of these stages. It shows that in juvenile, or still compacting, basins, the main water movement is outward from the deepest parts of the basins. At this time, shales may be overpressured, releasing waters into the sandstones. This is similar to the Gulf Coast basin in the United States (Woodruff and Foley, 1985). In intermediate basins with topographically high zones of recharge, meteoric water may be washing through the basins, displacing connate waters. In old basins, hydrostatic pressure dominates. The basins of Alberta (Toth, 1980) illustrate the topographic control of hydrodynamics (Figure 3.3.2).

Hydrologic recharge to geothermal systems in basins may be from either (or both) of two sources. Meteoric waters could precipitate on either surrounding highlands or onto the basin itself. Connate waters could be carried to depth in subsiding sedimentary columns, and then squeezed out during compaction.

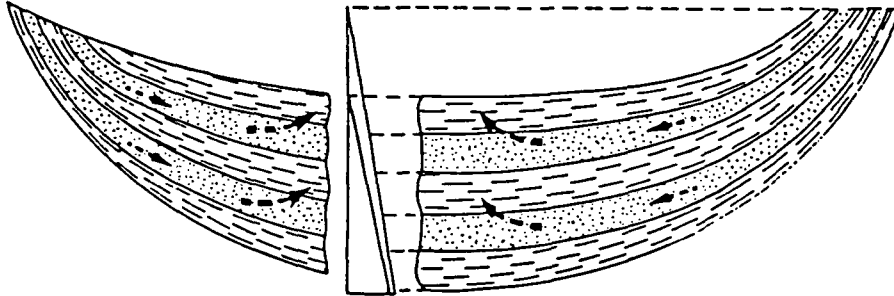
Permeability in a basin may be either intergranular or fracture controlled. Intergranular permeability is a product of such factors as original rock lithology (including as grain size, sorting, etc.), diagenesis (which is controlled by rock composition, water or contained fluid chemistry, pressure, time, and temperature), and amount of compaction. In most geothermal systems, intergranular permeability is of secondary importance. It is worth noting that, in geologic time, no rock is an aquiclude; all rocks can transmit some water. Sorey and others (1983) note the importance of including leaky beds surrounding a geothermal aquifer in calculating the amount of water that will be able to be produced.

Reduction of intergranular permeability may be important in some areas.

BASSIN JUVENILE OU CENTRIFUGE



BASSIN INTERMEDIAIRE OU CENTRIPETE



BASSIN SENILE : PRESSION HYDROSTATIQUE

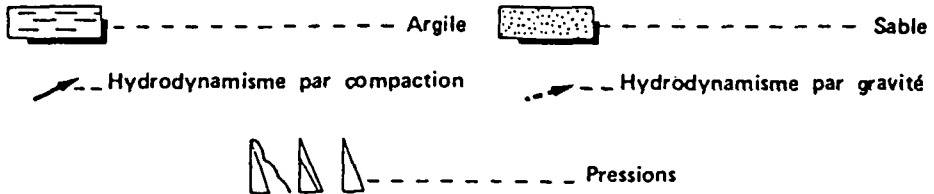
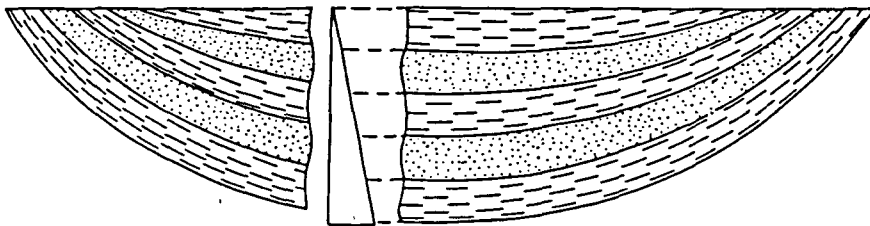
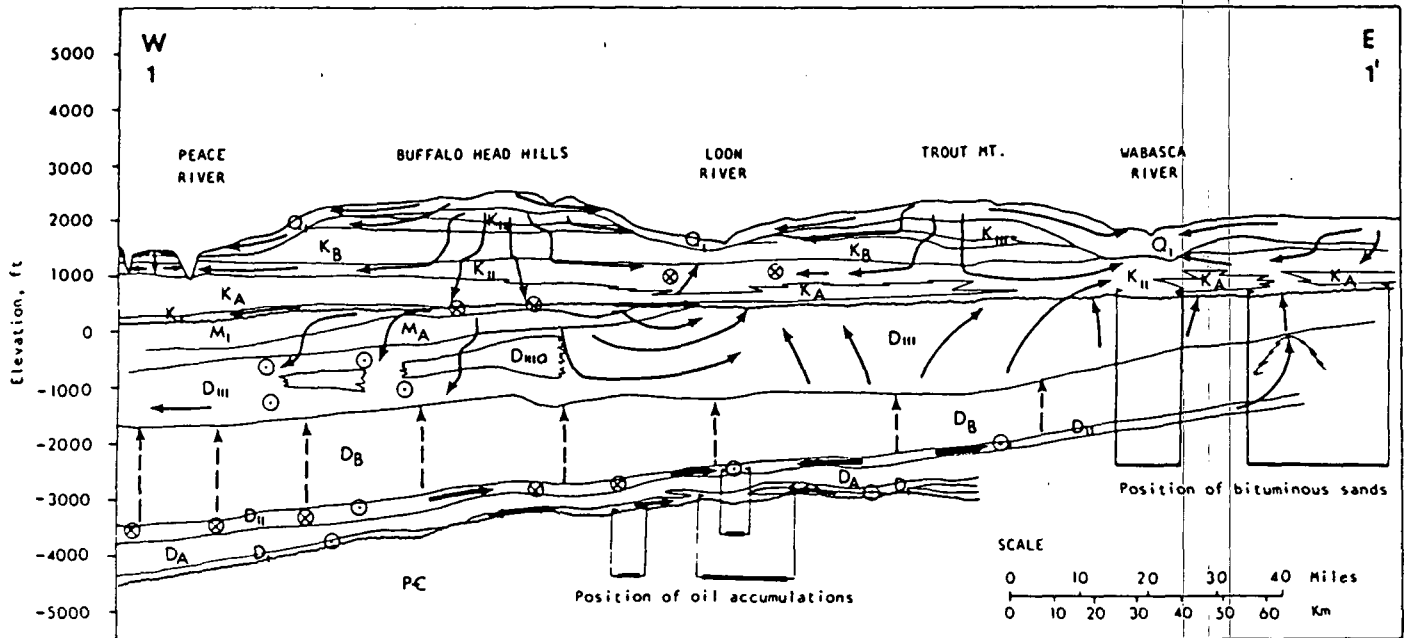


Figure 3.3.1 The three hydrodynamic types of basins (Coustau and others, 1975).



LEGEND

Direction of fluid flow

Flow significant on time scale of

- Holocene
- - - Pliocene-Pleistocene
- Tertiary-Cenozoic

- Toward front of diagram
- ⊗ Toward back of diagram

Figure 3.3.2 Present and paleohydrologic flows, Alberta (Toth, 1980).

Diagenetic fronts can serve as barriers to fluid flow. These barriers in some circumstances could trap thermal waters.

Fracture permeability is dominant in most geothermal systems. It may be either stratigraphically confined or throughgoing, and may range in dimension from less than one millimeter to major caves where limestones have been dissolved. In order for a major geothermal system to exist, however, both horizontal and vertical permeability along fractures are required.

Throughgoing fractures often have a tectonic origin. These may be faults, which do not have to be seismically active to impact hydrologic movement. Faults may serve as either permeability channels, where they are open (Price, 1976; Smith, 1965) or permeability barriers, where they are closed (Eremenko and Michalov, 1974). Either of these processes can redirect local or regional fluid flow. Abbott (1977) points out that extensive caverns have been dissolved along faults in Cretaceous limestones of Texas, but where these faults juxtapose rocks with different permeabilities, they may serve as barriers to flow (Maclay and Small, 1983).

Although seismically active (a Richter 7.3 earthquake occurred in 1983), the northern Rocky Mountains of Idaho do not have many geothermal systems; one contributing factor may be the disruption of recharge paths by thrusts (Foley and Street, in prep.). This hypothesis is similar to that postulated for the Canadian Rocky Mountains by Schwartz and others (1981).

Joints can also be important permeability channels. This may particularly be true in areas where tectonically inherited joint regimes intersect important cross-cutting geologic structures. An example of this would be an area where an inherited joint trend is oblique to and intersects a regional physiographic boundary (Foley and Street, 1985).

Joint permeability may be stratigraphically controlled. This is

particularly true in basins where more brittle limestone or sandstone are associated with more ductile shales. Fracture permeability dominates in the water- and petroleum-producing Madison Limestone of North Dakota and Montana. Stratigraphically controlled fracture permeability is also important in the geothermal systems of the young sediments in the Imperial Valley of California.

Fracture permeability is dominant in igneous terrains. In volcanic areas, permeability along unit boundaries may be locally important, particularly where these boundaries are flow tops or breccias. In some basin margin areas, fractures within and surrounding igneous plugs can be important.

3.4 Thermal Regime

The temperature at any point in a basin is a result of thermal input minus thermal losses at that point. Thermal input may come from heat flow from the mantle, heat generation in older rocks and in the lower crust, volcanic activity, or exothermic chemical reactions. Thermal losses are largely the product of conduction through rocks or convection by circulating waters. The discussion below is based on the assumption that young volcanic activity is not present, as this is the case in most sedimentary basins.

Heat flow is defined as:

$$q = k \frac{dT}{dz}$$

q = heat flow

k = thermal conductivity of rocks

T = temperature

z = depth

Heat flow in a basin may have a wide range of values, due to changes in con-

ductivity of rocks, changes in thermal gradients, and changes in additional factors, such as topography and water flow, that may affect the measurement of components of the equation. Figure 3.4.1 presents typical ranges for thermal conductivity in several rock types.

A heat flow of $> 100 \text{ mW/m}^2$ implies that convection is taking place (H. Heasler, personal communication, 1985), as in the absence of volcanic activity, mantle heat flow and the heat generation properties of rocks are not sufficient to generate such numbers. Very large heat flows are generated by convection systems in young volcanic environments. Heat flows calculated on the basis of raw data need to be evaluated, and if required, corrections for topography (Blackwell and others, 1980) and appropriate other factors should be applied.

Conductivity of a rock in the field is dependent on the degree of anisotropy of the unit, the porosity of the unit (including the nature of the medium filling the pores) and the mineralogy of the unit. Some factors, such as porosity, are depth dependent as a result of compaction. The lowering porosity may increase the thermal conductivity of units with depth; this particularly must be kept in mind when evaluating thermal gradient data from immature basins. Conductivity can also change with temperature and pressure (Clark, 1966).

In a typical basin, a greater thickness of shale with a lower conductivity can serve as an insulating blanket to retain heat. This has been found in several areas, such as the Great Plains (Gosnold and Eversoll, 1981) and the Atlantic Coastal Plain (Costain and others, 1980) in the U.S. In areas without the insulating shales, such as carbonate-dominated basins, no thermal anomalies are found (Renner and Vaught, 1979).

Two sources of data are common in sedimentary basins. The first is

THERMAL CONDUCTIVITY OF VARIOUS ROCKS AND POREFLUIDS AT ROOM TEMPERATURE, i.e. UNDER NEAR SURFACE CONDITIONS

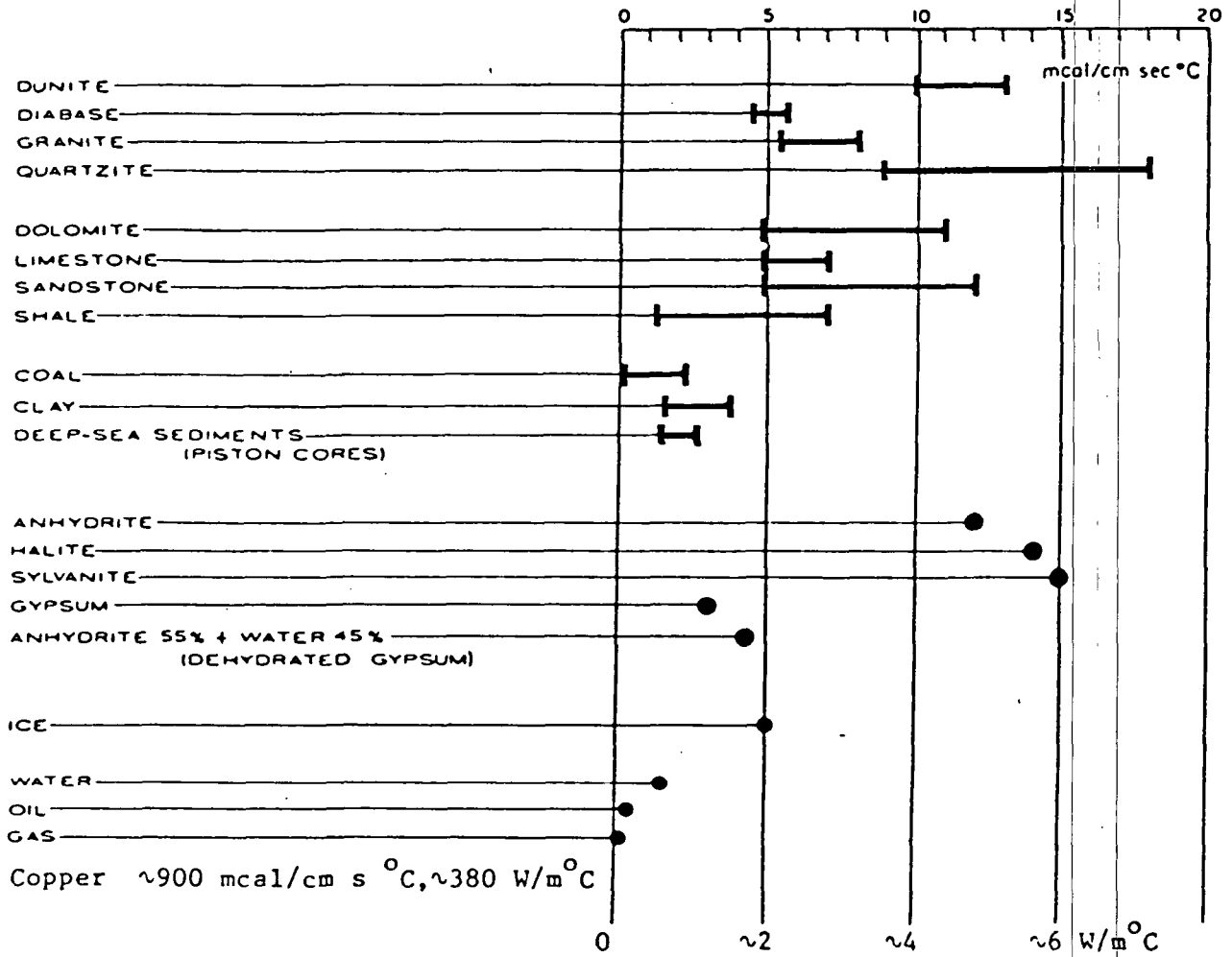


Figure 3.4.1

actual water temperature measurements. These are available from both springs and wells, and may or may not be instructive about thermal conditions at depth. If inaccurate thermometers or recording techniques are used, temperature data may be misleading.

The second major source is data from oil and gas wells. Bottom hole temperatures (BHTs) are routinely collected from the bottom of a well during geophysical logging. These are a commonly used tool in geothermal exploration of basins. Temperatures are also often recorded during the testing of production characteristics of a formation. These are known as drill stem tests (DSTs), and in some cases may be estimated rather than measured temperatures.

Bottom hole temperatures, although they may be the only source of data for an area, are notoriously unreliable as real formation temperatures. Some of the problems with these data include inaccurate thermometers, recording temperatures that are guessed rather than measured, and disruption of thermal conditions during drilling, by such processes as circulating mud or water that is not at formation temperature. BHTs may either be above or below the actual formation temperature. Many correction factors have been devised to cope with these problems (e.g. Oxburgh and others, 1972; Schoepel and Gilarranz, 1966; Cheung, 1978), but these are probably appropriate on scales no larger than the basin for which they were derived.

BHT data, despite these problems, can be very important in evaluating the deeper thermal conditions of basins. Thermal anomalies can be recognized by constructing maps depicting regional temperature gradient, temperatures recalculated to constant depth, or mapping temperatures and structures within one unit. Maps have also been constructed depicting temperature gradients to one lithology (Woodruff and others, 1984). It must be remembered, however,

that individual data points may be unreliable, and BHTs must be used in large data sets.

The source of heat in basins is the thermal flux of the earth. It is common to find, particularly on the margins of a basin, or in geologically complex interiors of basins, that thermal conditions change rapidly in relatively short distances. Most reports to date emphasize regional summations of thermal patterns (e.g. Roberts, 1981). Woodruff and Foley (in press) found, however, that in the highly faulted terrain of the Texas Gulf Coast, the "radius of influence" (Singer and Drew, 1976) of individual thermal data points is probably less than three kilometers. Heasler (1982) found a rapidly increasing temperature regime as the crest of an anticline is approached. This is a common phenomena (Roberts, 1981). These high-frequency perturbations to regional thermal regimes are the result of local water movements.

3.5 Conclusions

The hydrology of geothermal systems in basins has three major components in the flow path. The first is recharge to the system. This may be either meteoric or connate water, which can be moved to depth to be heated. Meteoric waters circulate downward through fractures, connate waters may be carried down with the subsiding sedimentary column. These waters are heated by either sweeping out heat from rocks as they circulate laterally through an area, or by circulating to depth and remaining long enough to be heated. Upward circulation, the third component, is either through fault or sedimentary units along the margins of geologic structures.

The driving force of geothermal systems in basins is pressure, although the thermal buoyancy of heated water may also contribute. The pressure may be generated from either regional topography (Hitchon, 1984) or from deeply

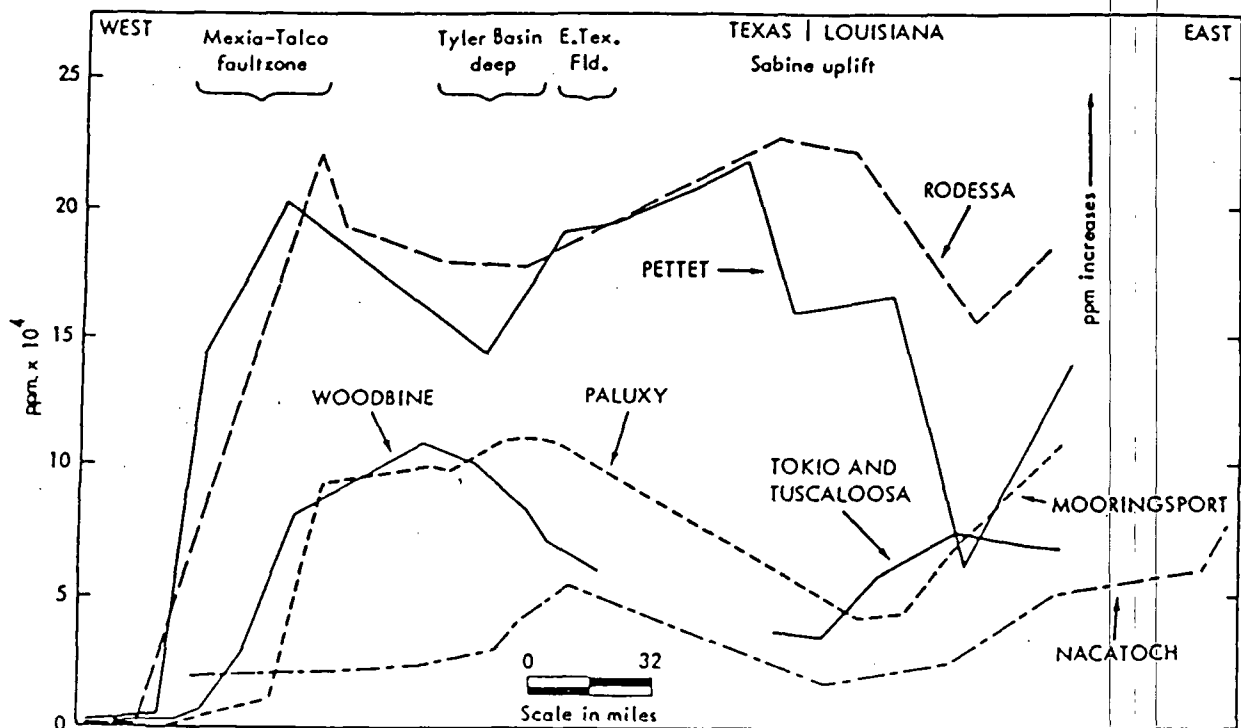
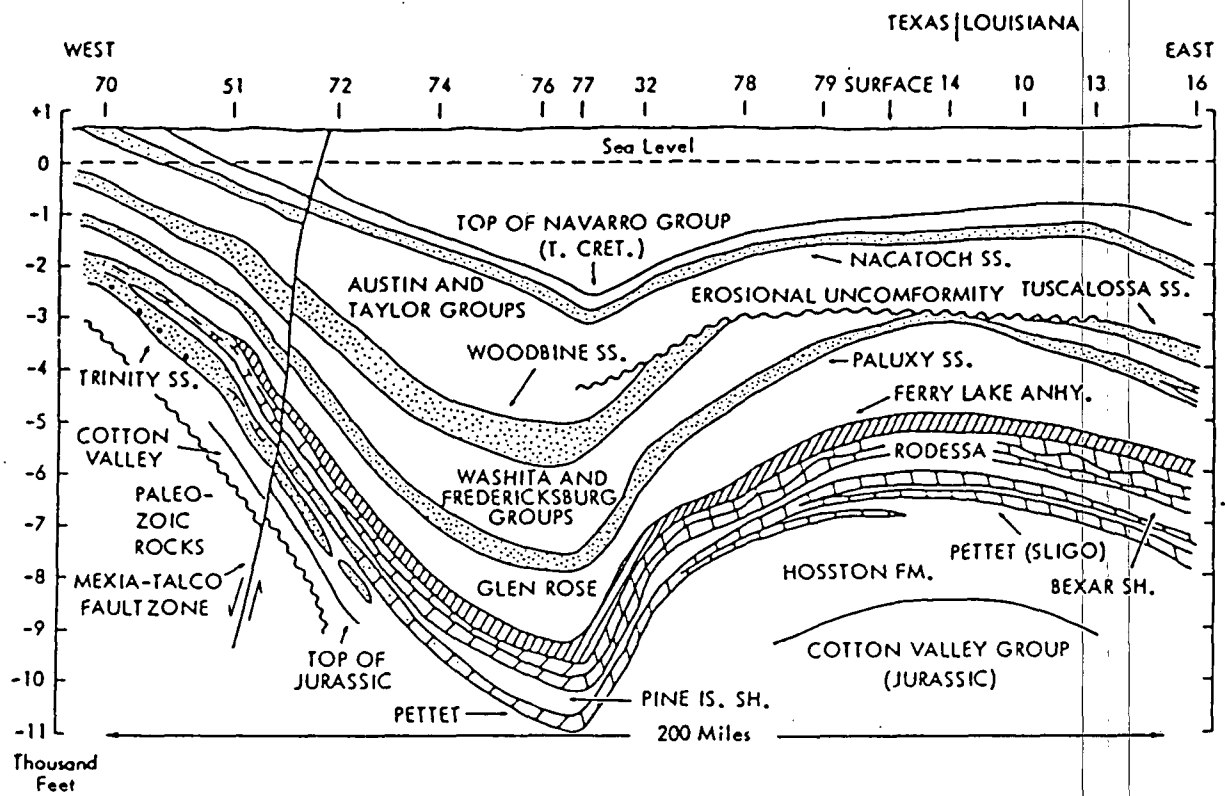


Figure 3.5.1 Geologic structures and salinities, east Texas (Parker, 1969).

TABLE 3.2.2

GULF COAST WATERS, TEXAS

Sample Type (all concentrations in mg/l unless noted)

<u>Element</u>	<u>Cold Recharge</u> ¹	<u>Mixing</u> ²	<u>Deep Brines</u> ³
Na	8.3	} 654	17.6 (g/l)
K	1.2		610
Ca	65	186	6.9 (g/l)
Mg	17	56	201
Fe	-	0.7	-
SiO ₂	12	28	-
B	-	1.7	-
Sr	1.3	-	615
HCO ₃	248	320	240
SO ₄	23	956	-
Cl	15	580	41.0 (g/l)
F	0.2	2.4	-
TDS	270	2620	-
depth (m)	520	-	4225
temperature (°C)	27.0	56	174

¹ Maclay and others (1980), well AY-68-36-908, limestone² Lang (1953), sandstone³ Land and Prezbirdowski (1981), J. A. Leppard No. 1 well

buried overpressurized zones.

Hydrologic, geochemical, structural, and thermal data can each be interpreted to provide information about geothermal resources in a basin, and about the other data sets. For instance, Parker (1969) depicts the relationship of geologic structure to salinity in east Texas (Figure 3.5.1 in this report). High salinity areas in this figure are related to fault zones or anticlines, and are also the areas where higher temperatures are encountered in the fluids. Upwelling fluids generate thermal highs, which can be complex in pattern, particularly where flow from deep basins is disrupted by faults.

Overall fluid flow patterns and chemical water types in sedimentary environments are summarized in Figure 3.5.2. This depiction is based on an analyses of the consolidated rocks in Alberta (Toth, 1980), where regional topography dominates hydrologic drive.

Geologic basins with greater complexity (i.e. several generations of tectonism, etc.) or long regional hydrologic flow patterns are favorable for the development of geothermal systems.

3.6 References

- Abbott, P. L., 1977, Effect of Balcones faults on groundwater movement, south central Texas: Texas Journal of Science, v. 29, p. 5-14.
- Blackwell, D. D., Steele, J. L., and Brott, C. A., 1980, The terrain effect on terrestrial heat flow: Journal of Geophysical Research, v. 85, p. 4757-4772.
- Carpenter, A. B., 1978, Origin and chemical evolution of brines in sedimentary basins: Oklahoma Geological Survey Circular 79, p. 60-77.
- Carpenter, A. B., 1985, Origin of Na-Ca-Cl brines in Jurassic and Cretaceous reservoirs of Gulf Coast (abs.): American Association of Petroleum Geologists Bulletin, v. 69, p. 242.
- Cheung, P. K., 1978, The geothermal gradient in sedimentary rocks in Oklahoma: unpub. M.Sc. thesis, Oklahoma State University, 55 p.
- Chilingarian, G. V., and Rieke, H. H. III, 1969, Some chemical alterations of subsurface waters during diagenesis: Chemical Geology, v. 4, p. 235-252.

- Clark, S. P., Jr., 1966, Thermal conductivity, in Clark, S. P., Jr., ed., Handbook of Physical Constants: Geological Society America, Memoir 97, p. 459-482.
- Clayton, R. N., Friedman, I., Graf, D. L., Mayeda, T. K., Meents, W. F., and Shimp, N. F., 1966, The origin of saline formation waters, 1. Isotopic composition: Journal of Geophysical Research, v. 71, p. 3869-3882.
- Collins, A. G., 1975, Geochemistry of Oilfield Waters: Elsevier Pub. Co., New York, 496 p.
- Costain, J. K., Glover, L. III, and Sinha, A. K., 1980, Low-temperature geothermal resources in the eastern United States: EOS, v. 61, p. 1-3.
- Coustau, H., 1977, Formation waters and hydrodynamics: Journal of Geochemical Exploration, v. 7, p. 213-241.
- Coustau, H., Rumeau, J. L., Sourisse, C., Chiarelli, A., and Tison, J., 1975, Classification hydrodynamique des bassins sedimentaires utilisation combinee avec d'autres methodes pour rationaliser l'exploration dans des bassins non-productifs: Ninth World Petroleum Congress Proceedings, v. 2, p. 105-119.
- Eremenko, N. A., and Michailov, I. M., 1974, Hydrodynamic pools at faults: Bulletin of Canadian Petroleum Geology, v. 22, p. 106-118.
- Foley, D., and Street, L. V., 1985, Geothermal systems of the Snake River Plain, Idaho Batholith and northern Rocky Mountains transition zone (abs.): Geological Society of America, Abstracts with Programs, v. 17, p. 218-219.
- Gosnold, W. D., and Eversoll, D. A., 1981, Usefulness of heat flow data in regional assessment of low-temperature geothermal resources with special reference to Nebraska: Geothermal Resources Council, Transactions, v. 5, p. 79-82.
- Gretener, P. E., 1981, Geothermics: Using temperature in hydrocarbon exploration: American Association of Petroleum Geologists, Continuing Education Course Notes, 156 p.
- Heasler, H. P., 1982, The Cody hydrothermal system, in Reid, S. G., and D. J. Foote, eds., Geology of Yellowstone Park Area: Wyoming Geological Association 33rd Annual Field Conference Guidebook, p. 163-174.
- Hitchon, B., 1984, Geothermal gradients, hydrodynamics and hydrocarbon occurrences, Alberta, Canada: American Association of Petroleum Geologists Bulletin, v. 68, p. 713-743.
- Hitchon, B., and Friedman, I., 1969, Geochemistry and origin of formation waters in the western Canada sedimentary basin - I. Stable isotopes of hydrogen and oxygen: Geochimica et Cosmochimica Acta, v. 33, p. 1321-1349.

- Hitchon, B., Billings, G. K., and Klovau, J. E., 1971, Geochemistry and origin of formation waters in the western Canada sedimentary basin - III. Factors controlling chemical composition: *Geochimica et Cosmochimica Acta*, v. 35, p. 567-598.
- Kingston, D. R., Dishroon, C. P., and Williams, P. A., 1983, Global basin classification system: *American Association of Petroleum Geologists Bulletin*, v. 67, p. 2175-2193.
- Land, L. S., and Prezbindowski, D. R., 1981, The origin and evolution of saline formation water, lower Cretaceous carbonates, south-central Texas: *Journal of Hydrology*, v. 54, p. 51-74.
- Land, L. S., and Prezbindowski, D. R., 1985, Chemical constraints and origins of four groups of Gulf Coast reservoir fluids: discussion: *American Association of Petroleum Geologists Bulletin*, v. 69, p. 119-121.
- Lang, J. W., 1953, Groundwater in the Trinity Group in the San Antonio area, Texas: U.S. Geological Survey Open-File Report, Austin, Texas, 5 p.
- Maclay, R. W., and Small, T. A., 1983, Hydrostatigraphic subdivisions and fault barriers of the Edwards aquifer, south-central Texas, U.S.A.: *Journal of Hydrology*, v. 61, p. 127-146.
- Maclay, R. W., Rettman, P. L., and Small, T. A., 1980, Hydrochemical data for the Edwards Aquifer in the San Antonio area, Texas: Texas Department of Water Resources, LP-131, 37 p.
- Manheim, F. T., and Bischoff, J. L., 1969, Geochemistry of pore waters from Shell Oil Company holes on the continental slope of the northern Gulf of Mexico: *Chemical Geology*, v. 4, p. 63-82.
- Ottlik, P., Galfi, J., Horvath, F., Korim, K., and Stegena, L., 1981, The low enthalpy geothermal resource of the Pannonian Basin, Hungary, in L. Rybach and L. J. P. Muffler, eds., *Geothermal Systems: Principles and Case Histories*: John Wiley & Sons, New York, p. 221-245.
- Oxburgh, E. R., Richardson, S. W., Turcotte, D. L., and Hsui, A., 1972, Equilibrium borehole temperatures from observation of thermal transients during drilling: *Earth and Planetary Science Letters*, v. 14, p. 47-49.
- Parker, J. W., 1969, Water history of Cretaceous aquifers, East Texas Basin: *Chemical Geology*, v. 4, p. 111-133.
- Price, L. C., 1976, Aqueous solubility of petroleum as applied to its origin and primary migration: *American Association of Petroleum Geologists Bulletin*, v. 60, p. 213-244.
- Reed, M. J., ed., 1983, Assessment of low-temperature geothermal resources of the United States - 1982: U.S. Geological Survey Circular 892, 73 p.
- Renner, J. L., and Vaught, T. L., 1979, Geothermal resources of the eastern United States: *Gruy Federal, Inc. Rept. DOE/NVO/1558-7*, 59 p.

- Rittenhouse, G., 1967, Bromine in oil-field waters and its use in determining possibilities of origin of these waters: American Association of Petroleum Geologists Bulletin, v. 51, p. 2430-2440.
- Roberts, W. H. III, 1981, Some uses of temperature data in petroleum exploration in Gottlieb, B. M., ed., Unconventional Methods in Exploration for Petroleum and Natural Gas II: Southern Methodist University, p. 8-49.
- Schoepfel, R. J., and Gilarranz, S., 1966, Use of well log temperatures to evaluate regional geothermal gradients: Journal of Petroleum Technology, v. 18, p. 667-673.
- Schwartz, F. W., Muehlebachs, K., and Chorley, D. W., 1981, Flow-system controls of the chemical evolution of groundwater: Journal of Hydrology, v. 54, p. 225-243.
- Singer, D. A., and Drew, L. J., 1976, The area of influence of an exploratory hole: Economic Geology, v. 71, p. 642-647.
- Smith, D. A., 1965, Sealing and non-sealing faults (abs.): Bulletin of American Association of Petroleum Geologists, v. 49, p. 1749.
- Sorey, M. L., Nathenson, M., and Smith, C., 1983, Methods for assessing low-temperature geothermal resources, in Reed, M. J., ed., Assessment of low-temperature geothermal resources of the United States - 1982: U.S. Geological Survey Circular 892, p. 17-30.
- Stoessell, R. K., and Moore, C. H., 1983, Chemical constraints and origins of four groups of Gulf Coast reservoir fluids: American Association of Petroleum Geologists Bulletin, v. 67, p. 896-906.
- Stoessell, R. K., and Moore, C. H., 1985, Chemical constraints and origins of four groups of Gulf Coast reservoir fluids: Reply: American Association of Petroleum Geologists Bulletin, v. 69, p. 122-126.
- Toth, J., 1980, Cross-formational gravity-flow of groundwater: a mechanism of the transport and accumulation of petroleum (the generalized hydraulic theory of petroleum migration), in W. H. Roberts III, and R. J. Cordell, eds., Problems of Petroleum Migration: American Association of Petroleum Geologists, Studies in Geology, no. 10, p. 121-167.
- White, D. E., 1957, Magmatic, connate and metamorphic waters: Geological Society of America Bulletin, v. 68, p. 1659-1682.
- Woodruff, C. M., and Foley, D., in press, Thermal regimes of the Balcones/Ouachita trend, central Texas: Gulf Coast Associated Geological Societies.
- Woodruff, C. M., Gever, C., and Wuerch, D. R., 1984, Geothermal gradient map of Texas (and generalized tectonic features): Texas Bureau of Economic Geology, map.

Zak, I., and Gat, J. R., 1975, Saline waters and residual brines in the Shiraz-Sarvistan Basin, Iran: Chemical Geology, v. 16, p. 179-188.

CHAPTER 4

CHEMICAL CHARACTERISTICS OF GEOTHERMAL FLUIDS

4.1 CLASSIFICATION OF FLUIDS

The composition of fluids that flow underground records their history in terms of time, temperature, and rock associations. Many systems have been devised to combine fluid compositional data into a visually simple but meaningful diagram. These diagrams range from bar graphs and divided circles to complex angular patterns. An excellent review of these methods has been given by Hem (1970).

The method we prefer is the trilinear, or Piper plot. This method was presented by Piper (1944), and is based on the relative amounts of Na+K, Mg, Ca, Cl+F, SO₄, and HCO₃+CO₃ in the fluid. These components are the major ions in cold and thermal fluids, and are thus used to discern gradation between geothermal and meteoric fluids flowing from springs and wells.

CALCULATION OF PIPER PLOT COORDINATES

To calculate a Piper plot, the units of concentration must first be transformed from ppm to milli-equivalents. This is accomplished by the equation

$$C_i(\text{meq}) = \frac{C_i(\text{ppm})}{M_i} \cdot (z_i), \quad (4.1.1)$$

where: $C_i(\text{meq})$ = concentration of component i in milliequivalents,

$C_i(\text{ppm})$ = concentration of component i in ppm,

M_i = molecular weight of component i ,

z_i = ionic charge of component i ,

i = Na, K, Ca, Mg, CO₃, HCO₃, SO₄, Cl, or F.

The molecular weights and ionic charges of these components are listed in Table 4.1.1.

The second step is to calculate cation and anion percentages by the use of the cation equation

$$C_j\% = \frac{C_i(\text{meq})}{(\text{Na} + \text{K} + \text{Ca} + \text{Mg})\text{meq}} \times 100, \quad (4.1.2)$$

and the anion equation

$$C_k\% = \frac{C_i(\text{meq})}{(\text{Cl} + \text{F} + \text{HCO}_3 + \text{CO}_3 + \text{SO}_4)\text{meq}} \times 100. \quad (4.1.3)$$

where: $C_j\%$ = percent j of total cations,

$C_k\%$ = percent k of total anions,

j = Na+K, Ca, or Mg, and

k = Cl+F, $\text{HCO}_3 + \text{CO}_3$, or SO_4 .

These percentages are then plotted on the diagram shown in Figure 4.1.1.

EXAMPLE OF CALCULATIONS

A typical water analysis would be reported and calculated as follows:

	<u>Reported</u> ppm	meq	<u>Calculated</u> % cations	% anions
Na	2390	103.99	85.	
K	98.1	2.51		
Ca	223	11.13	9.	
Mg	90	7.41	6.	
HCO_3	1270	20.82		14.
SO_4	2370	49.38		35.
Cl	2640	74.46		51.
F	.3	.02		

The meq column is derived by applying equation (4.1.1) to the reported data. For example,

$$\text{Na}(\text{meq}) = \frac{2390 \text{ ppm}}{22.99 \text{ mol}} \times 1 (\text{charge unit}) = 104 \text{ meq.}$$

TABLE 4.1.1

	<u>Molecular Weight</u>	<u>Charge</u>
Na	22.99	+1
K	39.10	+1
Ca	40.08	+2
Mg	24.31	+2
Cl	35.45	-1
F	19.00	-1
HCO ₃	61.02	-1
CO ₃	60.01	-2
SO ₄	96.06	-2

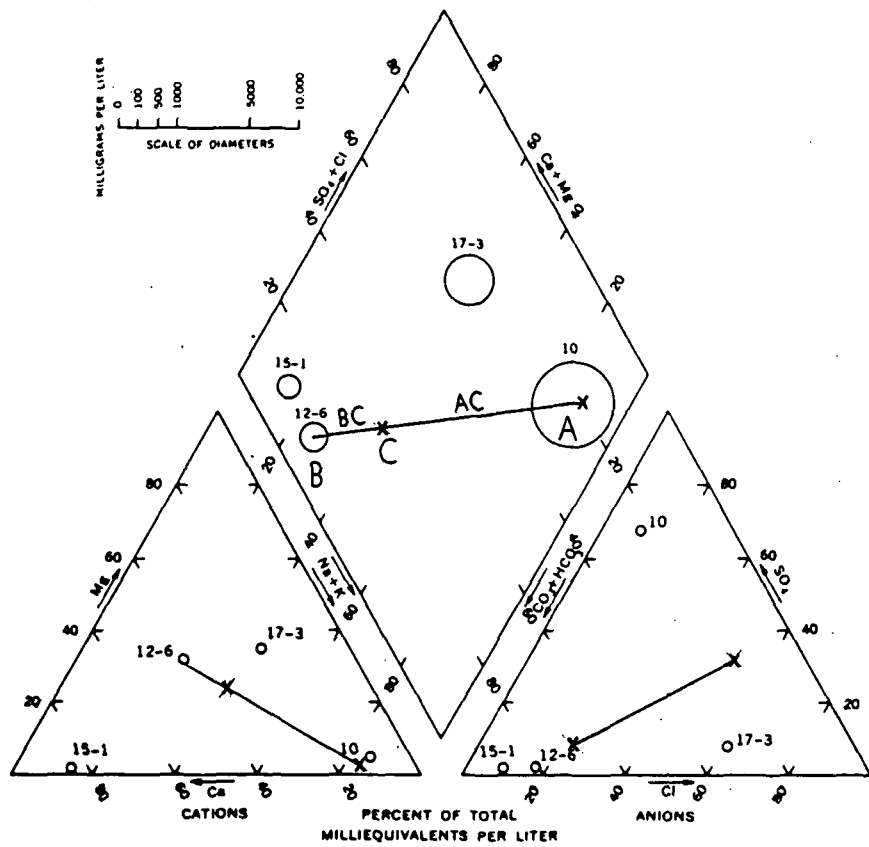


Figure 4.1.1

The % columns are calculated using equations (4.1.2) and (4.1.3). For Na+K and Cl+F:

$$(\text{Na+K})\% = \frac{103.99 \text{ meq} + 2.51 \text{ meq} \times 100}{103.99 \text{ meq} + 2.51 \text{ meq} + 11.13 \text{ meq} + 7.41 \text{ meq}} = 85\%$$

and

$$\text{Cl+F}\% = \frac{74.46 \text{ meq} + .02 \text{ meq}}{74.46 \text{ meq} + .02 \text{ meq} + 49.38 \text{ meq} + 20.82 \text{ meq}} = 51\%$$

The cation percentages are plotted on the lower left triangular and the anion percentages on the lower right, as shown in Figure 4.1.1. The cation and anion percentages are combined by projecting them into the central rhombohedron. The TDS content of the samples may be noted by varying the size of the sample point (not shown for sample calculation).

USE OF PIPER PLOTS

Piper plots can be used to characterize water types, and define the extent of mixing between waters. For example, a fluid is designated as a NaCl fluid when Na is > 50% of the cations, and Cl is > 50% of the anions. When no ion is greater than 50%, the two highest ions are hyphenated, such as Na HCO₃-SO₄. The fluid types have significance with respect to the processes that control the composition of the fluid. As shown in Figure 4.1.2, fluids that lie in the NaCl field are generally primary geothermal fluids. Fluids that lie in the Na HCO₃ or the Na HCO₃-SO₄ field are frequently meteoric fluids that have been heated and chemically enriched by gas and steam from an underlying geothermal fluid. Cool or warm meteoric waters are usually of the Ca HCO₃, Ca-Mg HCO₃, or mixed type. A good example of this application is given by Adams et al. (1985).

The second phase would be correlation of water types with spring

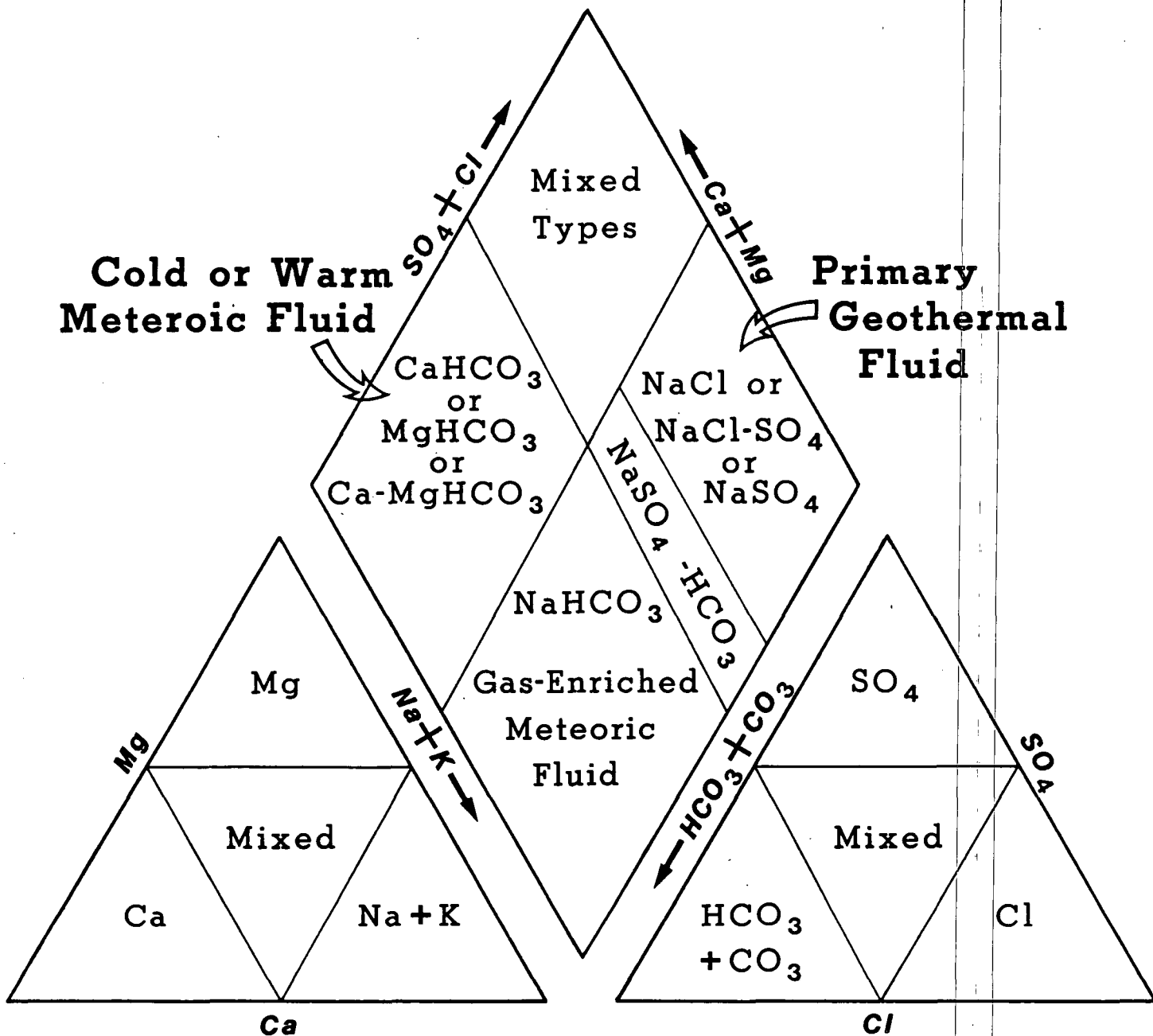


Figure 4.1.2

locations. This will aid in a combined hydrologic-geochemical interpretation by identifying the thermal-water recharge. An example of this technique is given in Struhsacker et al. (1983) and is shown in Figures 4.1.3 and 4.1.4.

The third phase would involve the determination of mixing. This is discussed in a later section.

4.2 COMPOSITIONAL VARIATIONS IN GEOTHERMAL FLUIDS

Most geothermal fluids begin the recharge-discharge cycle as meteoric water. Meteoric water is generally Ca HCO₃ to Mg HCO₃ in chemical character. Where shales and claystones are abundant meteoric water may also be Na HCO₃ to Na HCO₃-SO₄ in character. The concentrations of B and Li are low, while F is high, relative to geothermal water. As the fluid heats up and interacts with rock, several changes take place. Na, K, Li, B, SiO₂, and Cl increase, while Ca and Mg decrease. Changes in HCO₃ and SO₄ are variable. Some dissolved gases increase due to increased pressure and subsurface reactions. Increased temperature alters the ratio of Na to K. As the fluid circulates further and TDS contents rise above 5000 to 10,000 mg/l, the concentrations of Ca, SO₄, HCO₃ and F will increase above those of meteoric water, while Mg concentration will tend to decrease to below .5 mg/l.

Where a high-temperature NaCl reservoir exists at depth, several peripheral or overlying fluid types are possible. These are acid SO₄, Na HCO₃-SO₄, and mixed fluids. Examples of fluids of these compositions are given in Tables 4.2.1 and 4.2.2.

Solution of steam and gas into meteoric water is the driving force behind the creation of acid SO₄ waters. Some examples of the geologic configuration which have been shown to give acid SO₄ waters are shown on Figures 4.2.1 to 4.2.5. The steam is given off by a boiling NaCl fluid, and is rich in H₂S and

Table 4.2.1

EXAMPLES OF GEOTHERMAL WATER TYPES

TYPE	EXAMPLE	pH	Na	K	Ca	Mg	Fe	Cl	SO ₄	HCO ₃	SiO ₂	F	Mn	B	Li
SODIUM CHLORIDE	GEYSER - EL TATIO, CHILE	7.3	4340	520	272	.5	.1	7922	30	46	260	3.1	.4	178	45
ACID SULFATE	GEYSER - TOKAANU, N.Z.	2.8	43	11	27	3.5	8.2	32	347	0	280	—	—	2.5	—
ACID SULFATE-CHLORIDE	HOT SPRING - WAIOTAPU, N.Z.	2.8	405	74	40	7.5	5.0	612	666	0	370	—	—	10.1	—
	CRATER LAKE - RUAPEHA, N.Z.	1.2	740	79	1200	1030	900	9450	10950	0	852	260	34	13.8	1.6
BICARBONATE-SULFATE	WELL - (500 m) KAWAH KAMOJANG, INDONESIA	8.0	148	6.7	11.6	.1	.15	10	120	207	375	—	—	10	.35

GEOHERMAL WATER CLASSIFICATION

TYPE	ORIGIN	CHARACTER	OCCURRENCE
NEAR-NEUTRAL SODIUM CHLORIDE	REACTION OF HYDROTHERMAL FLUIDS WITH ROCKS	HIGH DISSOLVED SOLIDS GENERALLY 1,000 TO 30,000. ENRICHED IN: Na, K, Ca, Cl, SO ₄ , HCO ₃ , Si. DISSOLVED GASES: CO ₂ , H ₂ S, PREDOMINATE.	COMMON DEEP HIGH TEMP. RESERVOIR FLUID. WHERE THIS FLUID COMES TO SURFACE IT FORMS HOT SPRINGS.
ACID SULFATE	STEAM RISES FROM HIGH TEMP. WATER AND CONDENSES IN NEAR SURFACE OXIDIZING ENVIRONMENT	VERY DILUTE, ENRICHED IN SO ₄ FROM STEAM. OTHER ELEMENTS DERIVED FROM ACID LEACHING OF COUNTRY ROCK.	NEAR SURFACE, GENERALLY ABOVE THE WATER TABLE
ACID SULFATE- CHLORIDE	(1) MIXING OF SODIUM CHLORIDE AND ACID SULFATE WATERS (2) HIGH TEMP. VOLCANIC STEAM RICH IN F, Cl, AND S, RISES AND CONDENSES IN NEAR SURFACE (OXIDIZED) WATER	(1) COMPOSITION CAN VARY WIDELY (2) ENRICHED IN: Cl, SO ₄ , F	NEAR SURFACE
NEAR-NEUTRAL SODIUM BICARBONATE- SULFATE	VOLCANIC OR THERMAL STEAM RISES AND CONDENSES IN REDUCED GROUNDWATER	LOW DISSOLVED SOLIDS ENRICHED IN HCO ₃ , VARIABLE AMOUNTS OF SO ₄ .	ON PERIPHERY OR ABOVE THE HIGH TEMP. RESERVOIR

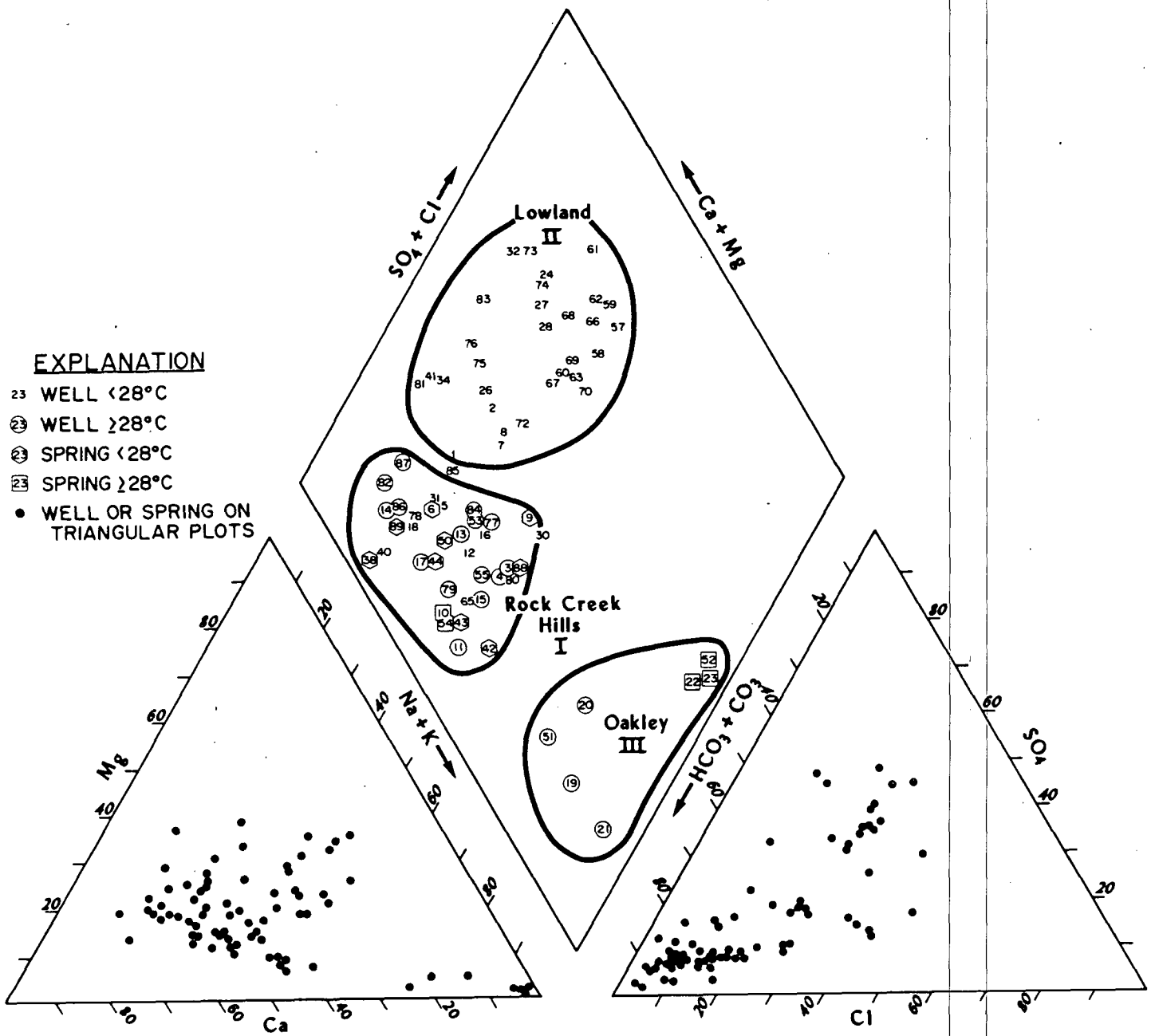


Figure 4.1.3

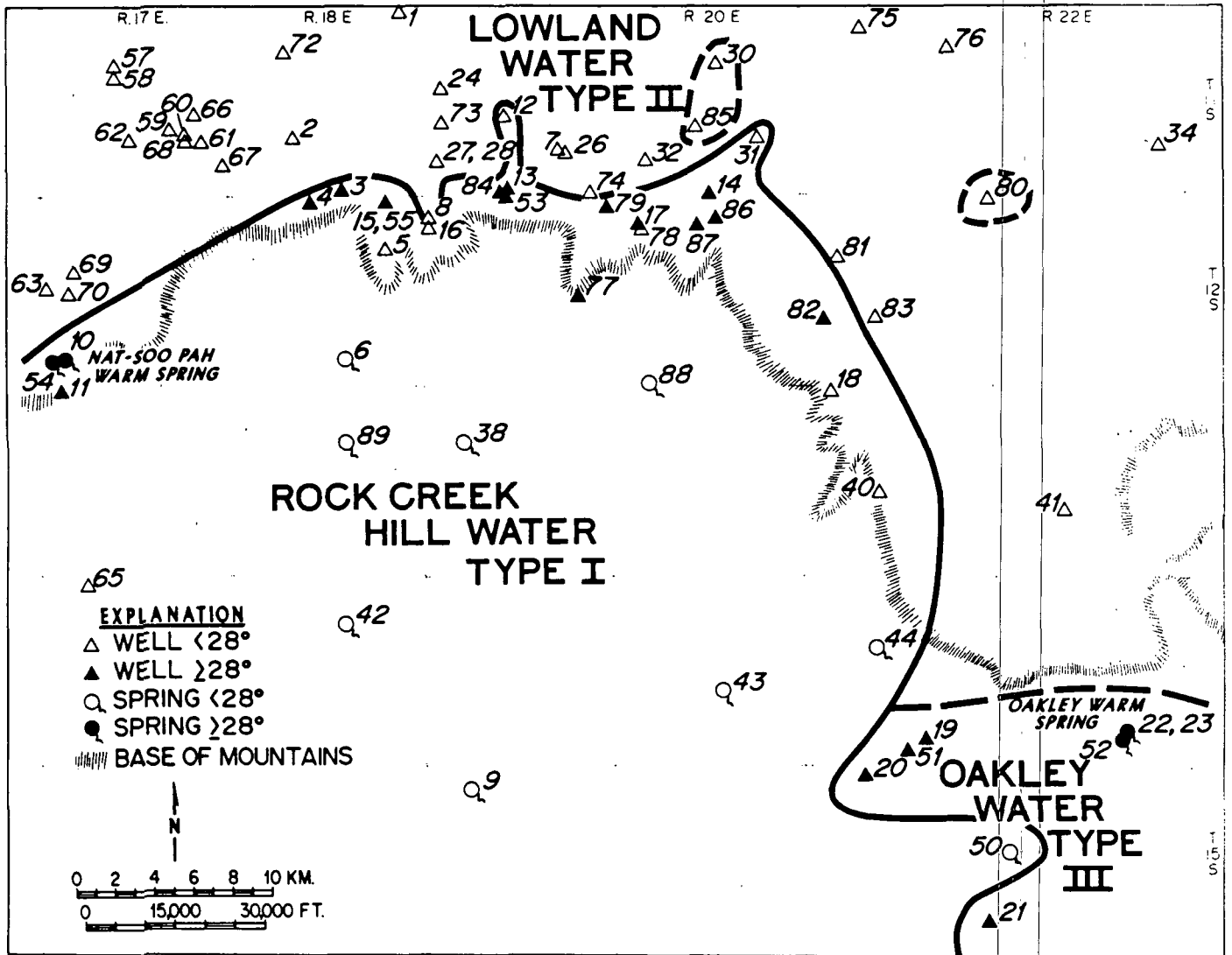


Figure 4.1.4

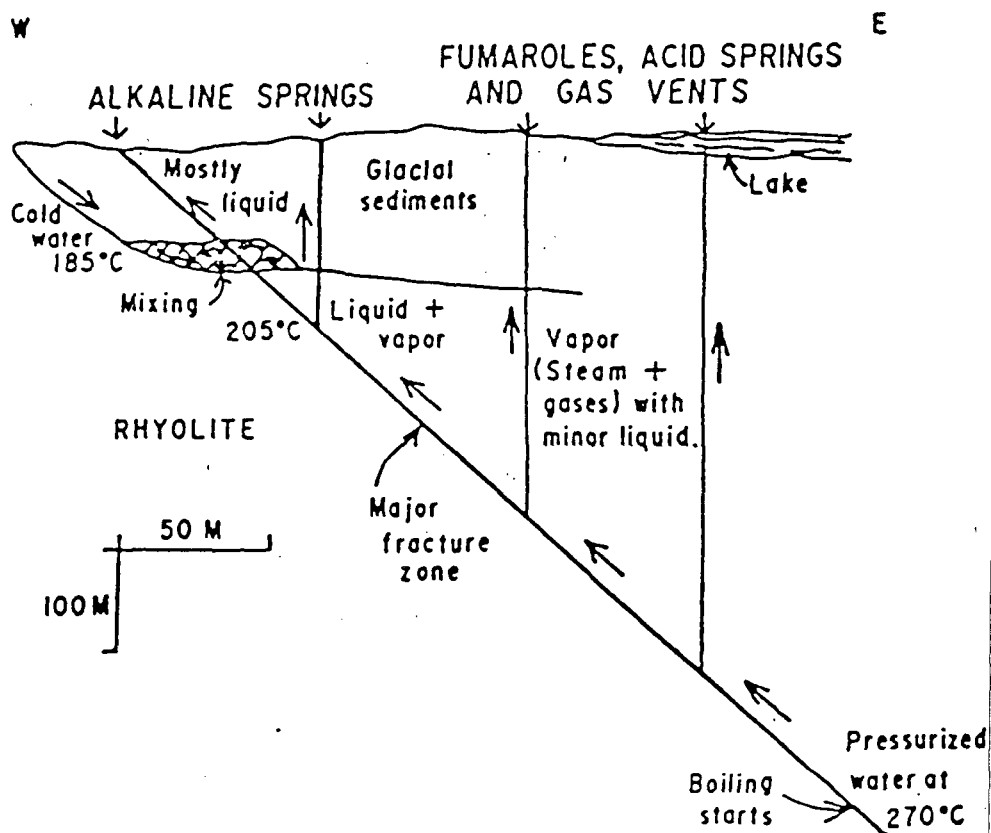


Figure 4.2.1
 from Truesdell and Thompson (1984)

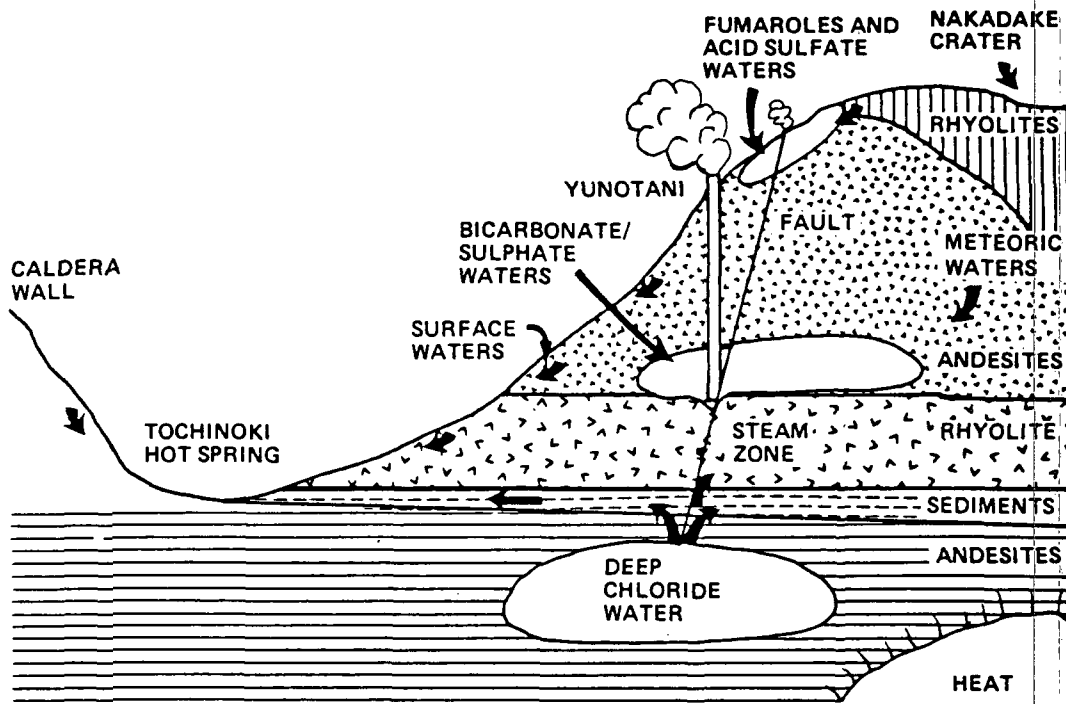
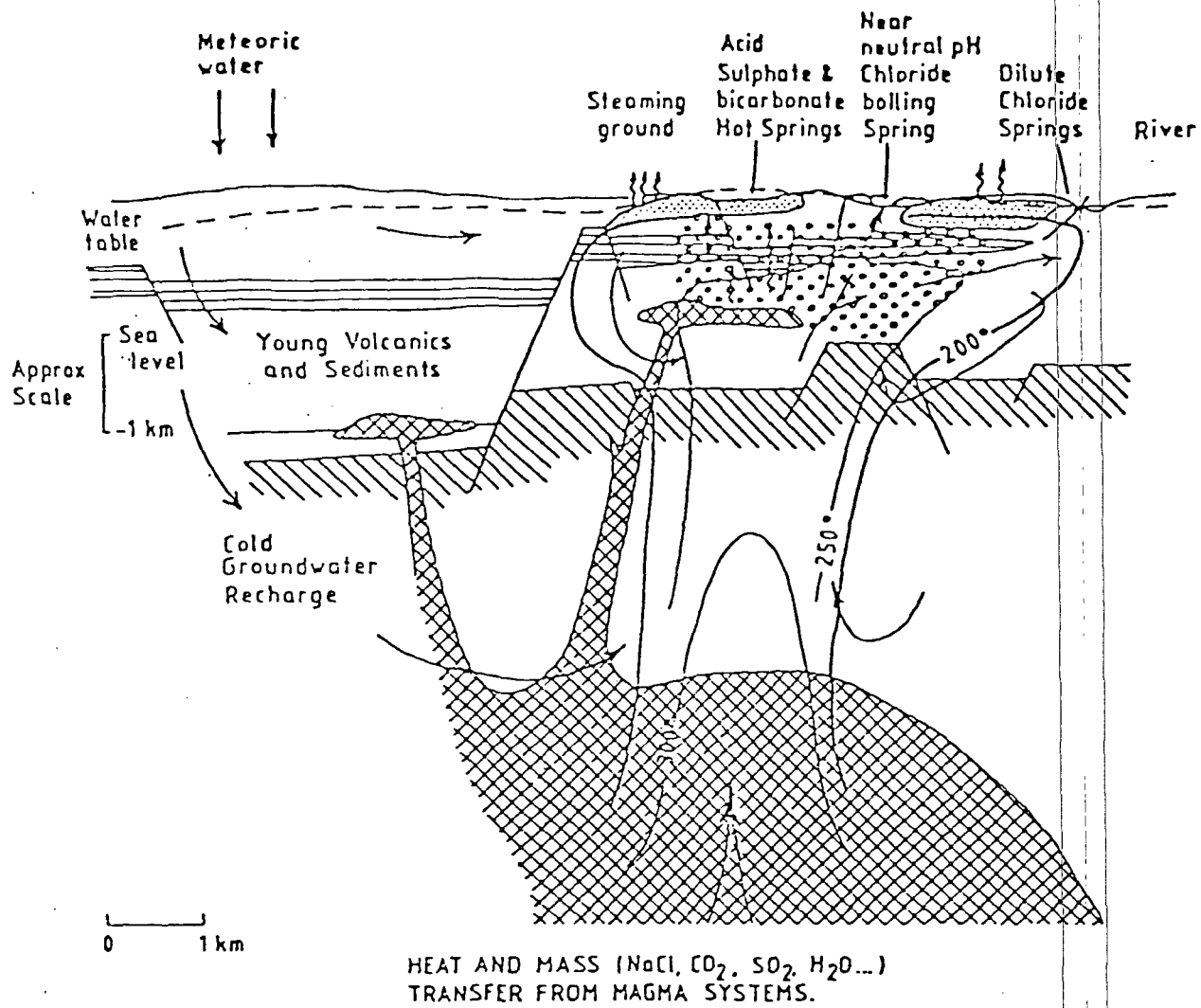


Figure 4.2.2 from Parmentier and Hagashi (1981)



KEY








	Pre-Volcanic Basement		Steam-heated Acid SO ₄ ²⁻ ± HCO ₃ ⁻ waters
	Intrusive Volcanics		SO ₄ ²⁻ -Cl ⁻ waters (fig 2)
	Low Permeability Stratum e.g. Mudstones		Near neutral Chloride waters (within 200° Isotherm approx.)
			Two Phase Region Water Liquid + Steam (+ Gas)

Figure 4.2.3
from Henly and Ellis (1982)

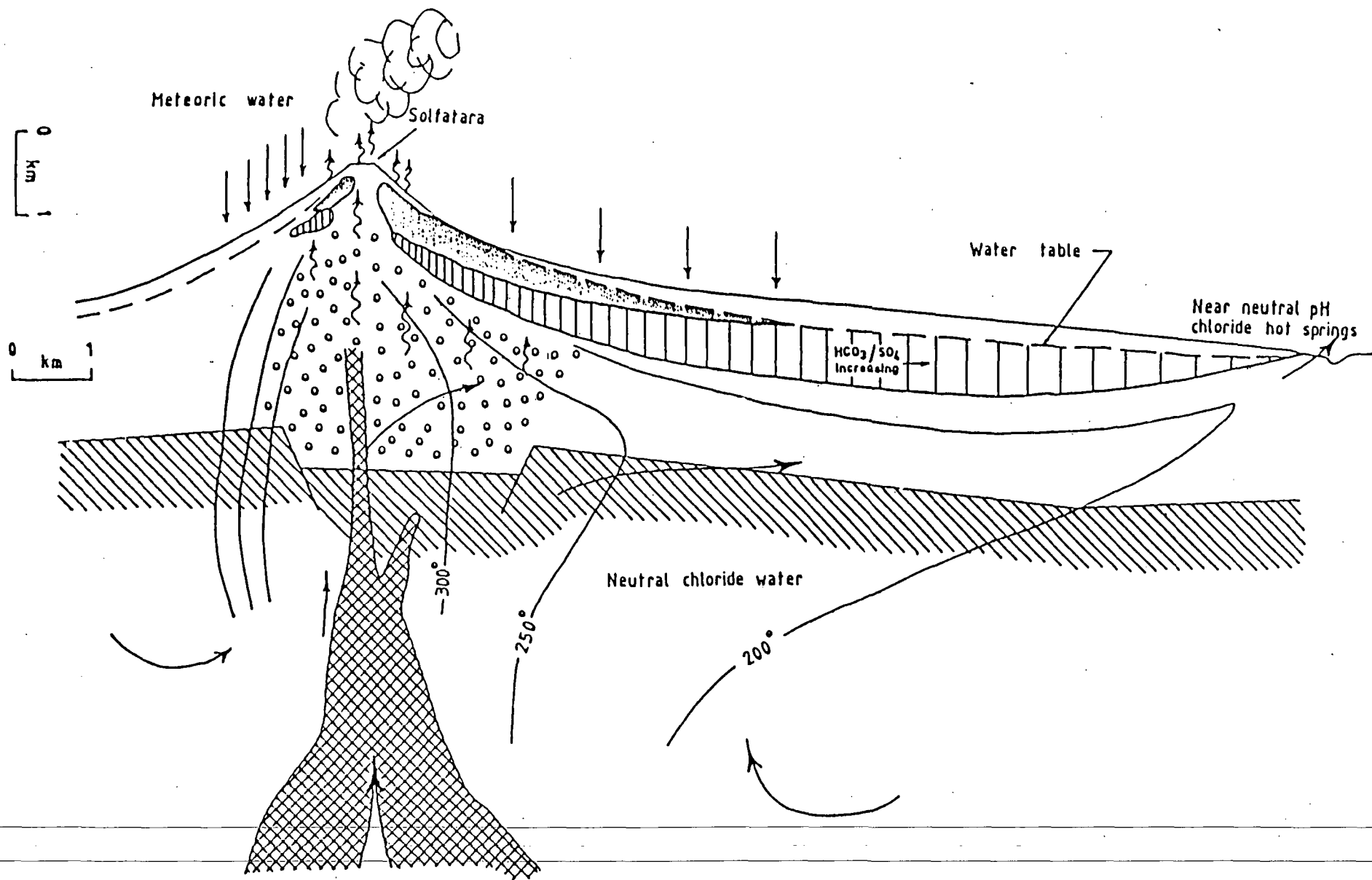
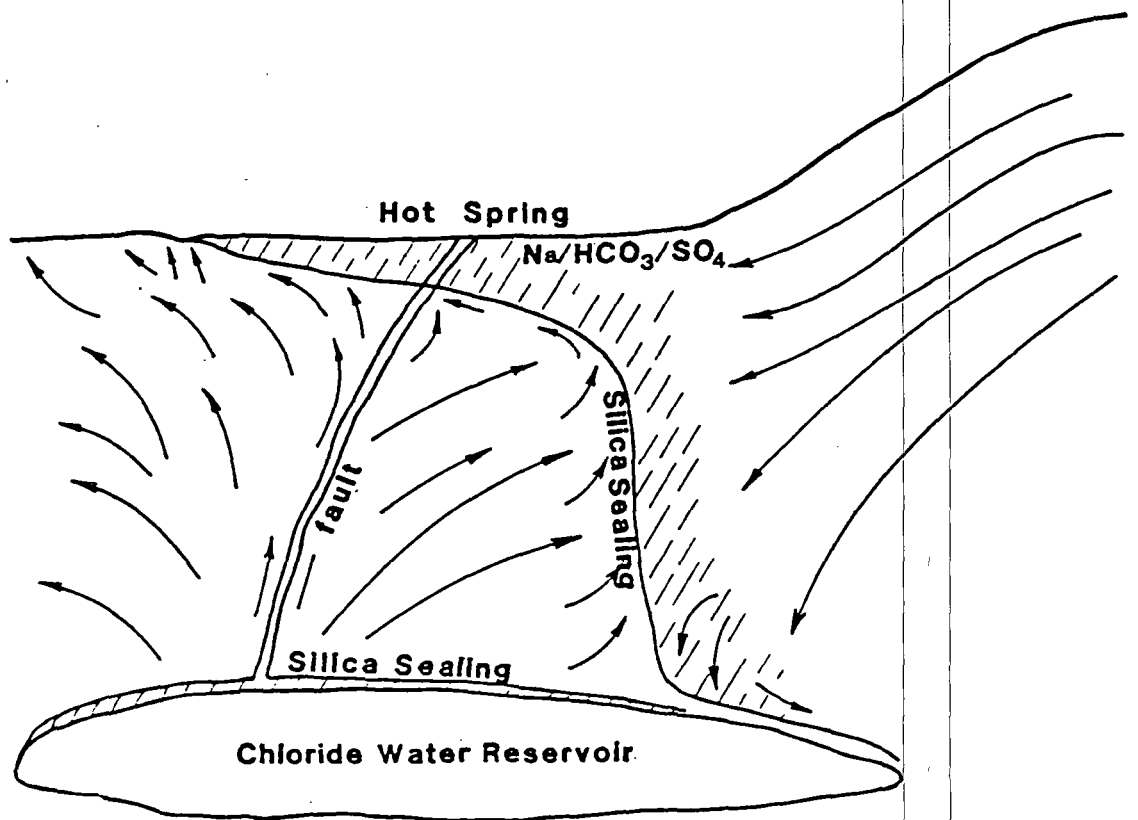
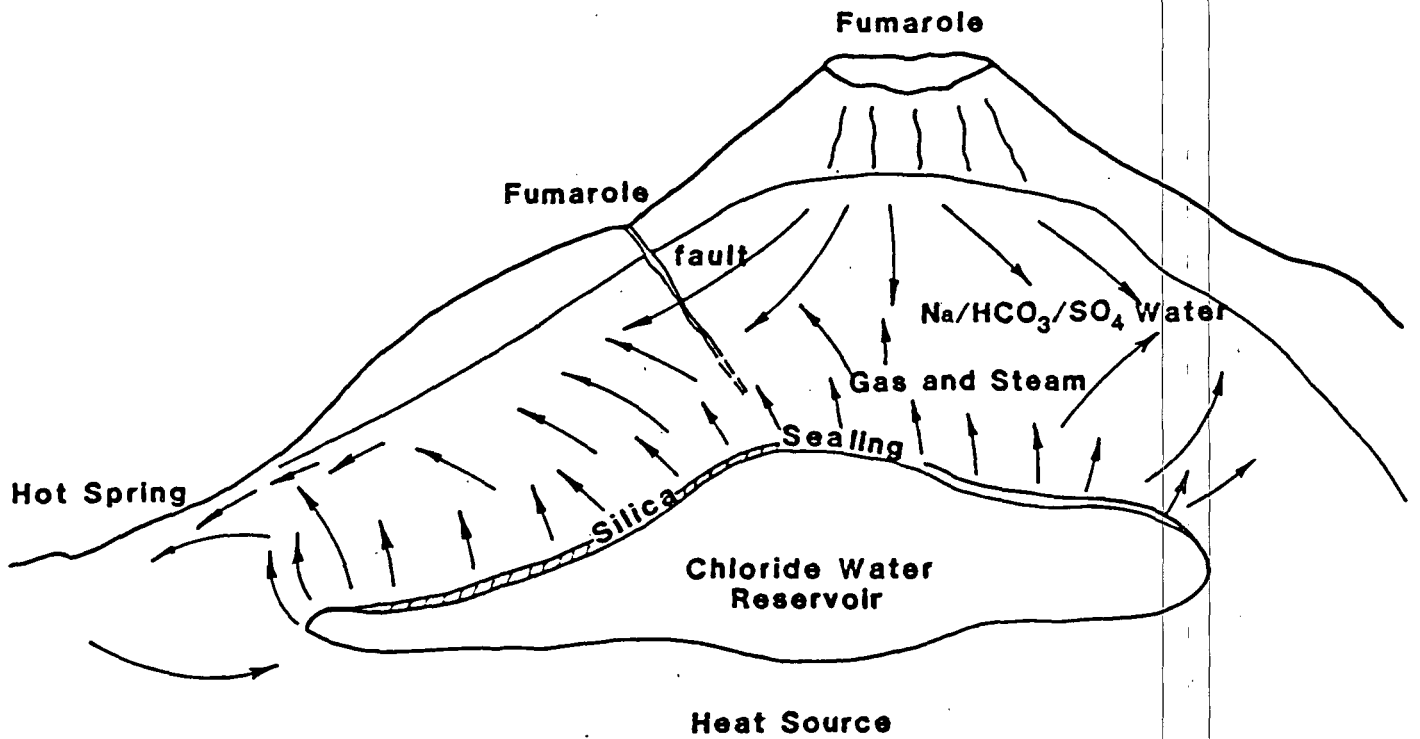


Figure 4.2.4
 from Henly and Ellis (1982)



(Mahon and others, 1980)

Figure 4.2.5

CO₂ gas. When these gases contact meteoric water they hydrate, ionize, and/or oxidize. These processes result in heated, acidic meteoric water. Compositions of these fluids will vary according to how much steam and gas have been added. Compositions will also vary according to how much the acid gases have reacted with rock.

As an acid SO₄ water reacts with rock, it will increase its concentrations of all ions. During the dissolution process the acidity of the fluid is neutralized. This results in a neutral pH (~ 7.0) fluid with a Na HCO₃-SO₄ character.

Mixed fluids result from hydrologic communication between the three thermal fluid types and meteoric waters. Methods of interpreting mixed fluid types are discussed below.

4.3 PROCESSES AFFECTING FLUID CHEMISTRY

Many physical processes can affect the composition of a geothermal fluid during its ascent between the deep fluid reservoir and hot springs at the surface. These include conductive heat loss, dilution with meteoric water, and boiling. The chemical effect of conductive cooling is generally negligible, which is the basis for many of the cation geothermometers currently in use. However, if the cooling path is long enough the Na/K/Ca ratios can adjust, and silica can be lost. These changes will seldom take place unless the fluid cools more than 100°C. Conductive cooling is indicated where hot springs with similar Cl contents display different temperatures.

Ascending hot water may mix with cold water either in the upper or marginal parts of hot-spring systems. The temperature of the resulting mixed water may be above or below the boiling temperature at atmospheric pressure, and complete or partial chemical reequilibration may or may not occur after

mixing. Chemical reequilibration is more likely if the temperature after mixing is greater than 100°C.

Some indications of mixing are as follows: (1) variations in chloride content of boiling springs too great to be explained by steam loss; (2) variations in the ratio of conservative elements, such as B/Cl; (3) variations in oxygen and hydrogen isotopes (especially tritium); (4) cool springs with large mass flow rates and much higher temperatures (greater than 50°C) indicated by chemical geothermometers; (5) systematic variations of spring compositions and measured temperatures. Generally, the cold water will be more dilute than the hotter water. However, in some situations the cold-water component could be more concentrated than the hot water, such as where ocean water or closed-basin saline lake water mixes with an ascending hot water. The above indications of mixing may be shown by different compositions of nearby springs or by seasonal variations in a single spring.

Although the presence of mixed waters make geochemical interpretation complex, techniques have been developed to deal with this situation (Fournier and Truesdell, 1974; Truesdell and Fournier, 1977; Fournier, 1977). The next section will illustrate some of these techniques.

Surface and subsurface boiling of thermal fluids also results in physical and chemical changes in the thermal fluids. Cooling of the boiling fluid is the most obvious change. In addition, concentration of the non-volatile chemical constituents will occur. The loss of CO₂ to the steam phase will result in an increase in pH generally from about 7.5 to 8.5 and a loss of Ca as a result of calcite deposition. The effects of boiling on mineral deposition are described more fully in Chapter 8. In moderate-temperature systems these effects are primarily surface phenomenae. In high-temperature systems the steam can be derived from subsurface boiling. This steam can also affect the

composition of meteoric water.

The acidification and subsequent neutralization of the steam-heated meteoric water will produce acid SO_4 and neutral $\text{NaHCO}_3\text{-SO}_4$ fluids, respectively. Where mixing of these fluids with themselves or NaCl fluid occurs, the pH and composition can vary to a large extent. Examples of the compositional variations among geothermal fluids within several systems are shown in Figures 4.2.1 to 4.2.5.

4.4 ROCK TYPE

The type of rock that the fluid flows through will also affect the fluid chemistry. This effect is generally most evident in the concentration of minor elements found in the thermal waters. For instance B/Cl ratios can vary according to rock type. The ratio B/Cl has been used in New Zealand (Mahon, 1970) to identify the host rocks of various geothermal fluids. However, these variations are minor compared to the variation between meteoric and geothermal B/Cl ratios. The B/Cl ratios can be used by an explorationist without regard to rock type in most terrains.

The presence of evaporites can have some effect on the salinity of the fluid but the ion ratios appear to be determined by temperature. For instance, the southern half of Starr Valley, Wyoming (Adams and Capuano, 1982) contains 1000 m of a halite-rich sandstone. Thermal fluids flow from the entire length of the graben; some thermal springs are located within .5 km of salt mines, and some are located in the volcanic-rock fill of northern Starr Valley. The cation geothermometer temperatures of these springs are all consistent with each other, ranging from $90^\circ\text{-}100^\circ\text{C}$. This indicates that the cation ratios are determined by temperature rather than halite contamination.

The influx of ions into meteoric water to create geothermal water is a

controversial subject. The following discussion is a review by A. J. Ellis in Barnes (1979).

Origin of Water and Solutes

"The origin of chemicals in natural thermal waters has been argued widely. The view that volcanic spring waters are entirely magmatic fluids is not in agreement with evidence from hydrogen and oxygen isotope ratio determinations (Craig, 1963; White, 1974), or from the compositions of dissolved inert gases. There is quantitative evidence that high-temperature thermal waters have predominantly a local meteoric water origin, but the methods of examination do not exclude the possibility of 5-10% of other water being present.

Facca and Tonani (1964) suggested that the carbon dioxide, hydrogen sulfide, hydrocarbons, and ammonia present in the Larderello steam could come from simple decomposition reactions in the hot sedimentary rocks. Ellis and Mahon (1964, 1967) showed by laboratory experiments that the typical elements in high-temperature natural waters could be derived from the simple reaction of volcanic rocks and water within a geothermal system. They demonstrated that the concentrations of major rock-forming elements such as Si, Na, K, Ca, Mg, Al, Fe, and Mn were controlled in solution by pressure- and temperature-dependent mineral/solution equilibria and that other constituents such as fluoride, carbonate, and sulfate were limited by the formation of sparingly soluble salts. Transfer of appreciable proportions of chloride, boron, ammonia, fluoride, and arsenic from the rocks occurred even before there was appreciable hydrothermal alteration, an important fact suggesting that these elements (and possibly others) were not held entirely within the crystal structures of the major rock minerals but concentrated in intercrystalline material.

Appreciable proportions of the Li, Rb, and Ce in the original rocks were released only after extensive alteration had occurred, which at the experimental times of 1-2 weeks required temperatures of 500-600°C. However, Chelishev (1967) showed that the distribution of rubidium and cesium between either mica or feldspar and water was increasingly in favor of the solution phase as temperatures were lowered from 600° to 250°C. An extended reaction period (2 years) at 210°C released 10 ppm lithium into solution from a Wairakei rhyolite breccia (R. B. Glover, personal communication), and parts per million concentrations of lithium resulted from the reaction of Iceland dolerite with 0.5 m NaCl solution at 300°C (Andrusenko and Moskalyuk, 1966).

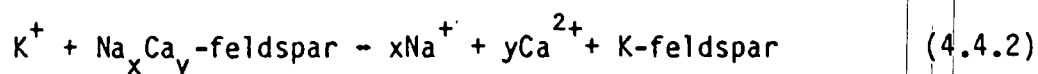
Further work by Mahon (1967) on the reaction of water with graywacke, shale, and mudstones at temperatures of 200-300°C produced solutions with chemical characteristics (e.g., Cl/B and Cl/NH₃ ratios and F concentrations), which were in line with those of hot waters found in these rock types. Similar experiments were reported by Kissen and Pakhomov (1967).

Specific Solutions and Mineral Reactions

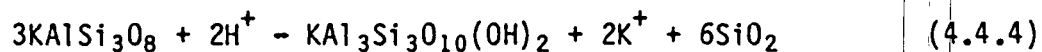
There are few elements in geothermal waters whose concentrations are not controlled by temperature- and pressure-dependent equilibria. The principal "soluble" elements with their chemistry dominated mainly by extraction and dilution processes are Cl, Br, I, B, Ce, and As. Some specific reactions are now reviewed. Unless noted, equilibrium data discussed below are for saturated water vapor pressures, since at the depths of observations in geothermal systems pressures do not greatly exceed these values.

Sodium and Potassium

Sodium is usually the dominant cation in high-temperature geothermal waters. A systematic variation in the ratio Na/K with temperature occurs in all but the acidic geothermal systems, and in many areas within a wide variety of rock types it has been possible to make a precise correlation between Na/K and water temperature (White, 1965; Ellis and Mahon, 1967; Ellis, 1970A; and Fournier and Truesdell, 1973).



Simple ion exchange may occur: K may react with a plagioclase feldspar to form potassium feldspar, and there may be direct precipitation of potassium feldspar.



From the equilibrium equations (4.4.1), (4.4.2) and (4.4.4), for the coexistence of albite, potassium mica, and potassium feldspar, at each temperature unique values of Na/K, K/H, and Na/H occur in high-temperature, low-calcium solutions. The hydrogen ion activity is related to the concentrations of the sodium and potassium ion but Na/K ratios are essentially independent of pH (Ellis, 1970a).

Lithium, Rubidium, and Cesium

The concentration of rare alkalis in geothermal waters reflects their abundance in the surrounding rocks, with waters in basaltic areas having low concentrations compared with those in rhyolitic and andesitic areas. Lithium and rubidium tend to decrease in concentration in waters

migrating to the surface due to incorporation of the ions in low-grade hydrothermal alteration products such as clays and zeolites. Hydrothermally formed lepidolite has been noted in shallow, altered rocks (Bargar et al., 1973). In individual areas the Na/Rb ratios follow trends in the Na/K ratios, but the differences in Na/Li ratios between deep and surface waters are less marked. The isotopic ratio $^6\text{Li}/^7\text{Li}$ tends to increase in hot waters migrating to the surface, presumably through the preferential inclusion of the isotope ^7Li in hydrothermal alteration minerals (H. J. Svec and Ellis, unpublished).

Calcium

Geothermal waters contain the ions of several sparingly soluble calcium salts, for example, CaCO_3 , CaSO_4 , CaF_2 . Most geothermal waters at deep levels are near saturation with calcite (Ellis, 1970a) and this mineral is frequently precipitated from the waters when they boil and lose carbon dioxide. The tendency to precipitate calcite in natural channelways and in drill pipes is particularly marked for waters containing high carbon dioxide concentrations.

The following equations express the relationship between carbon dioxide and calcium and hydrogen ion activities in the water, where K_{a1} is the first ionization constant of carbonic acid, and K_c is the equilibrium constant for the solution of calcite:



$$K_c = a_{\text{Ca}^{2+}} \cdot a_{\text{HCO}_3^-}^2 / K_{\text{CO}_2} \cdot a_{\text{CO}_2} \quad (4.4.6)$$

$$= a_{\text{Ca}^{2+}} \cdot a_{\text{CO}_2} \cdot K_{a1}^2 \cdot K_{a1}^2 \cdot K_{\text{CO}_2} / a_{\text{H}^+}^2 \quad (4.4.7)$$

In addition, for the coexistence of potassium and sodium feldspar and

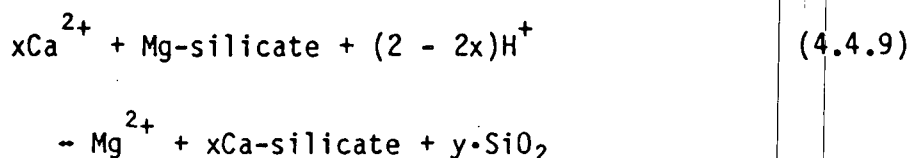
potassium mica (equations (4.4.1) and (4.4.4)) $a_{Na} / a_H = K_{fm}$. If geothermal waters are in equilibrium with calcite, potassium mica and sodium and potassium feldspars, then at a temperature the product $m_{Ca} \cdot m_{CO_2}$ should increase in proportion to m_{Na}^2 (or to m_{K_2}).

$$m_{Ca} \cdot m_{CO_2} = \frac{K_c \cdot m_{Na}^2 \cdot \gamma_{Na}^2}{K_{a_1}^2 \cdot K_{fm}^2 \cdot \gamma_{Ca}} \quad (4.4.8)$$

At constant carbon dioxide concentration, for a given temperature, calcium concentrations should vary approximately with the square of the sodium ion (or potassium ion) concentrations. Low salinity waters should have high Na/Ca ratios, and the converse for high salinity waters. For a given sodium ion concentration and temperature, waters with high carbon dioxide concentrations will tend to have low calcium concentrations.

Magnesium

In high-temperature geothermal waters of low salinity, magnesium concentrations are extremely low and frequently in the range 0.01-0.1 ppm. They appear to be controlled by the following type of reactions (Ellis, 1971):



The solutions are usually close to saturation with calcite, and common calcium silicates are montmorillonite, wairakite, or epidote. Chlorite is a common secondary magnesium-containing mineral.

For New Zealand geothermal fields with water temperatures in the range 235-255°C, with sodium concentrations of 0.02-0.04 m, and with P_{CO_2} ranging 1-30 bars, Ellis (1971) showed that value of $\log a_{Mg} / a_H^2$ for the deep solutions averaged 6.2 and showed no major trend with P_{CO_2} . As

a_{Ca}/a_{Mg} should be highest in waters with low m_{CO_2} . For a constant $\log a_{Mg}/a_{H^+}$ of approximately 6.0 at 250°C, m_{Mg} will be approximately 0.001, 0.10, and 10.0, at sodium concentrations of 0.01, 0.1, and 1.0 m, respectively.

Silica

Fournier and Rowe (1966) and Mahon (1966) have shown conclusively that high-temperature geothermal waters (above about 180°C) are saturated with silica in equilibrium with quartz. The concentration of silica in a sample of geothermal well water can be used to give an accurate estimate of the underground temperature (e.g., Fournier, 1970; Mahon and Finlayson, 1972). The high-temperature equilibrium solutions contain only monomeric silica species.

Metastable crystalline and amorphous forms of silica persist in contact with water to temperatures of at least 300°C and exhibit definite solubilities which are much higher than for quartz. As geothermal waters are concentrated by steam loss as they approach the surface in channels or drill-pipes, they pass from a stage of saturation with quartz and undersaturation with amorphous silica, to a condition of supersaturation with quartz, and eventually with amorphous silica. For example, the temperatures at which the solubility of amorphous silica is exceeded are 95, 150, and 200°C, for waters that were originally at underground temperatures of 200, 250, and 300°C, respectively. For these waters, growth of silica polymers in solution, with the associated tendency toward amorphous silica deposition does not begin until there is appreciable supersaturation with amorphous silica. It is only under near-surface conditions where the temperatures are too low for the quartz equilibrium to be rapidly reversible, and where solutions become appreciably supersaturated

with amorphous silica that extensive deposition of opal and silica occurs in the rocks or about outflows. The reactions involving silica polymerization and deposition are complex and detailed kinetic studies have been made observing the effects of pH, supersaturation, solution composition, presence of nucleir, and flow rates (Kitahara, 1960; Yanagase et al., 1970; and Rothbaum and Wilson, 1977).

Ellis and Mahon (1964) showed that at temperatures between 250 and 350°C the solubility of silica from volcanic igneous rocks was initially approximately equal to that for amorphous silica solubility. Arnorsson (1975) showed that Iceland thermal waters at temperatures up to approximately 150°C in basalt rocks dissolved silica and deposited chalcedony on cooling or dilution to retain equilibrium with this mineral. Hot waters moving into fresh volcanic rocks could cause extensive solution of silica and create concentration levels that would later require quartz or chalcedony to be deposited to attain equilibrium. The lateral migration of hot water from a reservoir system may therefore be hindered by the tendency of processes of solution and deposition to seal flow channels.

Ammonia

In sedimentary rock environments such as Ngawha, or Salton Sea, ammonia concentrations are higher than in geothermal systems contained within volcanic rocks. The ammonia distribution (solution/rock) is highest at high teperatures, and at low pHs (e.g., at Matsao). Whether this is an equilibrium distribution or simply more effective extraction is not clear, although under cooler near-surface conditions, ammonia is concentrated into low-grade hydrothermal alteration products (Erd et al., 1964).

Fluoride

The concentrations of fluoride in geothermal waters appear to be limited by the solubility of fluorite, which in the presence of silica is of the order of 10 ppm fluoride at temperatures of 200-300°C. High fluoride concentrations in general correlate with low calcium concentrations, in New Zealand geothermal waters (Mahon, 1964). Low calcium and high fluoride concentrations in geothermal waters are favored by low salinity, high carbon dioxide concentration, and high temperature.

Total fluoride concentrations may be increased in low pH waters due to the increased proportion of un-ionized HF, and the possible formation of SiF_6^{2-} or AlF_6^{3-} .

Calcium Sulfate

Most geothermal waters of temperature 200-300°C and of near-neutral pH and moderate salinity (0.02-0.1 m) have sulfate concentrations in the range 10-100 ppm. As the solubility of calcium sulfate (anhydrite) in high-temperature water is very low, an inverse correlation between calcium and sulfate concentrations is to be expected, except at low pHs where there is an appreciable proportion of total sulfate present as HSO_4^- . Very-high-temperature or very-high-salinity systems may have extremely low sulfate concentrations (e.g., Mexicali and Salton Sea).

Iron, Manganese, etc.

The general salinity/pH relationship affects the maximum concentration of metals such as iron, manganese, copper, and lead, that can be carried in geothermal solutions. The equilibrium solution of metal ions from oxides or sulfides involves the hydrogen ion, e.g., $\text{MO} + 2\text{H}^+ \rightarrow \text{M}^{2+} + \text{H}_2\text{O}$; or $\text{MS} + 2\text{H}^+ \rightarrow \text{M}^{2+} + \text{H}_2\text{S}$.

Within the limits of element availability from the surrounding rocks a

general relationship is to be expected between the concentration of iron, manganese, copper, lead, etc., and $(a_H)^2$, or in near-neutral pH waters $(m_{Na})^2$.

Redox Conditions

The waters of many high-temperature geothermal areas have hydrogen present at a partial pressure, P_{H_2} , of about 0.1 bars (Table 13-5?). For the gaseous reaction $2H_2O \rightleftharpoons 2H_2 + O_2$ the logarithm of the equilibrium constant, $K_{H_2O} = -45.9, -43.5, -41.3,$ and -39.2 at 225, 250, 275, and 300°C, respectively. If $P_{H_2} = 0.1$, P_{O_2} values are $10^{-42.5}, 10^{-40}, 10^{-37.5},$ and 10^{-35} , respectively. Seward (1974), and Kusakabe (1974) confirmed that P_{O_2} values of this order occurred in the Broadlands and Wairakei fields at approximately 250-260°C, and were close to the conditions for pyrite and pyrrhotite coexistence under the prevailing solution compositions.

Sulfur Species

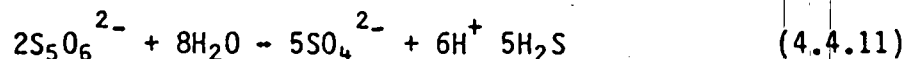
From the ratio of sulfide to sulfate and the pH of the deep hot waters, the partial pressure of oxygen necessary for equilibrium can be calculated from standard thermodynamic data (Ellis, 1967; Kusakabe, 1974). For example, at Wairakei underground P_{O_2} values of 10^{-36} - 10^{-35} bars are required. This suggests a more oxidizing situation than is found by direct measurement in the system, and the sulfide and sulfate may not have attained equilibrium. A similar situation apparently exists in the deep Broadlands waters (calculations of Seward, 1974).

Ellis and Giggenbach (1971) gave results for the sulfur hydrolysis equilibrium



The equilibrium constant K_s at saturated water vapor pressures was approximately $10^{-11.6}$ at 200°C, $10^{-8.7}$ at 250°C, and $10^{-6.4}$ at 300°C, where $K_s = m_{H_2S} \cdot m_{H^+} \cdot m_{HSO_4^-}$. For example, at 250°C the solution contains approximately 0.03 m H_2S and 0.01 m H_2SO_4 . These values are in approximate agreement with concentrations of sulfide and sulfate in the Matsuo well waters.

At temperatures of 250-300°C, dilute solutions of ions such as $S_2O_3^{2-}$, $S_4O_6^{2-}$, and $S_5O_6^{2-}$ disproportionate into sulfide and sulfate (Pryor, 1960; Ellis and Golding, unpublished).



However, Giggenbach (1974) demonstrated by high-temperature spectrophotometry that at temperatures less than 200°C, at near-neutral pHs, and with the total sulfur species concentrations at a level that brings the system close to the point of coexistence with sulfur, thiosulfate and several polysulfide species can exist, such as the S_4^{2-} ion and its dissociation products S_2^- or S_3^- . These intense blue radicals may account for the color of the cooling and partly oxidized waters of hot pools in many geothermal areas. With equal and equilibrium concentrations of sulfide and sulfate of, for example, 0.01 m, the point of coexistence with sulfur occurs at approximately pH 7 at 150°C, pH 3.6 at 200°C, and pH 0.7 at 250°C. Except in very acid waters or in solutions with very high total dissolved sulfur, species other than sulfide and sulfate are unlikely to be present in geothermal waters at temperatures in excess of approximately 200°C."

CHAPTER 4 REFERENCES

- Adams, M. C., Moore, J. N., and Forster, C., 1985, Fluid flow in volcanic terrains - hydrogeochemistry of the Meager Mountain thermal system: Geothermal Resources Council, Transactions, v. 9, in press.
- Adams, M. C., and Capuano, R. M., 1982, Evaluation of the geothermal reservoir associated with Auburn and Johnson Hot Springs, Upper Star Valley, Wyoming: Geothermal Resources Council, Transactions, v. 6, p. 73-76.
- Andrusenko, N. I., and Moskalyuk, A. A., 1966, Experiments on the hydrothermal treatment of dolerites with a bearing on the genesis of Iceland spar deposits: Geokhimiya, v. 9, p. 1119-1123.
- Annorsson, S., 1975, Application of the silica geothermometer in low temperature hydrothermal areas in Iceland: Am. J. Sci., 275, p. 763-784.
- Bargar, K. E., Beeson, M. H., Fournier, R. O., and Muffler, L. J. P., 1973, Present-day deposition of lepidolite from thermal waters in Yellowstone National Park: Am. Mineral., v. 58, p. 901-904.
- Chelishev, N. F., 1967, Laboratory studies in the distribution of rare alkalis between potassium minerals and aqueous solutions at high temperatures and pressures: Dokl. Aka. Nauk S.S.S.R., v. 175, p. 205-207.
- Craig, H., 1963, The isotope geochemistry of water and carbon in geothermal areas: in Nuclear Geology on Geothermal Areas, E. Tongiorgi, ed., Pisa: Consiglio Nazionale della Ricerca, Laboratorio di Geologia Nucleare, p. 17-23.
- Ellis, A. J., 1967, The chemistry of some explored geothermal systems, in Geochemistry of Hydrothermal Ore Deposits, H. L. Barnes, ed., New York: Holt, Rinehart and Winston, p. 465-514.
- Ellis, A. J., 1970, Quantitative interpretation of chemical characteristics of hydrothermal systems: Geothermics (Special Issue 2), 2(Pt. 1), p. 516-528.
- Ellis, A. J., 1971, Magnesium concentrations in the presence of magnesium chlorite, calcite, carbon dioxide, quartz: Am. J. Sci., v. 271, p. 481-489.
- Ellis, A. J., 1979, Explored geothermal systems, in Barnes, H., ed., Geochemistry of Hydrothermal Ore Deposits, John Wiley and Sons, New York, p. 632-683.
- Ellis, A. J., and Mahon, W. A. J., 1964, Natural hydrothermal systems and experimental hot water/rock interactions: Geochim. Cosmochim. Acta, v. 28, p. 1323-1357.
- Ellis, A. J., and Mahon, W. A. J., 1967, Natural hydrothermal systems and experimental hot water/rock interactions, Pt. 2: Geochim. Cosmochim. Acta, v. 31, p. 519-538.

- Ellis, A. J., and Giggenbach, W. J., 1971, Hydrogen sulphide ionization and sulphur hydrolysis in high temperature solution: *Geochim. Cosmochim. Acta*, v. 35, p. 247-260.
- Erd, R. C., White, D. E., Fahey, J. J., and Lee, D. E., 1964, Buddingtonite, an ammonium feldspar with zeolitic water: *Am. Mineral.*, v. 49, p. 831-850.
- Facca, G., and Tonani, F., 1964, Theory and technology of a geothermal field: *Bull. Volcanol.*, v. 27, p. 1-47.
- Facca, G., and Tonani, F., 1967, The self-sealing geothermal field: *Bull. Volcanol.*, v. 30, p. 271-273.
- Fournier, R. O., 1970, Silica in thermal waters: laboratory and field investigations, in *Proceedings Sympos. Hydrogeochemistry and Biogeochemistry*, v. 1, Wash., D.C.: The Clark Co., p. 122-140.
- Fournier, R. O., 1977, Chemical geothermometers and mixing models for geothermal systems: *Geothermics*, v. 5, p. 41-40.
- Fournier, R. O., and Rowe, J. J., 1966, Estimation of underground temperatures from the silica content of water from hot springs and wet-steam wells: *Am. J. Sci.*, v. 264, p. 685-697.
- Fournier, R. O., and Truesdell, A. H., 1973, An empirical Na-K-Ca geothermometer for natural waters: *Geochim. Cosmochim. Acta*, v. 37, p. 1255-1275.
- Fournier, R. O., and Truesdell, A. H., 1974, Geochemical indicators of subsurface temperature--Part 2, estimation of temperature and fraction of hot water mixed with cold water: *J. Res. U.S. Geol. Survey*, v. 2, p. 263-270.
- Giggenbach, W. F., 1974, Equilibria involving polysulfide ions in aqueous solutions up to 240°C: *Inorg. Chem.*, v. 13, p. 1724-1730.
- Hem, J. D., 1970, Study and interpretation of the chemical characteristics of natural water: *U.S. Geol. Survey Water-Supply Paper 1473*, 363 p.
- Kissen, I. G., and Pakhomov, S. I., 1967, Effect of high temperatures on the chemical composition of ground waters: *Geochem. Int.*, v. 4, p. 295-308.
- Kitahara, S., 1960, The polymerization of silicic acid obtained by hydrothermal treatment of quartz and the solubility of amorphous silica: *Rev. Phys. Chem. Japan*, v. 30, p. 131-137.
- Kusakabe, M., 1974, Sulphur isotopic variations in nature. 10. Oxygen and sulphur isotope study of Wairakei geothermal well discharges: *New Zealand J. Sci.*, v. 17, p. 183-192.
- Mahon, W. A. J., 1964, Fluorine in the natural thermal waters of New Zealand: *New Zealand J. Sci.*, v. 7, p. 3-28.

- Mahon, W. A. J., 1966, Silica in hot water discharged from drill holes at Wairakei, New Zealand: *New Zealand J. Sci.*, v. 9, p. 135-144.
- Mahon, W. A. J., 1967, Natural hydrothermal systems and the reaction of hot water with sedimentary rocks: *New Zealand J. Sci.*, v. 10, p. 206-221.
- Mahon, W. A. J., and Finlayson, J. B., 1972, The chemistry of the Broadlands geothermal area New Zealand: *Am. J. Sci.*, v. 272, p. 48-68.
- Piper, A. M., 1944, A graphic procedure in the geochemical interpretation of water analysis: *Amer. Geophys. Union, Trans.*, p. 914-923.
- Pryor, W. A., 1960, The kinetics of disproportionation of sodium thiosulfate to sodium sulfide and sulfate: *J. Am. Chem. Soc.*, v. 82, p. 4794-4797.
- Rothbaum, H. P., and Wilson, R. D., 1977, Effect of temperature and concentration on the polymerization rate of silica in geothermal waters, in *Geochemistry 1977*, A. J. Ellis and A. P. W. Hodder, eds., Wellington, New Zealand Dept. Sci. and Ind. Res. Bulletin, v. 218, p. 37-43.
- Seward, T. M., 1974, Equilibrium and oxidation potential in geothermal waters at Broadlands, New Zealand: *Am. J. Sci.*, v. 274, p. 190-192.
- Struhsacker, E. M., Smith, C., and Capuano, R. M., 1983, An evaluation of exploration methods for low-temperature geothermal systems in the Artesian City area, Idaho: *Geol. Soc. Amer., Bull.*, v. 94, p. 58-79.
- Truesdell, A. H., and Fournier, R. O., 1977, Procedure for estimating the temperature of a hot water component in a mixed water using a plot of dissolved silica versus enthalpy: *J. Res. U.S. Geological Survey*, v. 5(1), p. 49-52.
- White, D. E., 1957, Thermal waters of volcanic origin: *Bull. Geol. Soc. Am.*, v. 68, p. 1637-1658.
- White, D. E., 1965, Saline waters of sedimentary rocks, in *Fluids in Subsurface Environments—a Symposium*, *Memoir Amer. Assn. Petrol. Geologists*, v. 4, p. 342-366.
- White, D. E., 1974, Diverse origins of hydrothermal ore fluids: *Econ. Geol.*, v. 69, p. 954-973.
- Yanagase, K., Yamaguchi, K., Yanagase, T., Suginozawa, Y., Kozawa, S., and Yamazaki, H., 1970, Colloidal silica in hot-spring water: *Nippon Kagaku Zasshi*, v. 91, p. 1141-1148.

CHAPTER 5. GEOCHEMICAL METHODS APPLIED TO FLUID CHEMISTRY

5.1 OVERVIEW OF GEOTHERMOMETRY

An understanding of the temperatures at depth in the geothermal reservoir rocks is crucial to the development and exploitation of the resource. Temperatures can be determined directly through downhole measurements or estimated indirectly from the chemistry and stable isotopes (O, H, S, C) of the water, steam, gas and reservoir rocks themselves. Direct and indirect methods provide, however, different information about the reservoir.

The application of indirect methods plays a critical role in the initial assessment of a thermal field. Indirect methods based on the chemistry of the thermal fluids can provide information on deep thermal regimes within the high temperature parts of the reservoir that otherwise are inaccessible to shallow and even moderate-depth thermal gradient wells. Thus, indirect methods can be used to prioritize drilling targets and, when compared with thermal measurements made in shallow gradient wells, can be used to establish depth requirements for the deeper drilling program. During exploitation of a thermal field these geothermometers are used to monitor changes in the reservoir without requiring extensive shutting in of the wells.

The geothermometer techniques currently available require chemical or isotopic analyses of thermal waters, steam and gas from wells and springs. These quantitative techniques can be categorized into the following groups:

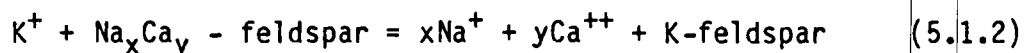
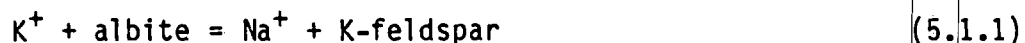
- 1) Chemical geothermometers
- 2) Mixing geothermometers
- 3) Isotope geothermometers

The underlying premise for all three categories is that temperature-dependent reactions between either the reservoir rock and fluid or evolving gases and the fluid attain equilibrium. Furthermore, no reequilibration

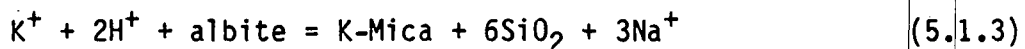
occurs after the fluid leaves the reservoir (see Fournier et al., 1974; Truesdell, 1976; Fournier, 1977; Ellis, 1979 for further details).

Several chemical geothermometers based on the concentrations of the major and minor elements occurring in thermal waters have been proposed and have proven extremely valuable in accurately estimating subsurface temperatures. The relationships between the concentrations of these elements and temperature are given in Tables 5.2.1 and 5.2.2 and are discussed in the following sections. An extensive review of the use of these geothermometers was recently published by Fournier (1981). A copy of this paper is included as an appendix to Chapter 5 (Appendix 5-A).

Although geothermometers are empirical in nature, there are field and laboratory data available to suggest that at relatively high temperatures the major element chemistry of the fluids is controlled by temperature/pressure-dependent reactions. For example, the reactions (Ellis, 1967; Fournier and Truesdell, 1973)



and



are believed to be important in controlling the K, Na, Ca contents and pH of fluids in many terrains where quartz and feldspar are abundant. The silica content appears to be limited above 180°C by the solubility of quartz (Fournier and Rowe, 1966; Mahon, 1966) and by the solubility of chalcedony at lower temperatures. At high temperatures the concentration of Mg is controlled by the formation of chlorite (Ellis, 1971).

Different geothermometers frequently give different results when applied to the same analyses, creating ambiguity in their interpretation. During the

early stages of an exploration program when data comes largely from springs and shallow wells, there is often no reason to choose one result over another. Comparison with other data, obtained from deep wells, thermal gradient studies, and qualitative fluid and mineral thermometers may help, however, in understanding these relationships. For example, concentrations of silica can be affected by pH, subsurface temperatures calculated from the Na-K-Ca geothermometer may be adversely affected by high contents of CO₂ (Paces, 1975) and Mg (Fournier and Potter, 1979), the Na/K ratio can also be affected by the addition of K and Na from sedimentary rocks or by interaction with montmorillonite (Weisberg and Wilson, 1977). Subsurface boiling, and mixing can also affect the cation ratios in different ways. In general, boiling does not affect the Na/K ratio but may cause loss of CO₂ and result both in the precipitation of calcite and Na-K-Ca geothermometer temperatures that are too high. Mixing can either decrease or increase the concentration of the components in solution. Goff and Donnally (1978) argued that some of the calculated Na-K-Ca temperatures of springs in The Geysers-Clear Lake area were anomalously high and reflected the mixing of ion-rich connate water trapped in rocks of the Great Valley Sequence with the thermal fluids. Higher concentrations of Cl in springs issuing from the Great Valley Sequence compared to waters of the same temperature which discharge from springs in the Franciscan rocks, and electrical resistivity data support their conclusions.

For systems undergoing mixing and/or boiling, the quartz mixing geothermometer and the chloride-enthalpy relationships can give information about the temperature and chemistry of the parent fluid and the extent of mixing with local groundwaters (see section 5.2). Calculations of this type indicate that extensive mixing occurs even in the deep parts of many systems. Figure 5.1.1 illustrates the results of the mixing calculation for

T26S
T27S

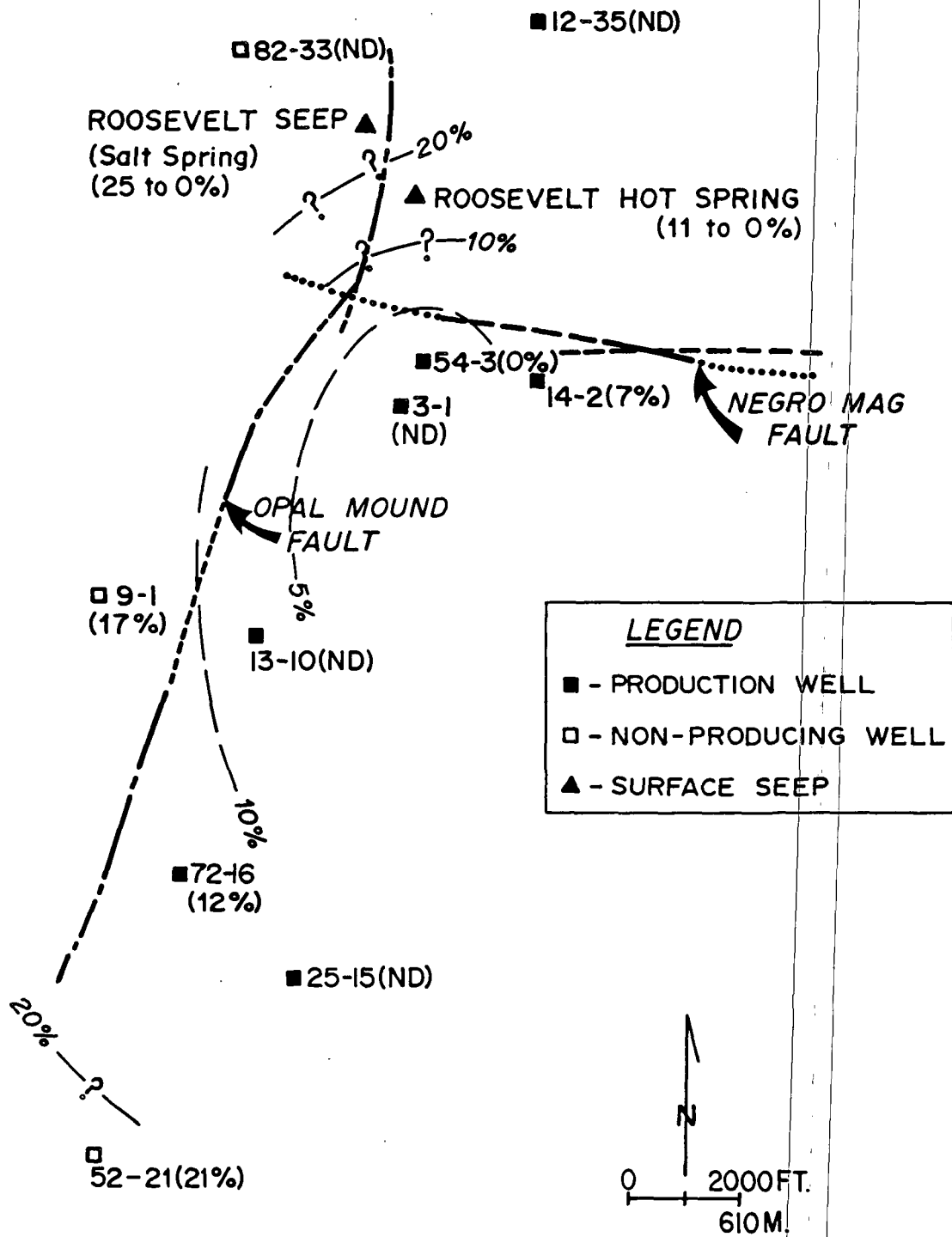


Figure 5.1.1

the Roosevelt Hot Springs thermal area, determined from chemical analyses of the wells and springs by Capuano and Cole (1981). These data indicate that the extent of groundwater mixing increases in all directions away from well 54-3 and that the center of upwelling is located near this well. The chloride-enthalpy relationships suggest that the reservoir fluid has a temperature of 284°C. Similar temperatures were estimated from other cation and isotope thermometers. The maximum measured temperatures are 269°C. These data strongly support 1) the initial model of the thermal system based on the geologic relationships, 2) subsurface temperatures based on the quantitative major element geothermometers applied to hot springs waters, and 3) qualitative fluid and mineral geothermometers (described below).

Stable isotopic fractionation data determined from coexisting gas-fluid, gas-gas and fluid-solid pairs can also provide quantitative temperature estimates. The co-existing pairs that have received the most attention and show the most promise as far as their application to geothermal systems include: 1) carbon isotopic fractionation between carbon dioxide-methane, 2) sulfur isotopic fractionation between sulfate-hydrogen sulfide, and 3) oxygen isotopic fractionation between sulfate-water, carbon dioxide-water and secondary alteration minerals (i.e., quartz, calcite)-water. The rates of isotopic reactions determine whether they will equilibrate in deep geothermal reservoirs and how rapidly reequilibration occurs in shallow reservoirs and during passage of fluids to the surface (Truesdell and Hulston, 1980). These differing rates of isotopic equilibration or reequilibration can be used to reconstruct the thermal history of the system.

Numerous qualitative thermometers, based on the cation and anion contents of the discharged fluids and on the distribution of various hydrothermal minerals and trace elements in the altered rocks, can also be used to estimate

Table 5.1.2 STEAM TABLES — THERMODYNAMIC DATA FOR WATER AT SATURATED VAPOR PRESSURES AND TEMPERATURES

0 - 374.136°C

Derivation: Equation of State of Keenan et al. (1969);
and calculated by P. Delaney (U.S. Geological Survey)

Reference:

Keenan, J.H., Keyes, F.G., Hill, P.G. and Moore, J.G., 1969, Steam Tables - thermodynamic properties of water including vapor, liquid, and solid phases (International Edition - metric units): Wiley, New York, 162 p.

Temp. (°C)	Press. (bars)	Specific Volume (cc/gm)		Enthalpy (J/gm)		
		vap.	liq.	vap.	liq.	evap.
0.01	0.01	206136	1.000	2501	0.01	2501
1	0.01	192577	1.000	2503	4.16	2499
2	0.01	179889	1.000	2505	8.37	2497
3	0.01	168132	1.000	2507	12.57	2494
4	0.01	157232	1.000	2509	16.78	2492
5	0.01	147120	1.000	2511	20.98	2490
6	0.01	137734	1.000	2512	25.20	2487
7	0.01	129017	1.000	2514	29.39	2485
8	0.01	120917	1.000	2516	33.60	2482
9	0.01	113386	1.000	2518	37.80	2480
10	0.01	106379	1.000	2520	42.01	2478
11	0.01	99857	1.000	2522	46.20	2475
12	0.01	93784	1.001	2523	50.41	2473
13	0.01	88124	1.001	2525	54.60	2471
14	0.02	82848	1.001	2527	58.80	2468
15	0.02	77926	1.001	2529	62.99	2466
16	0.02	73333	1.001	2531	67.19	2464
17	0.02	69044	1.001	2533	71.38	2461
18	0.02	65038	1.001	2534	75.58	2459
19	0.02	61293	1.002	2536	79.77	2456
20	0.02	57791	1.002	2538	83.96	2454
21	0.02	54514	1.002	2540	88.14	2452
22	0.03	51447	1.002	2542	92.33	2449
23	0.03	48574	1.002	2544	96.52	2447
24	0.03	45883	1.003	2545	100.7	2445
25	0.03	43360	1.003	2547	104.9	2442
26	0.03	40994	1.003	2549	109.1	2440
27	0.04	38774	1.003	2551	113.2	2438
28	0.04	36690	1.004	2553	117.4	2435
29	0.04	34733	1.004	2554	121.6	2433

Temp. (°C)	Press. (bars)	Specific Volume (cc/gm)		Enthalpy (J/gm)		
		vap.	liq.	vap.	liq.	evap.
30	0.04	32894	1.004	2556	125.8	2430
31	0.04	31165	1.005	2558	130.0	2428
32	0.05	29540	1.005	2560	134.1	2426
33	0.05	28011	1.005	2562	138.3	2423
34	0.05	26571	1.006	2563	142.5	2421
35	0.06	25216	1.006	2565	146.7	2419
36	0.06	23940	1.006	2567	150.9	2416
37	0.06	22737	1.007	2569	155.0	2414
38	0.07	21602	1.007	2571	159.2	2411
39	0.07	20533	1.007	2572	163.4	2409
40	0.07	19523	1.008	2574	167.6	2407
41	0.08	18570	1.008	2576	171.7	2404
42	0.08	17671	1.009	2578	175.9	2402
43	0.09	16821	1.009	2580	180.1	2400
44	0.09	16018	1.009	2581	184.3	2397
45	0.10	15258	1.010	2583	188.4	2395
46	0.10	14540	1.010	2585	192.6	2392
47	0.11	13861	1.011	2587	196.8	2390
48	0.11	13218	1.011	2589	201.0	2388
49	0.12	12609	1.012	2590	205.1	2385
50	0.12	12032	1.012	2592	209.3	2383
51	0.13	11486	1.013	2594	213.5	2380
52	0.14	10968	1.013	2596	217.7	2378
53	0.14	10476	1.014	2597	221.9	2376
54	0.15	10011	1.014	2599	226.0	2373
55	0.16	9569	1.015	2601	230.2	2371
56	0.17	9149	1.015	2603	234.4	2368
57	0.17	8751	1.016	2604	238.6	2366
58	0.18	8372	1.016	2606	242.8	2363
59	0.19	8013	1.017	2608	246.9	2361
60	0.20	7671	1.017	2610	251.1	2358
61	0.21	7346	1.018	2611	255.3	2356
62	0.22	7037	1.018	2613	259.5	2354
63	0.23	6743	1.019	2615	263.7	2351
64	0.24	6463	1.019	2617	267.9	2349
65	0.25	6197	1.020	2618	272.0	2346
66	0.26	5943	1.020	2620	276.2	2344
67	0.27	5701	1.021	2622	280.4	2341
68	0.29	5471	1.022	2623	284.6	2339
69	0.30	5252	1.022	2625	288.8	2336
70	0.31	5042	1.023	2627	293.0	2334
71	0.33	4843	1.023	2629	297.2	2331
72	0.34	4652	1.024	2630	301.4	2329
73	0.35	4470	1.025	2632	305.5	2326
74	0.37	4297	1.025	2634	309.7	2324
75	0.39	4131	1.026	2635	313.9	2321
76	0.40	3973	1.027	2637	318.1	2319
77	0.42	3822	1.027	2639	322.3	2316
78	0.44	3677	1.028	2640	326.5	2314
79	0.46	3539	1.028	2642	330.7	2311
80	0.47	3407	1.029	2644	334.9	2309
81	0.49	3281	1.030	2645	339.1	2306
82	0.51	3160	1.030	2647	343.3	2304
83	0.53	3044	1.031	2649	347.5	2301
84	0.56	2934	1.032	2650	351.7	2299

STEAM TABLES

Temp. (°C)	Press. (bars)	Specific Volume (cc/gm)		Enthalpy (J/gm)		
		vap.	liq.	vap.	liq.	evap.
85	0.58	2828	1.032	2652	355.9	2296
86	0.60	2726	1.033	2654	360.1	2293
87	0.63	2629	1.034	2655	364.3	2291
88	0.65	2536	1.035	2657	368.5	2288
89	0.68	2446	1.035	2658	372.7	2286
90	0.70	2361	1.036	2660	376.9	2283
91	0.73	2278	1.037	2662	381.1	2281
92	0.76	2200	1.037	2663	385.3	2278
93	0.79	2124	1.038	2665	389.5	2275
94	0.81	2052	1.039	2667	393.7	2273
95	0.85	1982	1.040	2668	398.0	2270
96	0.88	1915	1.040	2670	402.2	2268
97	0.91	1851	1.041	2671	406.4	2265
98	0.94	1789	1.042	2673	410.6	2262
99	0.98	1730	1.043	2674	414.8	2260
100	1.01	1673	1.043	2676	419.0	2257
101	1.05	1618	1.044	2678	423.3	2254
102	1.09	1566	1.045	2679	427.5	2252
103	1.13	1515	1.046	2681	431.7	2249
104	1.17	1466	1.047	2682	435.9	2246
105	1.21	1419	1.047	2684	440.1	2244
106	1.25	1374	1.048	2685	444.4	2241
107	1.29	1331	1.049	2687	448.6	2238
108	1.34	1289	1.050	2688	452.8	2236
109	1.39	1249	1.051	2690	457.1	2233
110	1.43	1210	1.052	2691	461.3	2230
111	1.48	1173	1.052	2693	465.5	2227
112	1.53	1137	1.053	2695	469.8	2225
113	1.58	1102	1.054	2696	474.0	2222
114	1.64	1069	1.055	2697	478.2	2219
115	1.69	1037	1.056	2699	482.5	2217
116	1.75	1006	1.057	2700	486.7	2214
117	1.80	975.6	1.058	2702	491.0	2211
118	1.86	946.7	1.059	2703	495.2	2208
119	1.92	918.8	1.059	2705	499.5	2205
120	1.99	891.9	1.060	2706	503.7	2203
121	2.05	865.9	1.061	2708	508.0	2200
122	2.11	840.8	1.062	2709	512.2	2197
123	2.18	816.6	1.063	2711	516.5	2194
124	2.25	793.2	1.064	2712	520.7	2191
125	2.32	770.6	1.065	2713	525.0	2189
126	2.39	748.8	1.066	2715	529.2	2186
127	2.47	727.7	1.067	2716	533.5	2183
128	2.54	707.3	1.068	2718	537.8	2180
129	2.62	687.6	1.069	2719	542.0	2177
130	2.70	668.5	1.070	2720	546.3	2174
131	2.78	650.1	1.071	2722	550.6	2171
132	2.87	632.3	1.072	2723	554.9	2168
133	2.95	615.0	1.073	2725	559.1	2165
134	3.04	598.3	1.074	2726	563.4	2163
135	3.13	582.2	1.075	2727	567.7	2160
136	3.22	566.6	1.076	2729	572.0	2157
137	3.32	551.4	1.077	2730	576.3	2154
138	3.41	536.8	1.078	2731	580.5	2151
139	3.51	522.6	1.079	2733	584.8	2148

Temp. (°C)	Press. (bars)	Specific Volume		Enthalpy		
		(cc/gm)		(J/gm)		
		vap.	liq.	vap.	liq.	evap.
140	3.61	508.9	1.080	2734	589.1	2145
141	3.72	495.6	1.081	2735	593.4	2142
142	3.82	482.7	1.082	2736	597.7	2139
143	3.93	470.2	1.083	2738	602.0	2136
144	4.04	458.1	1.084	2739	606.3	2133
145	4.15	446.3	1.085	2740	610.6	2130
146	4.27	435.0	1.086	2742	614.9	2127
147	4.39	423.9	1.087	2743	619.2	2124
148	4.51	413.2	1.088	2744	623.6	2120
149	4.63	402.9	1.089	2745	627.9	2117
150	4.76	392.8	1.090	2746	632.2	2114
151	4.89	383.0	1.092	2748	636.5	2111
152	5.02	373.5	1.093	2749	640.8	2108
153	5.15	364.4	1.094	2750	645.2	2105
154	5.29	355.4	1.095	2751	649.5	2102
155	5.43	346.8	1.096	2752	653.8	2099
156	5.57	338.4	1.097	2754	658.2	2095
157	5.72	330.2	1.098	2755	662.5	2092
158	5.87	322.3	1.100	2756	666.9	2089
159	6.02	314.5	1.101	2757	671.2	2086
160	6.18	307.1	1.102	2758	675.5	2083
161	6.34	299.8	1.103	2759	679.9	2079
162	6.50	292.7	1.104	2760	684.3	2076
163	6.66	285.9	1.106	2761	688.6	2073
164	6.83	279.2	1.107	2762	693.0	2070
165	7.00	272.7	1.108	2764	697.3	2066
166	7.18	266.4	1.109	2765	701.7	2063
167	7.36	260.2	1.110	2766	706.1	2060
168	7.54	254.3	1.112	2767	710.5	2056
169	7.73	248.5	1.113	2768	714.8	2053
170	7.92	242.8	1.114	2769	719.2	2050
171	8.11	237.3	1.116	2770	723.6	2046
172	8.31	232.0	1.117	2771	728.0	2043
173	8.51	226.8	1.118	2772	732.4	2039
174	8.71	221.7	1.119	2773	736.8	2036
175	8.92	216.8	1.121	2774	741.2	2032
176	9.13	212.0	1.122	2775	745.6	2029
177	9.35	207.3	1.123	2775	750.0	2025
178	9.57	202.8	1.125	2776	754.4	2022
179	9.79	198.4	1.126	2777	758.8	2018
180	10.02	194.0	1.127	2778	763.2	2015
181	10.25	189.8	1.129	2779	767.6	2011
182	10.49	185.8	1.130	2780	772.1	2008
183	10.73	181.8	1.132	2781	776.5	2004
184	10.98	177.9	1.133	2782	780.9	2001
185	11.23	174.1	1.134	2782	785.4	1997
186	11.48	170.4	1.136	2783	789.8	1993
187	11.74	166.8	1.137	2784	794.3	1990
188	12.00	163.3	1.139	2785	798.7	1986
189	12.27	159.9	1.140	2786	803.2	1982
190	12.54	156.5	1.141	2786	807.6	1979
191	12.82	153.3	1.143	2787	812.1	1975
192	13.10	150.1	1.144	2788	816.5	1971
193	13.39	147.0	1.146	2789	821.0	1968
194	13.68	144.0	1.147	2789	825.5	1964

STEAM TABLES

Temp. (°C)	Press. (bars)	Specific Volume (cc/gm)		Enthalpy (J/gm)		
		vap.	liq.	vap.	liq.	evap.
195	13.98	141.1	1.149	2790	830.0	1960
196	14.28	138.2	1.150	2791	834.5	1956
197	14.59	135.4	1.152	2791	839.0	1952
198	14.90	132.6	1.153	2792	843.4	1949
199	15.22	130.0	1.155	2793	847.9	1945
200	15.54	127.4	1.156	2793	852.4	1941
201	15.87	124.8	1.158	2794	857.0	1937
202	16.20	122.3	1.160	2794	861.5	1933
203	16.54	119.9	1.161	2795	866.0	1929
204	16.88	117.5	1.163	2796	870.5	1925
205	17.23	115.2	1.164	2796	875.0	1921
206	17.59	113.0	1.166	2797	879.6	1917
207	17.95	110.7	1.168	2797	884.1	1913
208	18.31	108.6	1.169	2798	888.7	1909
209	18.68	106.5	1.171	2798	893.2	1905
210	19.06	104.4	1.173	2798	897.8	1901
211	19.45	102.4	1.174	2799	902.3	1897
212	19.84	100.4	1.176	2799	906.9	1892
213	20.23	98.51	1.178	2800	911.5	1888
214	20.63	96.63	1.179	2800	916.0	1884
215	21.04	94.79	1.181	2801	920.6	1880
216	21.46	92.99	1.183	2801	925.2	1876
217	21.88	91.23	1.185	2801	929.8	1871
218	22.30	89.52	1.186	2802	934.4	1867
219	22.74	87.84	1.188	2802	939.0	1863
220	23.18	86.19	1.190	2802	943.6	1859
221	23.62	84.58	1.192	2802	948.2	1854
222	24.08	83.01	1.194	2803	952.9	1850
223	24.54	81.47	1.195	2803	957.5	1845
224	25.00	79.96	1.197	2803	962.1	1841
225	25.48	78.49	1.199	2803	966.8	1836
226	25.96	77.05	1.201	2803	971.4	1832
227	26.44	75.64	1.203	2804	976.1	1828
228	26.94	74.26	1.205	2804	980.8	1823
229	27.44	72.90	1.207	2804	985.4	1818
230	27.95	71.58	1.209	2804	990.1	1814
231	28.46	70.29	1.211	2804	994.8	1809
232	28.99	69.02	1.213	2804	999.5	1805
233	29.52	67.77	1.215	2804	1004	1800
234	30.06	66.56	1.217	2804	1009	1795
235	30.60	65.37	1.219	2804	1014	1791
236	31.15	64.20	1.221	2804	1018	1786
237	31.71	63.06	1.223	2804	1023	1781
238	32.28	61.94	1.225	2804	1028	1776
239	32.86	60.84	1.227	2804	1033	1771
240	33.44	59.76	1.229	2804	1037	1767
241	34.03	58.71	1.231	2804	1042	1762
242	34.63	57.68	1.233	2804	1047	1757
243	35.24	56.67	1.236	2803	1052	1752
244	35.86	55.68	1.238	2803	1056	1747
245	36.48	54.71	1.240	2803	1061	1742
246	37.11	53.75	1.242	2803	1066	1737
247	37.76	52.82	1.244	2802	1071	1732
248	38.40	51.90	1.247	2802	1076	1727
249	39.06	51.01	1.249	2802	1081	1721

Temp. (°C)	Press. (bars)	Specific Volume (cc/gm)		Enthalpy (J/gm)		
		vap.	liq.	vap.	liq.	evap.
250	39.73	50.13	1.251	2802	1085	1716
251	40.40	49.26	1.254	2801	1090	1711
252	41.09	48.42	1.256	2801	1095	1706
253	41.78	47.59	1.258	2800	1100	1700
254	42.48	46.77	1.261	2800	1105	1695
255	43.19	45.98	1.263	2800	1110	1690
256	43.91	45.19	1.266	2799	1115	1684
257	44.64	44.42	1.268	2799	1120	1679
258	45.38	43.67	1.270	2798	1124	1674
259	46.13	42.93	1.273	2797	1129	1668
260	46.89	42.21	1.276	2797	1134	1663
261	47.65	41.49	1.278	2796	1139	1657
262	48.43	40.79	1.281	2796	1144	1651
263	49.21	40.11	1.283	2795	1149	1646
264	50.01	39.43	1.286	2794	1154	1640
265	50.81	38.77	1.289	2794	1159	1634
266	51.63	38.12	1.291	2793	1164	1629
267	52.45	37.49	1.294	2792	1169	1623
268	53.29	36.86	1.297	2791	1174	1617
269	54.13	36.25	1.300	2791	1179	1611
270	54.99	35.64	1.302	2790	1185	1605
271	55.85	35.05	1.305	2789	1190	1599
272	56.73	34.47	1.308	2788	1195	1593
273	57.61	33.90	1.311	2787	1200	1587
274	58.51	33.34	1.314	2786	1205	1581
275	59.42	32.79	1.317	2785	1210	1575
276	60.34	32.24	1.320	2784	1215	1569
277	61.26	31.71	1.323	2783	1220	1563
278	62.20	31.19	1.326	2782	1226	1556
279	63.15	30.68	1.329	2781	1231	1550
280	64.12	30.17	1.332	2780	1236	1544
281	65.09	29.67	1.335	2778	1241	1537
282	66.07	29.19	1.338	2777	1246	1531
283	67.07	28.71	1.342	2776	1252	1524
284	68.07	28.24	1.345	2775	1257	1518
285	69.09	27.77	1.348	2773	1262	1511
286	70.12	27.32	1.352	2772	1268	1504
287	71.16	26.87	1.355	2771	1273	1498
288	72.22	26.43	1.359	2769	1278	1491
289	73.28	26.00	1.362	2768	1284	1484
290	74.36	25.57	1.366	2766	1289	1477
291	75.45	25.15	1.369	2765	1294	1470
292	76.55	24.74	1.373	2763	1300	1463
293	77.66	24.33	1.376	2761	1305	1456
294	78.79	23.94	1.380	2760	1311	1449
295	79.93	23.54	1.384	2758	1316	1442
296	81.08	23.16	1.388	2756	1322	1435
297	82.24	22.78	1.392	2755	1327	1427
298	83.42	22.40	1.396	2753	1333	1420
299	84.61	22.04	1.400	2751	1338	1412
300	85.81	21.67	1.404	2749	1344	1405
301	87.02	21.32	1.408	2747	1350	1397
302	88.25	20.97	1.412	2745	1355	1390
303	89.49	20.62	1.416	2743	1361	1382
304	90.75	20.28	1.420	2741	1367	1374
305	92.02	19.95	1.425	2739	1372	1366

STEAM TABLES

Temp. (°C)	Press. (bars)	Specific Volume (cc/gm)		Enthalpy (J/gm)		
		vap.	liq.	vap.	liq.	evap.
306	93.30	19.62	1.429	2737	1378	1358
307	94.59	19.29	1.434	2734	1384	1350
308	95.90	18.97	1.438	2732	1390	1342
309	97.23	18.66	1.443	2730	1395	1334
310	98.56	18.35	1.447	2727	1401	1326
311	99.92	18.04	1.452	2725	1407	1318
312	101.2	17.74	1.457	2722	1413	1309
313	102.6	17.45	1.462	2720	1419	1301
314	104.0	17.16	1.467	2717	1425	1292
315	105.4	16.87	1.472	2714	1431	1283
316	106.8	16.58	1.477	2712	1437	1275
317	108.3	16.30	1.482	2709	1443	1266
318	109.7	16.03	1.488	2706	1449	1257
319	111.2	15.76	1.493	2703	1455	1248
320	112.7	15.49	1.499	2700	1461	1239
321	114.2	15.22	1.504	2697	1468	1229
322	115.7	14.96	1.510	2694	1474	1220
323	117.2	14.71	1.516	2691	1480	1210
324	118.8	14.45	1.522	2687	1486	1201
325	120.3	14.20	1.528	2684	1493	1191
326	121.9	13.95	1.534	2681	1499	1181
327	123.5	13.71	1.541	2677	1506	1171
328	125.1	13.47	1.547	2673	1512	1161
329	126.8	13.23	1.554	2670	1519	1151
330	128.4	13.00	1.561	2666	1525	1141
331	130.1	12.76	1.568	2662	1532	1130
332	131.7	12.54	1.575	2658	1539	1119
333	133.4	12.31	1.582	2654	1545	1109
334	135.2	12.09	1.589	2650	1552	1098
335	136.9	11.87	1.597	2645	1559	1086
336	138.6	11.65	1.605	2641	1566	1075
337	140.4	11.43	1.613	2636	1573	1064
338	142.2	11.22	1.621	2632	1580	1052
339	144.0	11.01	1.629	2627	1587	1040
340	145.8	10.80	1.638	2622	1594	1028
341	147.7	10.59	1.647	2617	1601	1016
342	149.5	10.39	1.656	2612	1609	1003
343	151.4	10.18	1.665	2606	1616	990
344	153.3	9.983	1.675	2601	1624	977
345	155.2	9.784	1.685	2595	1631	964
346	157.1	9.587	1.695	2589	1639	951
347	159.1	9.391	1.706	2583	1647	937
348	161.1	9.197	1.717	2577	1654	923
349	163.1	9.005	1.728	2571	1662	908
350	165.1	8.813	1.740	2564	1671	893
351	167.1	8.623	1.753	2557	1679	878
352	169.2	8.435	1.765	2550	1687	863
353	171.3	8.247	1.779	2542	1696	847
354	173.4	8.060	1.793	2535	1704	830
355	175.5	7.873	1.807	2527	1713	814
356	177.6	7.688	1.822	2518	1722	796
357	179.8	7.502	1.839	2510	1731	778
358	182.0	7.317	1.855	2501	1741	760
359	184.2	7.131	1.873	2491	1751	741

Temp. (°C)	Press. (bars)	Specific Volume (cc/gm)		Enthalpy (J/gm)		
		vap.	liq.	vap.	liq.	evap.
360	186.5	6.945	1.892	2481	1761	721
361	188.7	6.759	1.913	2471	1771	700
362	191.0	6.571	1.934	2459	1781	678
363	193.3	6.381	1.958	2448	1792	655
364	195.7	6.190	1.983	2435	1804	631
365	198.0	5.995	2.011	2421	1816	606
366	200.4	5.797	2.041	2407	1829	578
367	202.8	5.593	2.076	2391	1842	549
368	205.3	5.380	2.114	2374	1857	517
369	207.7	5.162	2.159	2354	1873	482
370	210.2	4.925	2.213	2332	1890	442
371	212.8	4.671	2.280	2306	1911	395
372	215.3	4.380	2.369	2274	1936	338
373	217.9	4.019	2.509	2229	1971	258
374	220.5	3.404	2.880	2140	2049	91
374.136	220.9	3.155	3.155	2099	2099	0

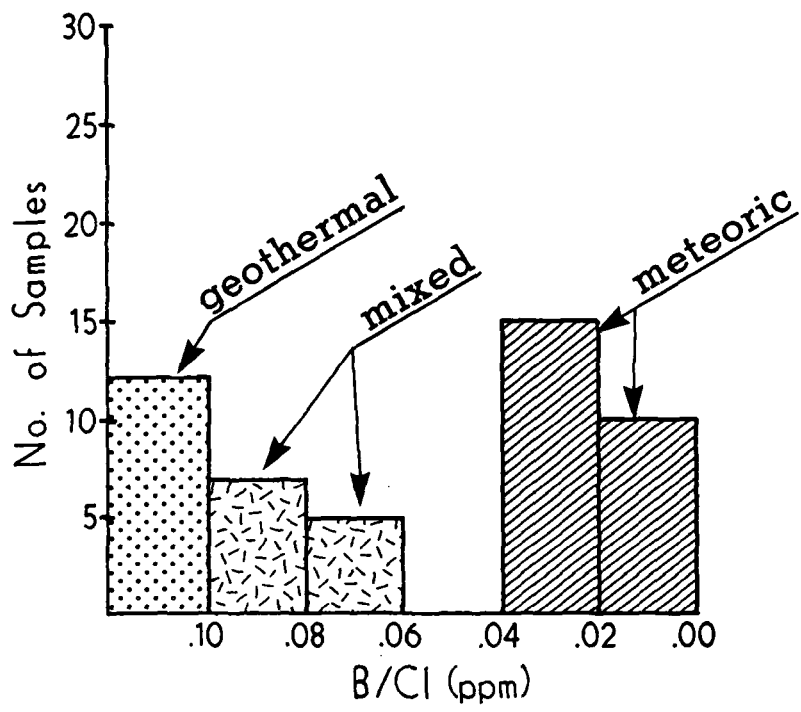


Figure 5.1.2

subsurface temperatures. The latter methods assume particular importance during the exploration drilling stage because they can provide immediate information on the temperatures and permeability in the well during the drilling program. In contrast, it may be several weeks after drilling before the thermal gradients in the wells "re-equilibrate" and accurate direct measurements can be made.

5.2 QUANTITATIVE FLUID GEOTHERMOMETERS

CHEMICAL GEOTHERMOMETERS

The chemical geothermometers are probably the most widely used (and misused) geothermometers. In this chapter we review the application of these various geothermometers. The equations of these geothermometers are listed in Tables 5.2.1 and 5.2.2.

SILICA GEOTHERMOMETERS

The concentration of silica in geothermal waters may be controlled by one of several different silica polymorphs (quartz, chalcedony, or amorphous silica). The solubilities of the different polymorphs is shown in Figure 5.2.1. At temperatures between about 150°C and 250°C, the silica content of geothermal waters is controlled by quartz. At higher temperatures reequilibration can take place rapidly and deposition of quartz is likely to occur as the solution cools. Furthermore, the solubility of amorphous silica may also be exceeded as the fluid cools, and because amorphous silica precipitates more rapidly than quartz, opal may be deposited in the near surface parts of the reservoir. As a result of silica precipitation, temperatures above about 225-250°C are generally not indicated by the silica geothermometer.

The quartz geothermometer may be affected by several other factors. These include: 1) the effects of steam separation, 2) polymerization of silica after sample collection as a result of improper preservation, 3) control of silica by other silica polymorphs, 4) the effect of pH (Fig. 5.2.2), and 5) dilution of the thermal waters. These effects are discussed in detail by Fournier (1981).

At temperatures below 150-180°C it appears that other silica polymorphs

Table 5.2.1 Equations expressing the temperature dependence of selected geothermometers.

C is the concentration of dissolved silica. All concentrations are in mg/kg.

GEO THERMOMETER	EQUATION	RESTRICTIONS
a. Quartz-no steam loss	$t^{0C} = \frac{1309}{5.19 - \log C} - 273.15$	$t = 0^{\circ}C-250^{\circ}C$
b. Quartz-maximum steam loss	$t^{0C} = \frac{1522}{5.75 - \log C} - 273.15$	$t = 0^{\circ}C-250^{\circ}C$
c. Chalcedony	$t^{0C} = \frac{1032}{4.69 - \log C} - 273.15$	$t = 0^{\circ}C-250^{\circ}C$
d. α -Cristobalite	$t^{0C} = \frac{1000}{4.78 - \log C} - 273.15$	$t = 0^{\circ}C-250^{\circ}C$
e. β -Cristobalite	$t^{0C} = \frac{781}{4.51 - \log C} - 273.15$	$t = 0^{\circ}C-250^{\circ}C$
f. Amorphous silica	$t^{0C} = \frac{731}{4.52 - \log C} - 273.15$	$t = 0^{\circ}C-250^{\circ}C$
g. Na/K (Fournier)	$t^{0C} = \frac{1217}{\log (Na/K) + 1.483} - 273.15$	$t > 150^{\circ}C$
h. Na/K (Truesdell)	$t^{0C} = \frac{855.6}{\log (Na/K) + 0.8573} - 273.15$	$t > 150^{\circ}C$
i. Na-K-Ca	$t^{0C} = \frac{1647}{\log (Na/K) + \beta[\log(\sqrt{Ca/Na}) + 2.06] + 2.47} - 273.15$	$t < 100^{\circ}C, \beta = 4/3$ $t > 100^{\circ}C, \beta = 1/3$
j. Mg correction for Na-K-Ca geothermometer* (see next page)		
k. $\Delta^{18}O(SO_4^{2-}-H_2O)$	$1000 \ln \alpha = 2.88(10^6 T^{-2}) - 4.1$	
	$\alpha = \frac{1000 + \delta^{18}O(HSO_4^-)}{1000 + \delta^{18}O(H_2O)}$ and $T = ^{\circ}K$	
l. Na/Li	$t^{0C} = \frac{1000}{\log(Na/Li) + 0.38} - 273.15$	$Cl^- < 11,000 \text{ mg/kg}$ $t < 350^{\circ}C$

Table 5.2.1 (cont.)

$$\begin{aligned}
 * \Delta t_{\text{Mg}} = & 10.66 - 4.7415R + 325.87(\log R)^2 - 1.032 \times 10^5 (\log R)^2 / T - \\
 & 1.968 \times 10^7 (\log R)^2 / T^2 + 1.605 \times 10^7 (\log R)^3 / T^2, \quad (1)
 \end{aligned}$$

and for $R < 5$

$$\begin{aligned}
 \Delta t_{\text{Mg}} = & - 1.03 + 59.971 \log R + 145.05 (\log R)^2 - 36711 (\log R)^2 / T - \\
 & 1.67 \times 10^7 \log R / T^2, \quad (2)
 \end{aligned}$$

where

$R = [\text{Mg}/(\text{Mg} + \text{Ca} + \text{K})] \times 100$, with concentrations expressed in equivalents.

Δt_{Mg} = the temperature correction in °C that should be subtracted from the Na-Ka-Ca calculated temperature.

T = the Na-K-Ca calculated temperature in °K.

For some conditions, equations 1 and 2 may give negative values for Δt_{Mg} . In that event, do not apply a Mg^{++} correction to the Na-K-Ca geothermometer.

TABLE 5.2.2

<u>Geothermometer</u>	<u>Equation</u>	<u>Restrictions</u>
<u>a</u> K/Mg (For fluids of oceanic origin)	$t^{0}C = \frac{4410}{13.95 - \log\left(\frac{K^2}{Mg}\right)} - 273.15$	$t < 200^{\circ}C$
<u>b</u> Na/Li (For brines)	$t^{0}C = \frac{1195}{\log Na/Li - .13} - 273.15$	$t < 300^{\circ}C$ $Cl^{-} > 11,000 \text{ mg/kg}$
<u>c</u> Mg/Li (For oilfield brines)	$t^{0}C = \frac{1900}{4.67 + \log(\sqrt{Mg/Li})} - 273.15$	$40^{\circ} < t < 250^{\circ}C$

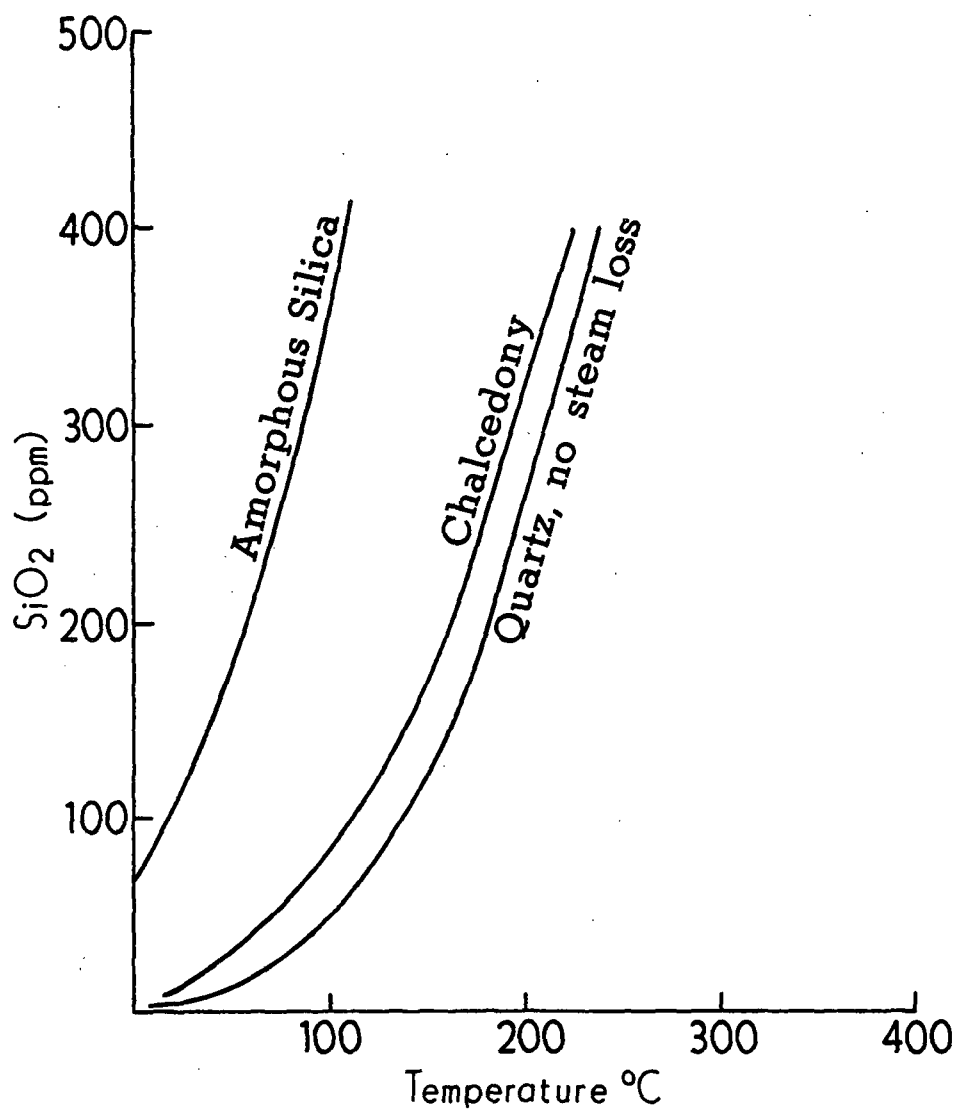
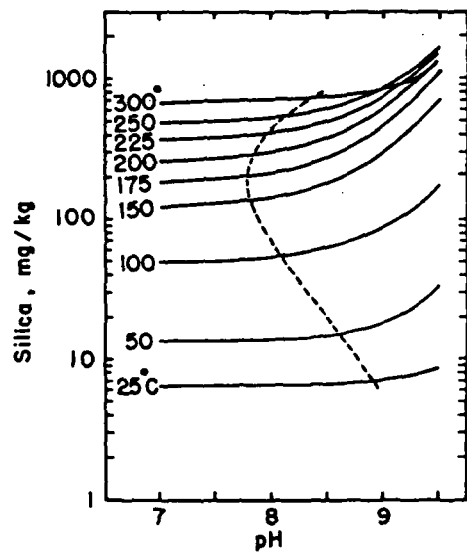


Figure 5.2.1



Calculated effect of pH upon the solubility of quartz at various temperatures from 25°C to 350°C, using experimental data of Seward (1974). The dashed curve shows the pH required at various temperatures to achieve a 10 per cent increase in quartz solubility compared to the solubility at pH 7.0
 © 7-0

Figure 5.2.2
 from Fournier (1981)

may control the silica contents of the fluid. Arnorsson (1975) showed that in basaltic rocks in Iceland the silica content of waters having temperatures between 50°C and 110°C is controlled by chalcedony. Either quartz or chalcedony controlled the aqueous silica in Icelandic waters between 110°C and 180°C. The temperature above which the fluids are in equilibrium with quartz in granitic rocks and sandstone appears to be slightly lower. Fouillac (1977, in Fournier, 1981) suggests that aqueous silica is controlled by quartz above 90°C and by chalcedony at lower temperatures in these terrains.

At reservoir temperatures below 90°C, however, non-equilibrium reactions may locally result in silica contents that are much higher than those predicted by quartz or chalcedony. In these areas high silica contents may reflect acid alteration of silicate minerals or sluggish precipitation of silica. Acid may be supplied by the decay of organic detritus, oxidation of sulfides or influx of H₂S or CO₂ (Fournier, 1981).

ALKALI GEOTHERMOMETERS

Several different geothermometers involving Na, K, Ca, Li and Mg have been proposed and modified during the last several years. These include the Na/K geothermometer of Fournier (1979) and of Truesdell (1976), the Na-K-Ca geothermometer of Fournier and Truesdell (1973), the Na/Li geothermometer of Fouillac and Michard (1981) and the K-Mg geothermometer proposed by Giggenbach et al. (1983).

THE Na/K GEOTHERMOMETER

The Na/K geothermometer is particularly useful in high-temperature environments above 150-180°C, although reliable temperature data can sometimes be obtained for reservoirs as low as 100°C. Henley et al. (1984), however, argue that at temperatures below about 200°C, ion exchange reactions between

the geothermal fluids and clay minerals may occur, resulting in temperature estimates that are too high. Despite the potential difficulties, the Na/K geothermometer often yields good results because it is less affected by dilution or steam separation than many of the other geothermometers.

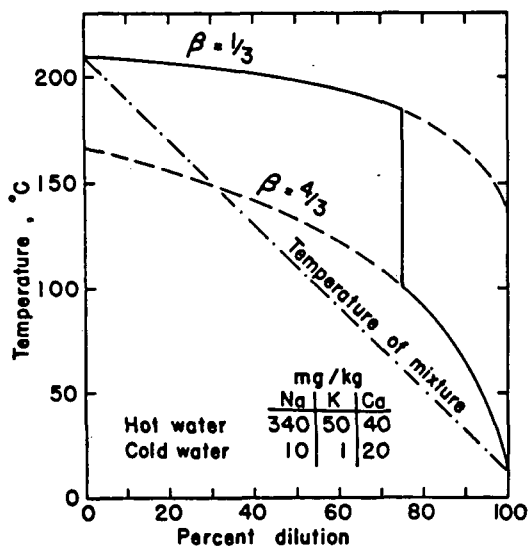
Na-K-Ca GEOTHERMOMETER

The Na-K-Ca geothermometer (Table 5.2.1) by Fournier and Truesdell (1973) is calibrated to give reliable temperature estimates over a much broader range, from 100-300°C. The value used for β in Equation 1 can be either 4/3 or 1/3. A value of 4/3 should be used if the calculated temperature is less than 100°C and $[\log(\sqrt{\text{Ca}/\text{Na}} + 2.06)]$ is greater than 0. If the calculated temperature with $\beta = 4/3$ is greater than 100°C or if $[\log(\sqrt{\text{Ca}/\text{Na}})]$ is negative then the geothermometer temperature should be calculated using $\beta = 1/3$.

Boiling, mixing with cold water, and high Mg and CO₂ contents can affect the geothermometer temperatures. The effect of boiling is to reduce the Ca content of the fluids through precipitation of calcite. In this case the calculated temperatures will be too high. The effect of dilution will be slight if the salinity of the high-temperature water is much greater than the cold water it mixes with. The effects of dilution increase with the amount of cold water (Fig. 5.2.3). Because it is very difficult to evaluate the extent of mixing, the geothermometer temperatures should be used with extreme care.

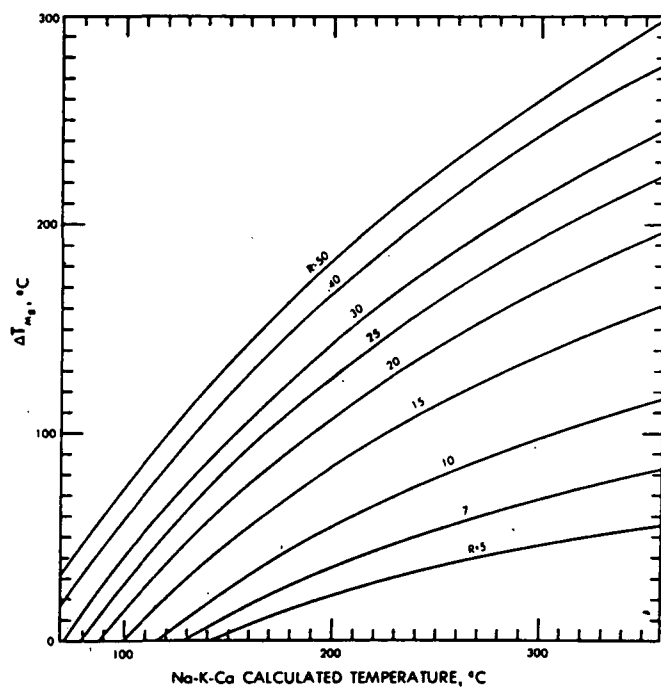
Geothermal waters containing high concentrations of Mg give Na-K-Ca temperatures that are too high. An empirical temperature correction that is subtracted from the calculated temperature was presented by Fournier and Potter (1979). The correction can be determined graphically (Fig. 5.2.4) for various R values or from the following equations.

For R between 5 and 50



For the indicated starting compositions, the effect of dilution of hot water by cold water upon the calculated Na-K-Ca temperature. Different starting compositions will give different results

Figure 5.2.3
from Fournier (1981)



Graph for estimating magnesium temperature correction, Δt_{Mg} , to be subtracted from the Na-K-Ca calculated temperature $R = 100 \text{ Mg}/(\text{Mg} + \text{Ca} + \text{K})$, expressed in equivalents. (From Fournier and Potter, 1979)

Figure 5.2.4

$$\Delta t_{Mg} = 10.66 - 4.7415R + 325.87(\log R)^2 - 1.032 \times 10^5 (\log R)^2 / T - 1.968 \times 10^7 (\log R)^2 / T^2 + 1.605 \times 10^7 (\log R)^3 / T^2, \quad (5.2.1)$$

and for $R < 5$

$$\Delta t_{Mg} = -1.03 + 59.971 \log R + 145.05(\log R)^2 - 36711(\log R)^2 / T - 1.67 \times 10^7 \log R / T^2, \quad (5.2.2)$$

where

$R = [Mg / (Mg + Ca + K) \times 100]$, with concentrations expressed in equivalents.

Δt_{Mg} = the temperature correction in °C that should be subtracted from the Na-K-Ca calculated temperature.

T = the Na-K-Ca calculated temperature in K ($^{\circ}\text{C} + 273.15$).

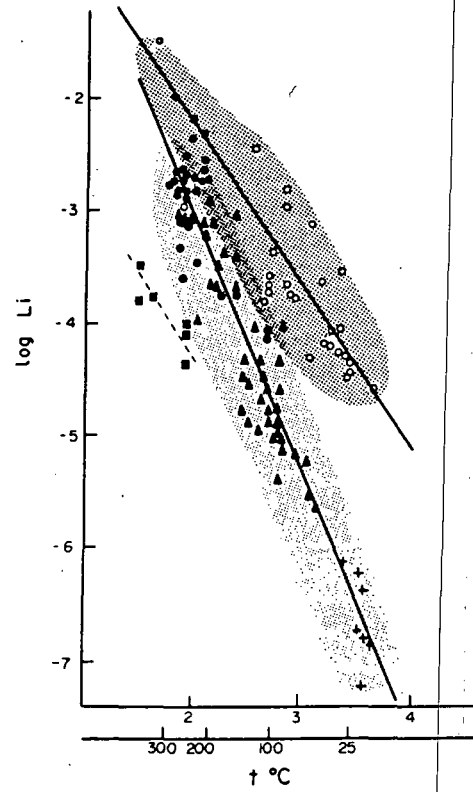
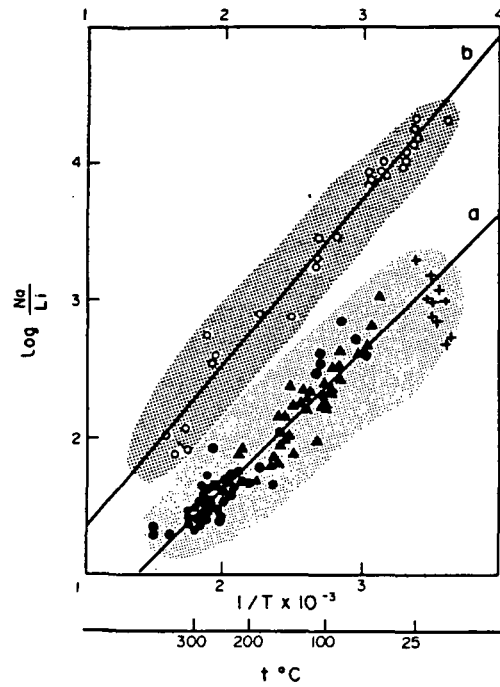
If the value of Δt_{Mg} is negative, do not apply a Mg^{++} correction to the Na-K-Ca geothermometer. Moreover, where $R > 50$ the measured temperature of the spring is taken as the temperature of equilibration.

Na/Li GEOTHERMOMETER

Another cation geothermometer, proposed by Fouillac and Michard (1981), is the Na/Li geothermometer. This method is based on the empirically derived correlation of $\log \text{Na/Li}$ with temperature. The Na/Li geothermometer is less sensitive to reequilibration than the Na/K or the Na/K/Ca geothermometer.

Two equations for the Na/Li method are provided here. Both methods are good to 350°C. The first method listed in Table 5.2.1 is to be used for fluid of meteoric origin. The second listed in Table 5.2.2 is to be used with fluids of known marine origin or brines with Cl greater than 11000 mg/kg. The data points used to calibrate these geothermometers are shown in Figure 5.2.5.

Lithium minerals are uncommon in geothermal systems, and thus it is



Log Na/Li in waters vs the inverse of absolute temperature. Key: (a) general line, closed symbols; (b) brine line, open symbols. ○, ● Measured temperatures. ▲ Estimated temperatures. + Surface waters. ■ Experimental water-rock interactions.

Log Li in waters vs the inverse of absolute temperature. Same symbols as in Fig. 1. Darker shading is for saline waters, lighter shading for low salinity waters.

Figure 5.2.5
from Fouillac and Michard (1981)

unlikely that the concentration of Li is related to any specific mineral equilibria. It is more likely that the concentration of Li is controlled by cation exchange reactions among clays and zeolites.

GEOOTHERMOMETRY OF BASIN BRINES AND MODIFIED SEA WATER

Several geothermometers have been developed empirically to predict the subsurface temperatures of basin brines and thermally-modified seawater. These include the Na/Li (Fouillac and Michard, 1981), the K/Mg (Giggenbach et al., 1983), and the Mg/Li (Kharoka et al., 1985) geothermometers. Equations for these geothermometers are listed in Table 5.2.2.

The K/Mg geothermometer of Giggenbach (1983) has been proposed for situations where Na and Ca do not equilibrate rapidly enough, such as in seawater in a low-temperature aquifer. This geothermometer has been used successfully by us at Ascension Island (Adams, unpublished report).

The Mg/Li method proposed by Kharoka et al. (1985) has been calibrated with more than 200 formation-water samples from 30 oil and gas fields in the U.S.A. Temperatures of these brines ranged from 40°-200°C. Quartz, Mg/Li, Na-K-Ca-Mg, and Na/Li geothermometers give concordant subsurface temperatures that are within 10°C of the measured values for reservoir temperatures higher than about 70°C. Mg/Li, Na/Li, chalcedony, and Na/K geothermometers give the best results for reservoir temperatures from 40° to 70°C.

The thermal modification of seawater has been studied experimentally by Bischoff and Seyfried (1978), Mottl and Holland (1978), and Seyfried and Bischoff (1979), among others. Although the validity of some of these experiments is not clear-cut, comparison of the results of these experiments with the in-situ studies of ocean-derived geothermal brine in Iceland does allow us to make some generalizations.

Annorsson (1978) compared the Icelandic Reykjanes brine to seawater.

This comparison is shown in Table 5.2.3. It can be seen that the primary modification of seawater is the dramatic loss of Mg and SO_4 , and the gain of K, Ca, CO_2 and SiO_2 . Experimental work has attributed these changes to the precipitation of $\text{Mg SO}_4(\text{OH})_x \cdot (\text{H}_2\text{O})_y$, dissolution of calcite and quartz, leaching of basalt, and influx of volcanic gases. It has been suggested that these changes happen when seawater is heated above 150° to 250°C .

Mizukami and Ohmoto (1983) have studied the geochemistry of heated seawater in tuff-rich environments. Their data indicate that the concentrations of Na, K, Ca, Mg, Sr, Co, and SO_4 reflect the meteoric to seawater ratio, cation exchange reactions involving smectite and feldspar, equilibria involving gypsum, anhydrite and calcite, and the water to rock ratios. The actual reactions involved are not yet well understood and probably vary from field to field (Adams, 1984, unpub. data).

MIXING GEOTHERMOMETERS

Mixing and boiling can adversely affect the geothermometer calculations. The effect of mixing on geothermometers is generally one of dilution. The geothermometers that are affected adversely by dilution are the Na-K-Ca-Mg, the Mg/K, the Mg/Li, and the silica geothermometers. Those geothermometers that retain their signature despite dilution are the Na/K and the Na/Li.

There are many situations which can result in fluid mixing. These all involve vertical or lateral spreading and mixing of geothermal fluid with each other or with meteoric water. These fluids can be mathematically unmixed to obtain the composition, mixing proportions, and temperature of the original unmixed fluids (end members), i.e. a mixing geothermometer can be applied. This approach can reveal information on the true compositional variability of the thermal fluids as well as information on the direction of hydrologic flow

Table 5.2.3 The concentration of analytical components in sea-water and geothermal waters in the Reykjanes Peninsula.

Figures in ppm

Component	Sea-water	Reykjanes well 8		Svartsengi well 4	Krisuvik well 6	Krisuvik well 5
	10°C	269°C	283°C			
Na	10556	10135	9629	6279	700	210
K	380	1480	1409	973	119	13.8
Ca	400	1628	1551	950	42.4	10.6
Mg	1272	1.0	1.0	6.0	0.4	0.2
SiO ₂	3.0	600	572	444	514	220
CO ₂	114	1438	1764	457	62.2	63.0
H ₂ S	-	26.7	32.7	1.9	6.6	4.4
SO ₄	2649	22.2	21.2	34.0	49.6	178.2
F	1.3	0.10	0.10	0.12	0.50	0.45
Cl	18980	19727	18785	12070	1094	118.0

and on the mechanisms of mixing. However, there is little use in mathematically unmixing fluids whose end-member compositions are not constant. Thus NaCl fluids, which are generally constant in composition, rather than acid SO_4 or NaHCO_3 fluids, are generally used in mixing calculations. There are two types of mixing; simple mixing where there is no loss or gain of constituents after mixing, and complex mixing, where precipitation, dissolution, or ion exchange takes place.

Simple mixing can best be examined using a Piper diagram. As shown in Figure 5.2.6, a mixture (C) of fluids A and B will always plot on a line drawn between A and B. The ratio of the distances AC/AB will be the fraction of fluid B in the mixture C, and BC/AB will define the fraction of fluid A in the mixture.

Complex mixing occurs when the temperature sensitive components of a mixed fluid re-equilibrate at a new temperature. The relative proportion of Na and K can exchange, Ca and SO_4 concentrations can increase from the dissolution of calcite and anhydrite (gypsum), and SiO_2 concentration can be reduced by the precipitation of a silica polymorph.

However, some elements do not form or react with minerals at the salinities and temperatures of most geothermal fluids. These are Cl, B, Br, and I. Because the concentrations of Br and I were generally too low to measure in moderate-temperature geothermal fluids not derived from seawater, Cl and B are generally used to develop mixing models.

In any calculation of mixing the most basic and important tool is the mixing equation, which is also called the lever rule. This equation is applied to the chloride-enthalpy and silica-enthalpy methods discussed below, and can also be applied wherever mixing is suspected and the concentration of the conservative elements (i.e., B, Cl) are known.

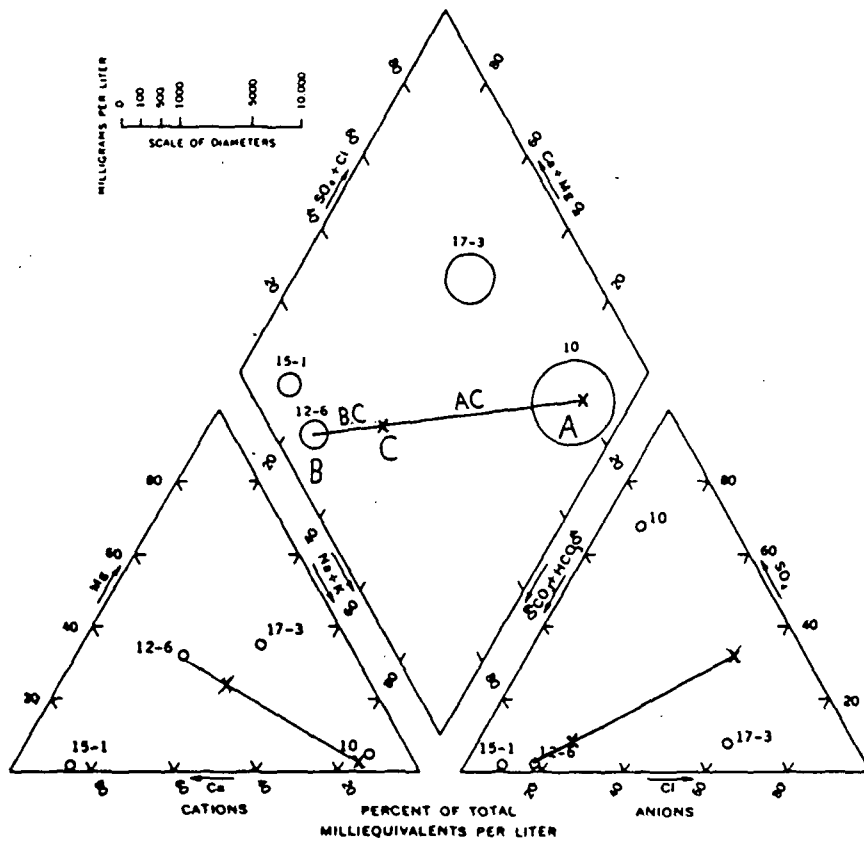


Figure 5.2.6

from Hem (1970), x = sample calculation in text

The composition of a mixed fluid is determined by the composition and proportions of each end-member. This is defined by:

$$C_{\text{mix}} = C_{\text{cold}} \times C_{\text{geothermal}} (1-X). \quad (5.2.3)$$

The composition of the undiluted geothermal fluid is determined by:

$$C_{\text{geothermal}} = \frac{C_{\text{mix}} - C_{\text{cold}}}{1 - X} \quad (5.2.4)$$

where C_{mix} = the mixed fluid sample concentration,

C_{cold} = the concentration of the cold fluid,

$C_{\text{geothermal}}$ = the geothermal concentrations, and

X = the fractional brine in the mixed fluid.

In order to use this method the composition of the cold water must be known. This can generally be determined by regional sampling or by using the most dilute sample as an end-member.

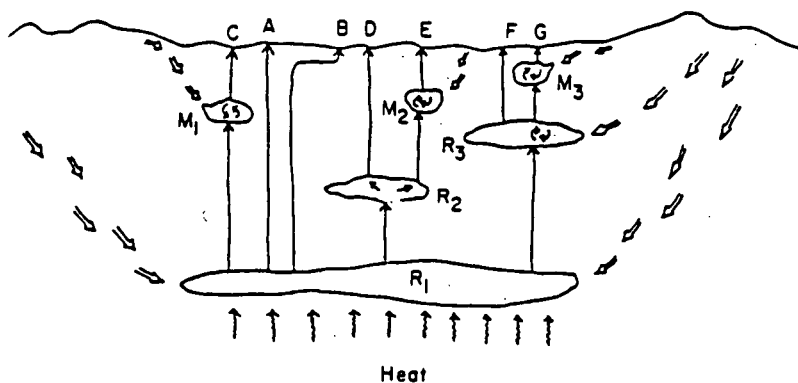
CHLORIDE-ENTHALPY DIAGRAMS

One means of examining the relationships among the various processes and fluids in a geothermal system is through the use of chloride-enthalpy diagrams. These diagrams make use of the fluids' heat content combined with any indications of dilution or concentration to elucidate processes such as conductive cooling, boiling, and mixing. These processes affect the estimated subsurface temperature, which is obtained from chemical geothermometers. Temperature estimation by the use of chemical geothermometers is reviewed above. The most extensive study of chloride-enthalpy relationships is that of Fournier (1979). In order to use the relationship between composition and enthalpy we must first consider what happens during conductive cooling, boiling, and mixing.

If conductive cooling has occurred, the spring temperature may be much lower than the maximum reservoir temperature, and changes in the composition of the water will probably occur as a result of mineral precipitation and reactions with the rocks. Table 5.2.4 shows the maximum rates of mass flow required for conductive cooling without boiling and the minimum rates for adiabatic cooling (boiling) with negligible conductive cooling if 200°C water moves vertically along a pipe and cools to 100°C (Truesdell et al., 1977). Bodvarsson (1950) has shown that fluids which move laterally, even with much larger mass flow rate, may also cool entirely conductively. Conductive cooling is likely where warm springs are characterized by different temperatures but with Cl concentrations that are similar to each other. The Cl contents of the springs will in this case be nearly the same as those of the deep reservoir. Both the silica and alkali contents of the waters may, however, change during conductive cooling.

Geothermal waters flowing directly to the surface at large mass rates will cool by boiling (adiabatic cooling) if the initial temperatures are above 100°C. During boiling the concentration of the nonvolatile species can increase. If cooling is entirely the result of boiling then it is very simple to calculate the concentrations of each component prior to boiling. Most boiling springs cool both by adiabatic and conductive processes. Generally, however, the relative effect of each is unknown, and these must be estimated.

Figure 5.2.7 summarizes the effects of boiling and mixing on the temperatures and compositions of spring waters above a deep geothermal reservoir. In this model, presented by Fournier (1979), it is assumed that only a single rock type is present, and that the fluids have equilibrated with the rock in reservoirs R_1 , R_2 and R_3 . Even if it is assumed that no chemical changes occur as a result of chemical reactions during upward flow, only



Schematic section through a hypothetical hot-spring system. The stippled areas represent reservoirs of hot water with the temperature of $R_1 > R_2 > R_3 > 100^\circ\text{C}$. Hot springs emerge at points A through G. Each spring illustrates a different condition of upward flow that may affect the water temperature and chemical composition: A = direct to surface from R_1 ; adiabatic cooling with fast flow and conductive cooling with slow flow. B = horizontal flow near the surface; conductive cooling possible even with fast flow. C = direct to surface from R_1 , but mixing with colder water at M_1 on the way, without chemical reequilibration after mixing. D = chemical reequilibration in intermediate reservoir R_2 . E = after reequilibration in R_2 , mixing with colder water at M_2 ; no chemical reequilibration after mixing. F = chemical reequilibration after mixing with cold water in shallow reservoir R_3 . G = mixing with colder water after leaving R_3 ; no chemical reequilibration after mixing at M_3 .

Figure 5.2.7
from Fournier (1979)

springs A and B provide direct information on the deep reservoir (R_1). The chemistry of D, after correcting for boiling, provides information on the temperature of R_2 and the salinity of R_1 and R_2 . Spring F gives data on only the temperature of R_3 . The chemistry of R_3 reflects mixing of R_3 and R_1 .

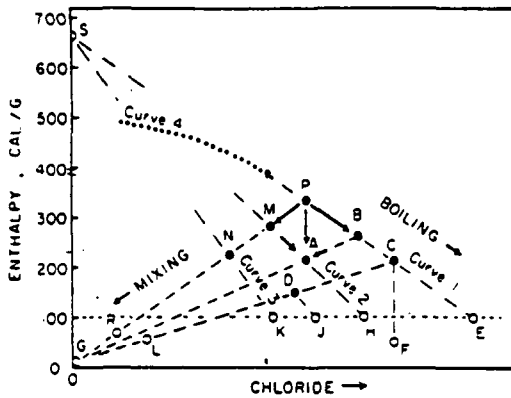
The following discussion on enthalpy chloride diagrams is taken from Fournier (1979).

Enthalpy is the heat content of water at a given temperature, pressure, and a specified phase (i.e., liquid). With these parameters an enthalpy can be assigned to each sample.

Enthalpies are listed in Table 5.2.5. The enthalpy/liq. column should be used for water samples. Once the enthalpy is assigned to a sample the chloride content and enthalpy should be plotted as the horizontal and vertical axes, respectively.

"Enthalpy-chloride diagrams have been used in several papers (Fournier et al., 1976a,b; Truesdell and Fournier, 1976; Fournier, 1977) to predict underground temperatures, salinities, boiling and mixing relations. The following discussion is intended to clarify procedures and assumptions used to construct such diagrams.

Referring to Figure 5.2.8, waters that result from mixing of a low-enthalpy (low-temperature) water, such as G, with high-enthalpy waters such as P, B, or C lie along lines radial to G. For example, waters M, N, and R could result from the mixing of waters G and P in different proportions. Similarly, waters D and L could result from the mixing of G and C in different proportions. Generally the low-temperature end member is much lower in chloride than the thermal waters. There are places where this may not be true, however, such as where sea water is involved or where the anions in thermal water are mainly bicarbonate.



Hypothetical plot of enthalpy relative to chloride for various waters that result from boiling and mixing of hot and cold waters. Dots refer to waters that have equilibrated chemically with the surrounding rock at a temperature corresponding to the indicated enthalpy. Circles refer to springs and waters that have not equilibrated after attaining their final enthalpy and temperature. The horizontal dashed line at 100 cal/g shows where boiling springs plot at one bar atmospheric pressure.

Figure 5.2.8
from Fournier (1979)

In Figure 5.2.8, waters initially at 300°C or less, that lose heat only by the formation and separation of steam (boiling) resulting in the evaporative concentration of chloride, lie along approximately straight lines extending away from the enthalpy of steam at the steam separation temperature. These evaporative concentration or boiling lines are slightly curved because the enthalpy per unit mass of steam ranges from 626 cal/g* at 340° to a maximum of 670 cal/g at 240°C and then back down to 639 cal/g at 100°C**. Using a constant value of 664 cal/g as a point of origin, point S in Figure 5.2.8, and drawing straight lines radial to that point introduces very little error if subsurface boiling takes place below 340°C (liquid water enthalpy of 380 cal/g). The dot-dashed straight lines labeled 1, 2, and 3 are drawn radial to the point at zero chloride and 664 cal/g. Points B, C, and E can be related to P by boiling along curve 1. Point K can be related to N by boiling along curve 3. The straight-line approximation is progressively poorer at temperatures higher than 300° because the enthalpy of steam changes very quickly as the critical temperature is approached; at 370°C the enthalpy of steam is only 557 cal/g. The heavy dotted curve labeled 4 shows the marked departure of curve 1 from linearity above 340°C up to 370°C.

In Figure 5.2.8, the water represented by point L is well below boiling after mixing, and unless that water remains underground at that temperature for several weeks or months, water-rock chemical reequilibration is not likely to occur after mixing. Also, because the temperature is below boiling, the chloride content is not likely to change during subsequent movement of the

* 1 cal/g = 4.18 Joules/g

** As salt concentrations increase the enthalpies of the solutions and coexisting steam depart from those of pure water and pure steam. In the system NaCl-H₂O the departure is very small for salinities less than about 10,000 mg/kg (R. W. Potter, oral communication) and no enthalpy corrections for changing salt concentrations have been applied to the diagrams presented in this paper.

water to the surface unless more mixing occurs or evaporite deposits are involved. In contrast, the water represented by D has a temperature well above 100°C after mixing, and water-rock chemical reequilibrium may occur in hours or days owing to the higher temperature. Also, water D could boil as it moves upward to the surface, and this boiling could cause the final chloride content to be as high as that of water J.

Point A in Figure 5.2.8 is drawn to illustrate that a deep parent water, P, can be related to water such as A by various mechanisms: (1) water P can first boil to produce water B, and then B can mix with some G to give A; (2) water P can first mix with some G to give water M, and M can then boil to produce A; or (3) water P may cool conductively to give A directly without boiling or mixing. Although the chloride and enthalpy of A are the same regardless of the route taken from P to A, it is likely that volatile chemical constituents would vary depending on whether boiling took place before or after mixing, or not at all.

In many places all the hot-spring waters that reach the surface are mixed waters or have equilibrated chemically in shallow or intermediate reservoirs or aquifers. Thus, direct information about deeper and hotter water in the system is not obtained by the simple application of chemical geothermometers such as silica (Fournier and Rowe, 1966) or Na-K-Ca (Fournier and Truesdell, 1973). A consideration of the enthalpy and chloride relations may overcome this difficulty. Information about enthalpies and chloride contents of subsurface waters such as A, C, and N in Figure 5.2.8 can be obtained by various methods: (1) direct measurement of waters produced from shallow wells; (2) estimates based on hot-spring compositions using chemical geothermometers such as silica and Na-K-Ca, and then correcting for possible steam loss as discussed by Fournier et al. (1974, 1976a); and (3) estimates

based on warm-spring mixing models (Truesdell and Fournier, 1977). As an illustration of the use of hot-spring data, the enthalpy of point C might be obtained from the composition of spring E, F, or L or a combination of these springs. If the composition of a vigorously boiling spring with a discharge greater than about 300 l/minute such as E is used, then a correction must be made for the probable maximum evaporative concentration of chloride owing to boiling on the way to the surface. Proceed as follows: calculate the temperature of the water supplying spring E using chemical geothermometers (Fournier and Rowe, 1966; Fournier and Truesdell, 1973) and then convert that calculated temperature to enthalpy using steam tables (Keenan et al., 1969). This gives the enthalpy of point C. Next plot point E on the enthalpy-chloride diagram using the measured temperature and chloride content of that spring water, and then draw a straight line from E to S, the steam point at zero chloride and 664 cal/g. Along this line mark the previously calculated enthalpy of C. This gives a graphical determination of the chloride content of C, correcting for maximum possible separation of steam. Boiling springs with flows less than about 200-300 l/minute may have cooled partly by conduction and partly by the formation of steam. In this event the calculated initial chloride content of the deep water is ambiguous. If a nonboiling spring such as F is used (and, using criteria discussed by Fournier et al., 1976b, it seems likely that either F is not a mixed water or chemical equilibration occurred after mixing), it can be assumed that no steam separated during movement to the surface and point C will plot directly above F at the enthalpy obtained using chemical geothermometers and steam tables.

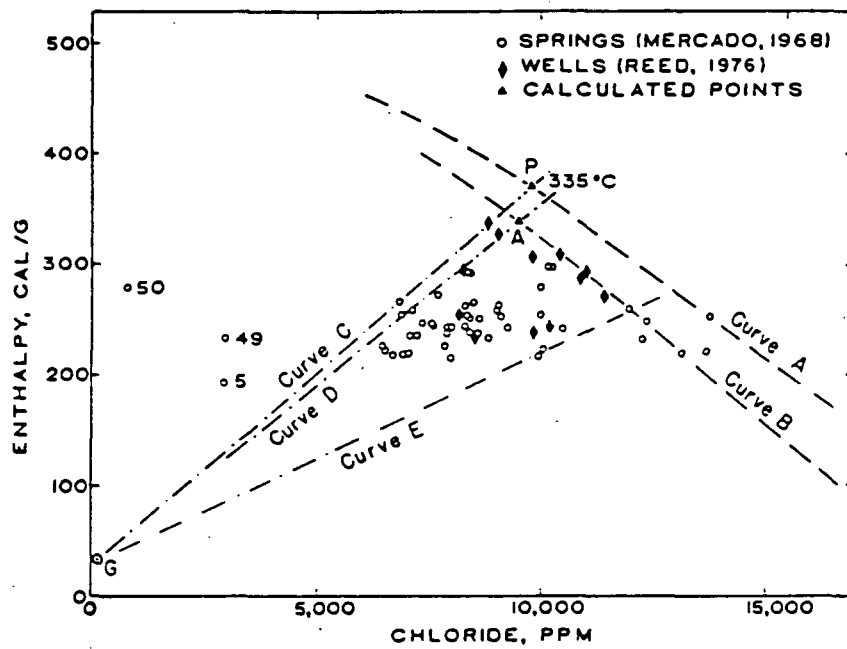
In Figure 5.2.8, assume that the enthalpy and chloride content of A and N have been estimated using hot-spring data and the above procedures. (Point N could have been obtained either from the mixed-water warm spring R or from

boiling spring K, and point A from the boiling spring H). If it is further assumed that A and N are related to a common parent water, then that parent water must lie in the enthalpy chloride field on or above and to the left of the extension of the mixing line G-N-M and on or above and to the right of the extension of the boiling curve H-A-M (curve 2). The minimum possible enthalpy of that parent water is given by the intersection of the two lines, point M. Similarly, if points C and N are known from shallow-well data or from estimates using hot-spring compositions, the minimum enthalpy of a common parent water is given by point P, the intersection of the mixing and boiling lines passing through N and C, respectively. The above principles have been used to interpret subsurface temperatures and mixing relationships in several geothermal systems from hot-spring data in order to test the usefulness of the model.

The circles in Figure 5.2.9 show calculated subsurface enthalpy-chloride values for hot spring waters at Cerro Prieto, Mexico, using hot-spring data published by Mercado (1968). Most of the springs are below boiling temperature, and the silica contents are irregular with respect to spring temperatures (Fig. 5.2.9), suggesting that some silica precipitated during movement of the waters to the surface. Therefore, Na-K-Ca-estimated temperatures (Fournier and Truesdell, 1973) were used to calculate enthalpies of the plotted points. Springs 5, 49, and 50 (Fig. 5.2.9) may be in part steam-heated waters so that the calculated enthalpies are anomalously high and the chlorides are anomalously low. Therefore, they were not included in determining the upper mixing line, curve C. Curve C is drawn radiating from G, the assumed enthalpy and chloride content of the nonthermal groundwater in the region. Curve C is the mixing line that is the upper boundary for all of the estimated points except for the three noted above. Curve A is the upper bounding boiling curve. The intersection of curves A and C is at P where the

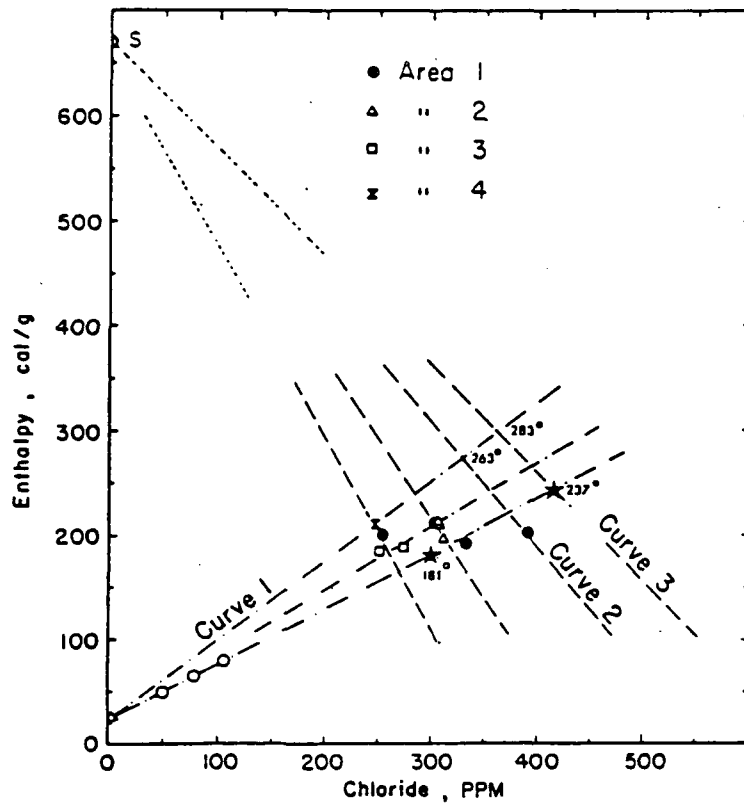
enthalpy of liquid water, 372 cal/g, requires a temperature of 335°C. Curves D and B give a more conservative boundary for most of the data points, and the intersection of these two curves is at an enthalpy that requires 315°C water. Curve E sets a lower limit for the waters that seem to be mixed waters. If a common parent water is present in the system, it should have a temperature at least as high as 315°C and possibly higher than 335°C. Thus, using only these hot-spring data and the enthalpy-chloride mixing model, it would have been possible before drilling to predict accurately that temperatures in excess of 300°C would be found and that mixed waters would be found in some parts of the system. If one takes a very optimistic position and assumes that springs 5 and 49 (Fig. 5.2.9) are valid points (do not have a "steam-heated" component) for determining the upper limit of mixing relationships in the enthalpy-chloride diagram, a minimum subsurface temperature of about 370°C is indicated. This is close to the temperature reported by Mercado (1970) for well M-10. The diamonds show enthalpy chloride data for deep waters produced from wells, using data presented by Reed (1976). Several of the wells produce waters that plot along or close to curve B (Fig. 5.2.9), a boiling curve. Therefore, the waters entering those wells probably are related by simple boiling. Other wells produce waters that plot far to the left of curve B, inside the region bounded by curves C and E. These wells produce mixed water.

Figure 5.2.10, showing calculated subsurface enthalpy-chloride values for waters at Orakeikorako, New Zealand, was constructed using data of W. A. J. Mahon (in Lloyd, 1972). The silica geothermometer was used to estimate subsurface temperatures of waters from boiling springs. The highest underground temperature indicated by the silica geothermometer is about 215°C. The starred waters at 237° and 181°C represent aquifers calculated to be present



Enthalpy-chloride graph of data from springs at Cerro Prieto, Mexico.

Figure 5.2.9
from Fournier (1979)



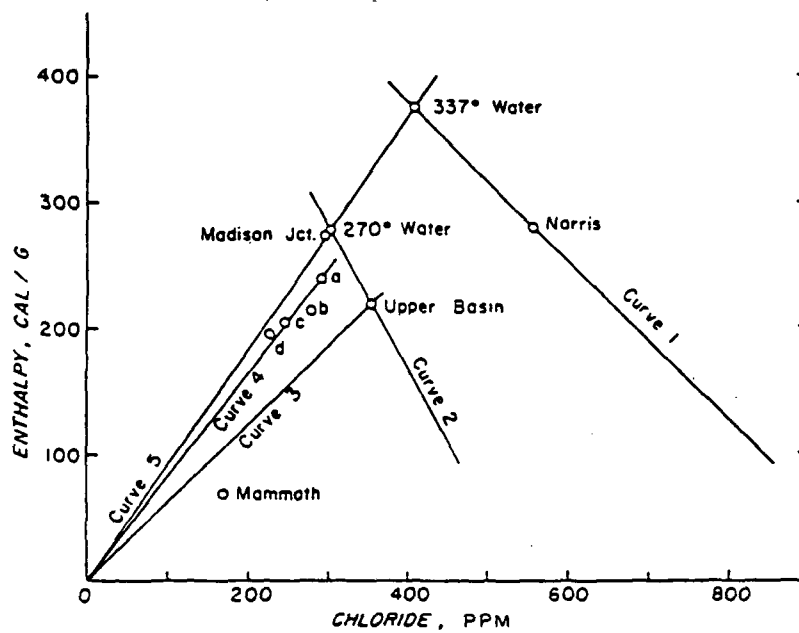
. Enthalpy-chloride graph of data from springs at Orakeikorako, New Zealand. Circles are warm springs with discharge rates greater than 5 l/s. Stars represent high-temperature components of mixed waters calculated from the warm-spring mixing model of Truesdell and Fournier (1977). The other symbols represent estimated subsurface conditions using groups of compositionally similar, boiling or near-boiling springs from the four geographic areas denoted by W.A.J. Mahon (in Lloyd, 1972).

Figure 5.2.10
from Fournier (1979)

using the springs shown by circles and the warm-spring mixing model technique of Truesdell and Fournier (1977). If only the boiling-spring data are considered, a parent water at 263°C (minimum temperature) with about 340 ppm Cl (~475 ppm Cl after decompressional cooling and steam separation at atmospheric pressure) can be inferred from the intersection of curves 1 and 2. A temperature of 260°C is reported (Ellis, 1966) for a well (hole 2) at Orakeikorako. However, the chloride in that well water is 546 ppm rather than 475 ppm after steam separation at atmospheric pressure. But, if the warm-spring mixing model point at 237°C is assumed to be valid, a parent water at 283°C with about 370 ppm Cl (~555 ppm Cl after steam separation) can be inferred from the intersection of curves 1 and 3. Although the 283°C water has not been confirmed by deep drilling, the predicted chloride content after maximum boiling to atmospheric pressure (555 ppm) is very close to that found in the water produced from hole 2. This strongly suggests that an aquifer at a temperature higher than 260°C is present at depth greater than the present drilled depth.

Measured temperatures of aquifers found by three other comparatively shallow wells are as follows: OK-6, 212°; OK-2, 218-224°; and OK-3, 232-241°C. The aquifer predicted at 237°C using the warm-spring mixing model falls nicely within the temperature range of the actual aquifer found in well OK-3, 232-241°C.

Figure 5.2.11 shows calculated enthalpy-chloride values for subsurface waters at Yellowstone National Park. Points on the diagram were calculated by Fournier et al. (1976a) using groups of springs of similar composition found in different geographic localities. Figure 5.2.11 shows that waters in localities a through d, curve 4, from within the Yellowstone caldera are related by mixing of hot water with cold water. Although the highest

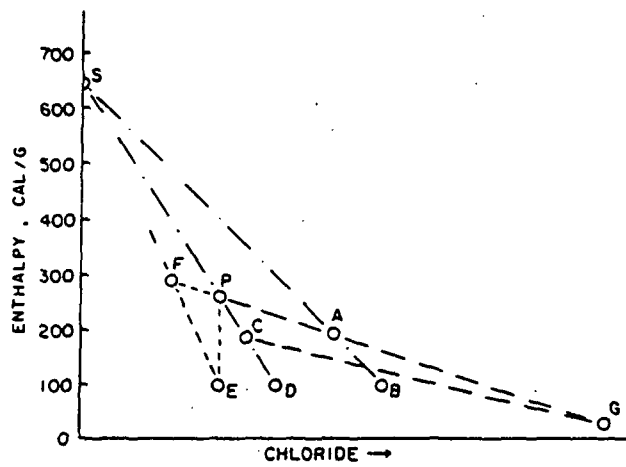


Enthalpy-chloride graph of data from Yellowstone National Park, Wyoming (after Fournier et al., 1976a).

Figure 5.2.11
from Fournier (1981)

temperature found in shallow drillholes (less than 330 m deep) was 238°C (White et al., 1975), it is reasonable to expect the hydrothermal system at Yellowstone Park to attain much higher temperature because the top of a large body of magma is believed to exist beneath the caldera at a relatively shallow depth (Eaton et al., 1975). The highest temperature predicted by applying chemical geothermometers directly without mixing models is about 270°C at Norris, and most spring waters elsewhere give predicted temperatures of 170° to 215°C (points b, c, and d and Upper Basin in Figure 5.2.11) (Fournier et al., 1976a). Drilling in Midway and Lower Geyser basins showed that aquifers at 170°C and about 200°C do exist there. Drilling at Norris showed that the aquifer temperature is greater than 238°C (White et al., 1975). If a common parent water does exist at Yellowstone Park, it should have a minimum temperature of 337°C.

In the preceding discussion the situation was not illustrated in which the cold-water component has a larger chloride content than the deep hot-water component. Where this occurs the boiling and mixing relationships may be difficult to sort out because both the mixing and evaporative concentration lines may trend in the same direction. In Figure 5.2.12, the cold, nonthermal water, G, is at the extreme lower right side of the diagram and P is the deep hot-water component. Mixing lines G-A-P and G-C are radial to G and have slopes less than the evaporative concentration lines S-P-C and S-A-B. If point G and at least two other points such as A and C are known, an estimate can be made of the minimum enthalpy and maximum chloride content of a possible common parent water, P. Point P is at the intersection of the evaporative concentration line drawn through C and the mixing line drawn through A. Note that care must be taken to distinguish between waters related by evaporative concentration and those related by conductive cooling. For example, in Figure



Enthalpy-chloride graph showing relations where the nonthermal water, *G*, has a higher chloride content than the hot-water component, *P*. See text for additional discussion.

Figure 5.2.12
from Fournier (1981)

5.2.12, assume that point E is related to P by conductive cooling. If the water represented by E is mistakenly assumed to have cooled adiabatically, a parent water at F would be estimated erroneously.

In Figure 5.2.12 if the cold-water component happened to have a chloride content near or between points D and E it would be necessary to use some other dissolved constituent to sort out the boiling and mixing relationships."

SILICA-ENTHALPY MIXING EQUATIONS

The concentration of silica, unlike Cl, is regulated by temperature. However, in high-flow rate springs and springs below 150°C, silica of a high-temperature origin can persist. Thus, the silica-enthalpy method can sometimes give additional information about original temperature where the chloride-enthalpy cannot. This is especially true where conductive cooling has eliminated a lot of original enthalpic information. The best treatment of silica-enthalpy is by Fournier and Truesdell (1974), and the following discussion is from that study. A simplified method, as given by Truesdell and Fournier (1977), is also discussed.

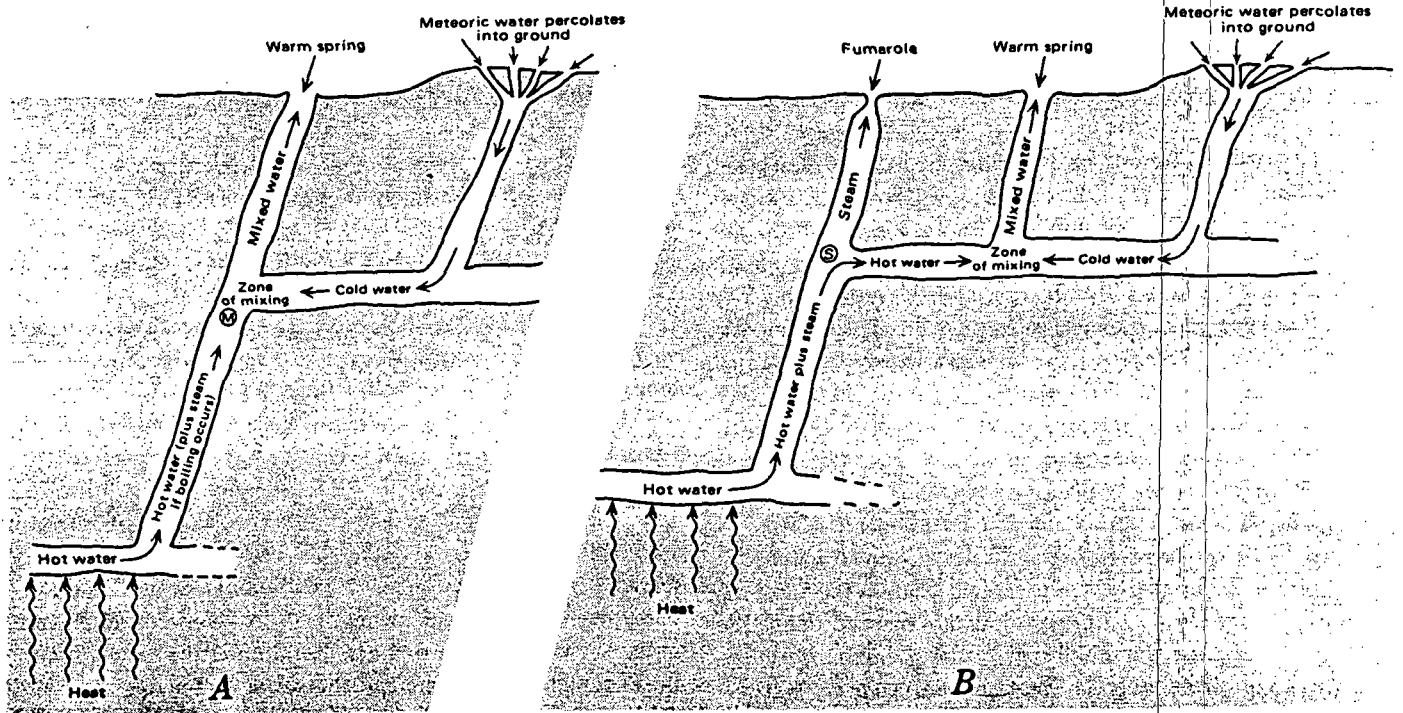
"The silica geothermometer (Fournier and Rowe, 1966) has been the most reliable single chemical indicator of reservoir temperature in spring systems that are high in silica and are characterized by sinter deposits and boiling waters. There is an ambiguity, however, in using the silica content of a warm spring to test for water-rock equilibration at the spring temperature: a high silica content in the spring water may be due to either solution of quartz at a much higher temperature (with or without subsequent mixing of hot and cold waters) or solution of cristobalite or amorphous silica at the spring temperature. Therefore, the silica geothermometer (Fournier and Rowe, 1966) should be used with great caution to test for water-rock equilibration at the

spring temperature. Although supersaturated silica solutions may occur in nature over a wide range in temperatures, they are not likely to persist for long periods of time above about 150°C (Fournier, 1973). This is critical for the models that we present in this paper.

MIXING MODELS

Two mixing models that allow calculation of the temperature and fraction of the hot water component are shown schematically in Figure 5.2.13. In model 1, Figure 5.2.13, hot water ascends from depth along a permeable channel, possibly a fault or joint. Depending on the initial temperature, the water may boil (cool adiabatically) as it rises. In this event, the water and newly forming steam rise together. At some point, M in Figure 5.2.13, the hot water encounters cold water from a permeable stratum. At the depth of mixing the weight of a column of cold water extending up to the surface is greater than the weight of the warm mixed water. Thus, the pressure relations are such that cold water enters the hot-water channel and the mixture flows to the surface and is discharged as a warm spring. Depending on the proportion of hot to cold water and the initial enthalpies of each, the spring may have a temperature ranging from very low to boiling.

In model 2, Figure 5.2.13 we assume that boiling occurs in the rising hot water and that some or all of the resulting steam escapes from that water (point S) before the hot water mixes with cold water. We show a fumarole where the steam emerges and a warm spring where the hot water mixed with cold water emerges. Alternatively, the separated steam might possibly condense and combine with shallow ground water and give rise to other warm springs that are not amenable to the methods suggested here. For this reason attention must be paid to be the chemical character of the springs.



—Schematic model (A) for obtaining a mixed-water warm spring in which both the enthalpy and silica content of the hot-water content are the same as in the original deep water (model 1) and schematic model (B) in which the hot-water component has lost steam before mixing with cold water (model 2). (See text for discussion.)

Figure 5.2.13

from Fournier and Truesdell (1974)

If the channel above S is filled with steam, boiling at S will be at atmospheric pressure, provided there are few constrictions in the channel or impediments to the escape of steam (no throttling occurs). If throttling of the steam occurs, or if the channel is partly or completely filled with water, boiling and escape of steam at S will be at greater than atmospheric pressure.

In both models of Figure 5.2.13 the calculations depend upon knowledge of the temperature and silica content of the cold water before mixing* and those of the warm spring water after mixing. In addition, it must be assumed that the initial silica content of the deep hot water is controlled by the solubility of quartz and that no further solution or deposition of silica occurs before or after mixing. Numerous observations have shown that natural water deep in hot-spring systems generally is just saturated with quartz (Mahon, 1966; Fournier and Truesdell, 1970; Ellis, 1970; Fournier, 1973). Furthermore, our observations in Yellowstone National Park (Fournier and Truesdell, 1970) and elsewhere (White, 1974) suggest that ascending boiling water generally does not dissolve or precipitate silica if the rate of upflow is fast.

In the calculations that follow, model 1 gives a probable maximum subsurface temperature attained by the hot-water component, and model 2, a probable minimum subsurface temperature. On the basis of the total chemical and physical character of the warm spring, its relation to other hot springs and fumaroles, and its geologic environment, it may be possible to choose the temperature that is more likely to be correct. Even where this is not possible, information on the range of possible subsurface temperatures will be of great interest.

* If the average temperature and silica content of nonthermal ground water in the region are not known, we suggest estimating the mean annual temperature and using 25 mg/l of silica as a first approximation.

CALCULATIONS

Model 1

In this model the enthalpy of the hot water plus steam that heats the cold water is the same as the initial enthalpy of the deep hot water. Two equations can be written to solve for the two unknowns--the temperature of the hot water and the proportions of the hot and cold water--because the silica content and temperature of the warm spring are different functions of the original temperature of the hot-water component. The first equation relates the heat contents or enthalpies of the hot water, H_{hot} ; cold water H_{cold} ; and spring water, H_{spg} ; and the fractions of cold water, X , and of hot water, $1-X$, as follows

$$(H_{cold})(X) + (H_{hot})(1-X) = H_{spg} \quad (5.2.5)$$

Below 100°C the enthalpy of liquid water coexisting with steam (saturated water) in calories per gram is essentially equivalent in magnitude to the temperature of the water in degrees Celsius. Above 100°C the relation of temperature and enthalpy of saturated water can be found in steam tables (Table 5.2.5).

In a similar manner the second equation relates the silica contents of hot water, Si_{hot} ; cold water, Si_{cold} ; and spring water, Si_{spg} :

$$(Si_{cold})(X) + (Si_{hot})(1-X) = Si_{spg} \quad (5.2.6)$$

The relation of dissolved silica to the temperature of the aquifer supplying the hot-water component is given by the solubility of quartz at the vapor pressure of the solution (Morey and others, 1962; Fournier, unpub. data, 1974). A graphical solution can be obtained as follows:

1. Assume a series of values of enthalpy of hot water for the temperatures

listed in Table 1 and calculate χ_t for each, as follows:

$$\chi_t = \frac{(\text{Enthalpy of hot water}) - (\text{Temperature of warm spring})}{(\text{Enthalpy of hot water}) - (\text{Temperature of cold spring})} \quad (5.2.7)$$

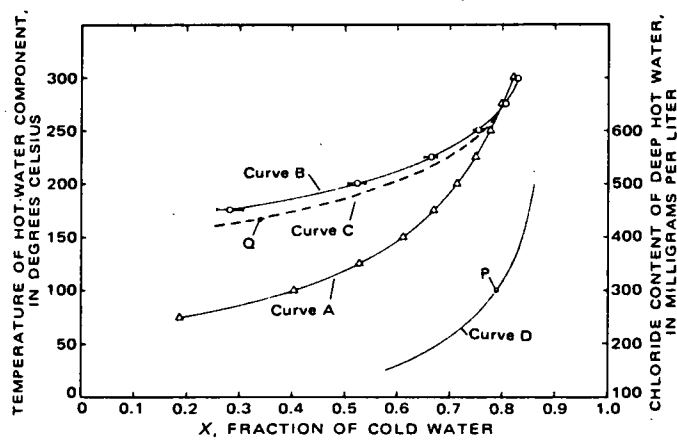
2. Plot the calculated values of χ_t in relation to the temperatures from which the assumed hot-water enthalpy values were derived (see Fig. 5.2.14, curve A).
3. Assume a series of silica contents of hot water appropriate for a variety of temperatures and evaluate χ_{Si} for each silica content, as follows:

$$\chi_{Si} = \frac{(\text{Silica in hot water}) - (\text{Silica in warm spring})}{(\text{Silica in hot water}) - (\text{Silica in cold spring})} \quad (5.2.8)$$

4. On the graph previously used, plot the calculated values of χ_{Si} in relation to the temperatures for which the silica contents were obtained (see Fig. 5.2.15, curve B).
5. The point of intersection gives the estimated temperature of the hot-water component and the fraction of cold water.

The two curves possibly may not intersect (Fig. 5.2.15) or they may intersect at an unreasonably high temperature. These situations would arise if the ascending hot water lost steam or heat before mixing with the cold water (model 2) or if the mixed water dissolved additional silica owing to contact with amorphous silica or rock containing glass. Therefore, we recommend that the mixing model described above be used with extreme caution for warm spring water that has silica contents about equal to the solubility of amorphous silica at the temperature of the spring. For temperatures below 200°C, the approximate solubility of amorphous silica can be calculated from the equation

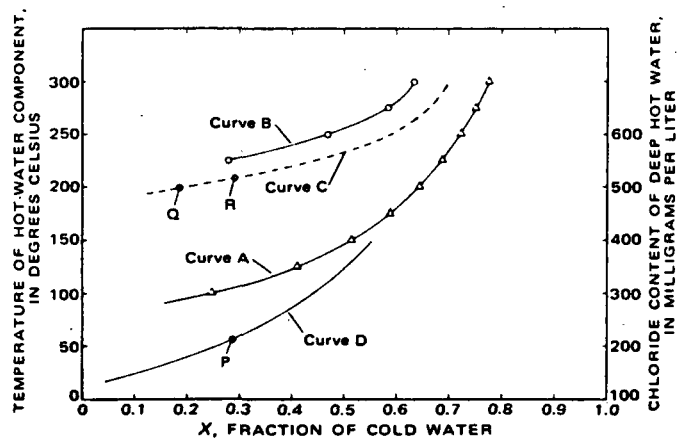
$$-\log C = \frac{731}{T} - 4.52 \quad (5.2.9)$$



—Fraction of cold water relative to temperature and chloride content of hot-water component in Terrace Spring. Triangles, X_t values listed in table 2; circles, X_{S_1} values. The horizontal bars show the possible error due to uncertainty in the silica analysis of the spring water. Points P and Q discussed in text. Curve A, Fraction of cold water based on model 1 enthalpy considerations. Curve B, Fraction of cold water based on model 1 silica considerations. Curve C, Fraction of cold water based on model 2 silica considerations. Curve D, Required chloride contents of deep water.

Figure 5.2.14

from Fournier and Truesdell (1974)



—Fraction of cold water relative to temperature and chloride content of hot-water component in Interchange Spring. Points P, Q, and R discussed in text. See figure 2 for explanation of symbols and curves.

Figure 5.2.15

from Fournier and Truesdell (1974)

where C is silica solubility in milligrams per liter and T is absolute temperature.

The actual temperature and silica content of the "cold" component at the point of mixing can seldom if ever be known with certainty. If either the temperature or silica content of the cold water were higher than the assumed value, the resulting estimated temperature of the hot-water component would be too high.

Model 2

The enthalpy of the hot water in the zone of mixing is less than the enthalpy of the hot water at depth owing to escape of steam during ascent. The silica content of the hot-water component, however, is fixed by quartz solubility at depth and subsequent enrichment in the liquid water fraction as steam separates. At the point where steam escapes from the ascending hot water and steam mixture, S in Figure 5.2.13, the residual silica concentration in the hot water increases and is given by the equation

$$\text{Residual silica} = \frac{\text{Original silica}}{1-y} \quad (5.2.10)$$

where y is the fraction of steam formed during movement of water from depth to S.

If one assumes a temperature, T_s , at which steam escapes, it is possible to calculate the residual silica for that condition and, using that information, estimate the original hot-water temperature before steam separates. In general, we set T_s equal to the boiling temperature imposed by local atmospheric conditions. This requires that escape of steam at point S of Figure 5.2.13 occurs at atmospheric pressure, and our calculation yields a minimum probable temperature for the hot-water aquifer. The calculation is carried out as follows:

1. Use the atmospheric boiling temperature for the value of H_{hot} in equation 5.2.5 and calculate the corresponding value of X .
2. Use that value X in equation 5.2.6 to estimate the residual silica content of the hot water at T_S .
3. Use the calculated residual silica content and curve A of Fournier and Rowe (1966, Fig. 5) to estimate the original subsurface temperature before separation of steam. Curve A of Fournier and Rowe is roughly approximated by the equation

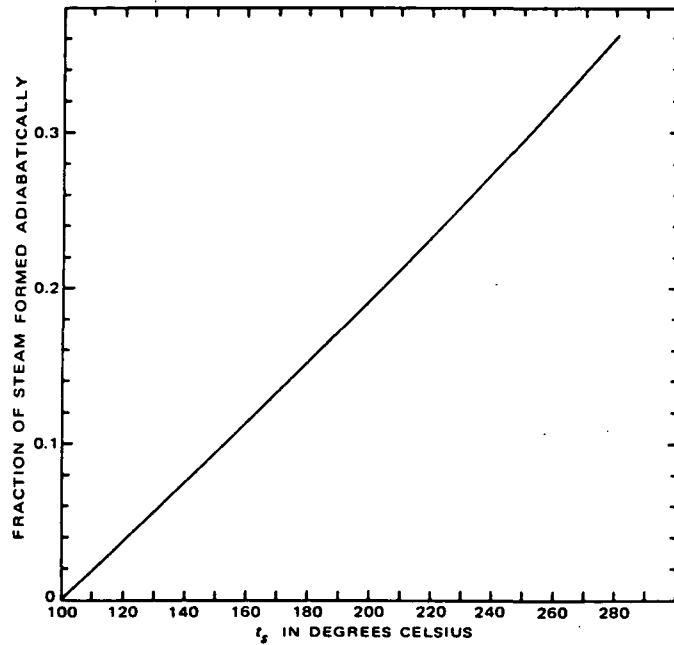
$$-\log C = \frac{1522}{t_{0C} + 273} - 5.75. \quad (5.2.11)$$

If superheated steam emerges from nearby fumaroles or if there are other reasons for believing that steam escapes at greater than atmospheric pressure, an alternate procedure should be used:

1. Assume a value of T_S appropriate for the pressure at which steam is thought to escape at point S of Figure 5.2.13.
2. Use steam tables to determine the heat content of liquid water in calories per gram at T_S and substitute that value in equation 5.2.5 to estimate a corresponding value of X .
3. Use that value of X in equation 5.2.6 to estimate the residual silica content of the hot water at T_S .
4. Estimate the silica content, C , that would have been present in the hot-water component if steam had escaped at atmospheric pressure using the relation

$$C = \frac{\text{Residual silica}}{1 - \frac{x}{1-y}} \quad (5.2.12)$$

where X is the fraction of steam that would be formed in going from T_S to the boiling temperature at atmospheric pressure (see Fig. 5.2.16) and y is the



—Fraction of steam that would form by adiabatic cooling from t_s to 100°C.

Figure 5.2.16

from Fournier and Truesdell (1974)

fraction of steam formed in going from the original temperature to T_s . Both y and C are unknown in equation 5.2.11. However, the value of y will generally range from 0 to about 0.3, and as a first approximation it can be set equal to 0.1.

5. Use the value of C and Curve A of Fournier and Rowe (1966, Fig. 5) or equation 5.2.11 to estimate the original subsurface temperature before separation of steam.

A more precise estimate is possible if an iterative process is used in which the value of y is adjusted to reflect successive estimates of the original temperature. In general, we do not believe that the overall accuracy of the method warrants this additional effort.

EXAMPLES OF APPLICATION

These mixing models proposed have been applied to a few large-flowing warm springs in Yellowstone National Park. The results are geologically reasonable but have been substantiated by shallow drilling in the proximity of only one (Interchange Spring) of the springs in question.

The average silica content of the nonthermal ground water in the park was found to be 25 ± 2 mg/l and the temperature of the coldest spring was 5°C , in good agreement with the mean annual temperature of 4°C .

Terrace Spring near Madison Junction flows at about 5,500 l/min, the water temperature is 62°C , and silica content is 140 mg/l (Allen and Day, 1935, p.353-354). The Na, K, and Ca contents of the water yield an estimated aquifer temperature of 200°C , using the method of Fournier and Truesdell (1973). As this temperature is far greater than the spring temperature of 62°C , the spring is assumed to be mixed-water type.

Calculated fractions of cold water, assuming various temperatures of hot

water and using model 1 and equations 5.2.7 and 5.2.8 are plotted in Figure 5.2.14, curves A and B. The curves intersect at 265°C and a cold water fraction of 0.79. This is a very high estimated aquifer temperature and can be thought of as the maximum probable temperature of the hot-water component.

Although there are no nearby fumaroles, boiling pools, or other physical evidence that points to model 2 as a reasonable possibility, we have applied that model to Terrace Spring in order to establish a lower limit to the probable maximum subsurface temperature at that locality.

Curve C of Figure 5.2.14 was generated by assuming various values of T_s and using equations 5.2.10 and 5.2.12 and other relations as discussed in the section on calculations. If steam escaped at atmospheric pressure from an ascending boiling water, the hot-water component would have been at about 92°C at the time of mixing with cold water, and the original temperature of that hot water would have been 165°C (point Q, Figure 5.2.14). This is the minimum probable temperature of the aquifer supplying the hot-water component. If higher pressures are assumed for escape of steam, larger fractions of cold water are required and higher estimated aquifer temperatures result, as shown by curve C, Figure 5.2.14. Again, the probable upper temperature limit is about 265°C where curves A, B, and C intersect at a common point.

For Terrace Spring the aquifer supplying the hot water is probably closer to 265° than 165°C. The spring is located between Lower Geyser Basin (9 km to the south) and Norris Geyser Basin (14.5 km to the northeast) at a relatively low topographic position along the bounding fault of a large caldera (Keefer, 1971; Christiansen and Blank, 1972). Recent drilling by the U.S. Geological Survey has shown that subsurface temperatures beneath parts of Lower Geyser Basin exceed 205°C; those beneath Norris Geyser Basin exceed 240°C (White and others, 1968). Silica and Na-K-Ca geothermometers applied to boiling hot-

spring water at Norris suggest subsurface temperatures of 250° to 270°C.

The Cl content of Terrace Spring, 64 mg/l is consistent with the higher aquifer temperature and correspondingly large calculated fraction of cold water. Given the Cl concentration in the spring and the average Cl in nonthermal water in the region (< 1 mg/l), the Cl content of the deep hot water can be calculated, assuming any given proportion of hot and cold water. Curve D, Figure 5.2.14 shows the results of that calculation. For a cold-water fraction of 0.79, the Cl content of the hot-water fraction would be about 300 mg/l (point P, Figure 5.2.14). This is close to the Cl content of thermal water (before steam loss) found at Lower Geyser Basin.

The second example is one in which mixing model 1 fails, but model 2 gives excellent results. Interchange Spring in Black Sand Basin came into being as a result of an excavation for a highway interchange for diverting traffic around the Old Faithful area. The spring had a temperature of 76°C, a silica content of 270 mg/l, and a flow rate of about 2,000 l/min. The Na-K-Ca content suggests a temperature of 205°C. The calculated fractions of cold water at given temperatures of the hot-water component are plotted in Figure 5.2.15.

The most notable feature of Figure 5.2.15 is that curve A, based on enthalpy considerations, and curve B, based on model 1 silica considerations, do not intersect. Evidently either steam escaped from the hot-water component before mixing or the warm spring water dissolved extra silica after mixing occurred. The warm water may be picking up extra silica, for it emerges from sands and gravels composed mostly of fresh obsidian. The obsidian glass could dissolve and raise aqueous silica to saturation with respect to amorphous silica. At 76°C the solubility of amorphous silica is 266 mg/l, which is within the analytical error of the 270 mg/l silica found in the spring water.

We favor the first alternative because the large rate of flow makes equilibration with amorphous silica unlikely and because model 2 gives results in close agreement with what is known about subsurface temperatures near Interchange Spring.

The variation of original hot water temperature relative to the fraction of cold water in the warm spring, curve C, Figure 5.2.15 is based on model 2 silica considerations. If steam escaped at atmospheric pressure before mixing of hot and cold water, the remaining hot water would have been at 92°C (boiling temperature at the altitude of the spring) and its original temperature would have been about 200°C (point Q, Fig. 5.2.15).

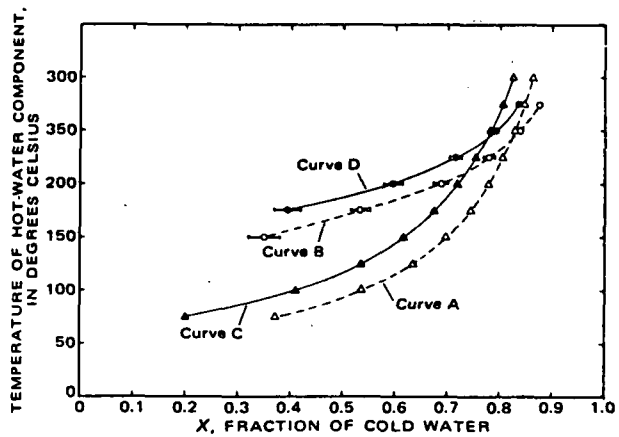
About the same temperature is estimated from Cl considerations. The chloride content of Interchange Spring is 224 mg/l, the calculated chloride contents of the hot-water component, assuming various fractions of mixed cold water, are shown by curve D, Figure 5.2.15. The highest concentration of Cl found in discharging boiling springs and geysers in Black Sand Basin was 315 mg/l. Presumably this is the residual Cl concentration attained after maximum separation of steam owing to adiabatic cooling of the ascending water. Therefore, the maximum Cl content of the hot-water component in Interchange Spring is likely to have been 315 mg/l; the corresponding maximum fraction of cold water 0.285 (point P, Fig. 5.2.15). This requires that the hot-water component has a temperature of 110°C or less at the time of mixing. For a cold water fraction of 0.285, curve C of Figure 5.2.15 shows an original hot-water temperature of about 208°C (point R).

The silica contents of boiling springs and geysers in the vicinity of Interchange Spring indicate an aquifer temperature of 190° to 205°C. In addition, two shallow holes drilled nearby indicate subsurface temperatures exceeding 170° to 180°C. Both holes were terminated before a maximum or

leveling off temperature was attained. One hole is about 900 m to the southeast and had a bottom-hole temperature of 180°C (Tenner, 1936). The other is about 600 m to the west and had a bottom-hole temperature of 170°C (White and others, 1968; Honda and Muffler, 1970).

Apparently the hydrologic system supplying water to Interchange Spring is very similar to model 2. We suggest that the hot-water fraction of the mixed water in Interchange Spring comes from an aquifer at 200° to 208°C. That water cools adiabatically, forming steam as it rises toward the surface. At a shallow level, but before mixing with cold water occurs, the high-enthalpy steam fraction escapes from the remaining lower enthalpy liquid water. This low-enthalpy water at 92° to 110°C then encounters cold ground water and a mixed water at 76°C results. The separated steam fraction probably emerges 350 m northwest of Interchange Spring at the Pine Springs group, where violently boiling springs occur with little or no discharge.

Ideally, large-flow warm springs in a given locality with different temperatures and different compositions should give the same estimated hot-water temperature. Such is found for two large-flow unnamed springs located between Biscuit Basin and Midway Geyser Basin in Yellowstone National Park. The springs have temperatures of 49° and 61°C and silica contents of 100 and 122 mg/l respectively. Applying model 1, the intersection of curves A and B, Figure 5.2.17, indicates a cold-water fraction of 0.82 for the 49°C spring and 243°C as the maximum probable temperature of the hot-water component. The intersection of curves C and D, Figure 5.2.17 gives exactly the same temperature, 243°C, for the high-temperature component of the 61°C water. As expected, the fraction of cold water, 0.77, is less in the 61°C water than in the 49°C water. Applying model 2, and assuming $T_s = 100^\circ\text{C}$, a minimum probable temperature of 166°C is obtained for the original temperature of the hot-water



—Fraction of cold water relative to temperature of hot-water component in two springs located between Biscuit and Midway Basins. See figure 2 for explanation of curves and symbols; open symbols refer to the 49°C water and solid symbols to the 61°C water.

Figure 5.2.17

from Fournier and Truesdell (1974)

component in each spring, which indicates clearly that two waters are mixing in different proportions. Unfortunately, additional data is insufficient to indicate whether the higher or lower estimated temperature of hot-water component is more nearly correct.

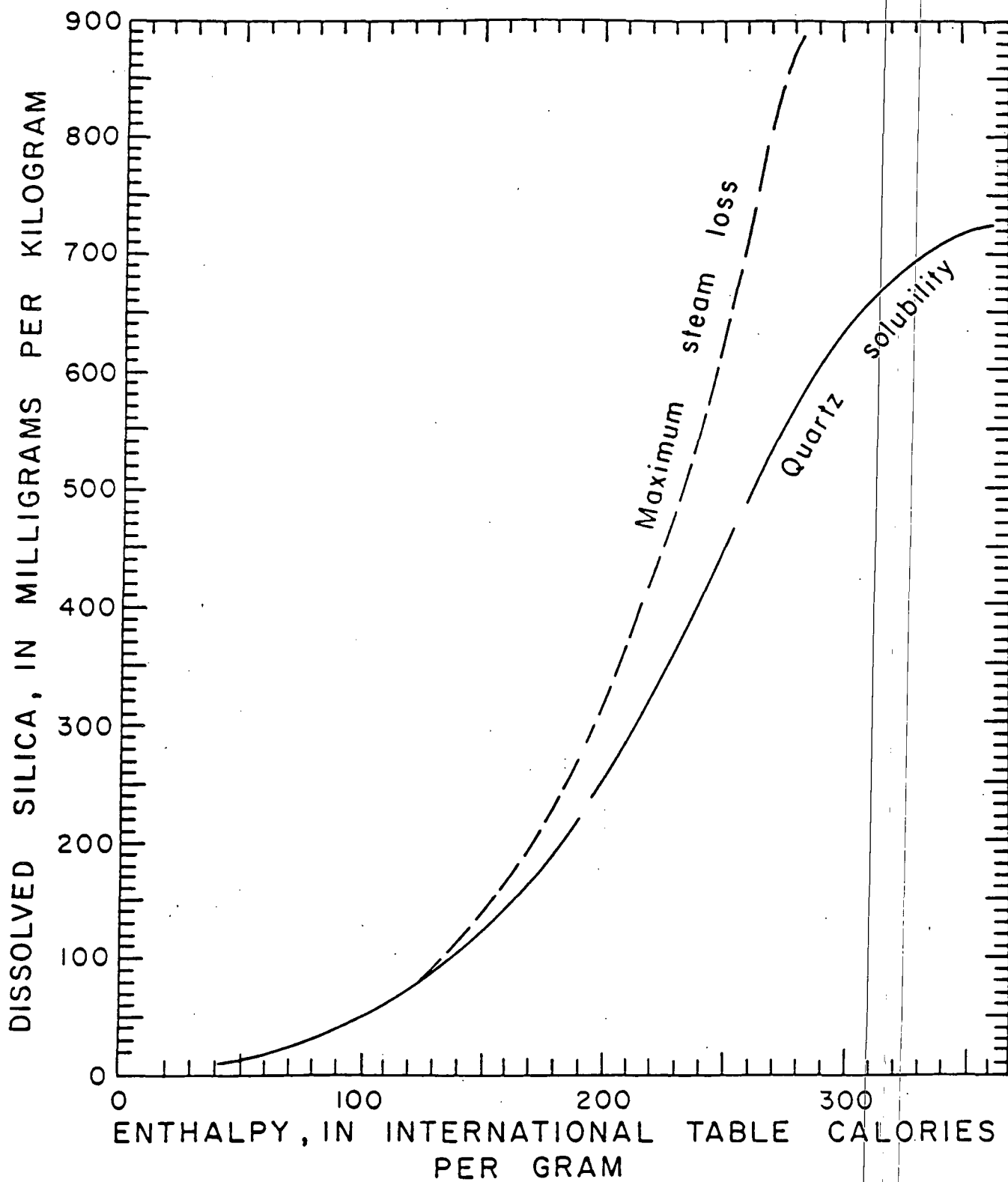
SILICA-ENTHALPY: SIMPLIFIED METHOD

Here we present simplified graphical procedures for obtaining silica-enthalpy results. The method makes use of the dissolved silica-versus-temperature graph of Fournier and Rowe (1966, Fig. 5), replotted in Figure 5.2.18 as dissolved silica versus enthalpy of liquid water in equilibrium with steam. To simplify the procedure, we have chosen to plot enthalpy in International Table calories (cal_{IT} per gram (above 0°C)) rather than joules per gram because the enthalpy of liquid water is numerically approximately the same as the temperature.

In using Figure 5.2.18, one may assume either that no steam or heat had been lost from the hot-water component before mixing or that steam had separated from the hot-water component at an intermediate temperature before mixing. In either event, it is necessary to assume that no loss of heat occurs after mixing, that the initial silica content of the deep hot water is controlled by the solubility of quartz, and that no further solution or deposition of silica occurs before or after mixing.

Procedure

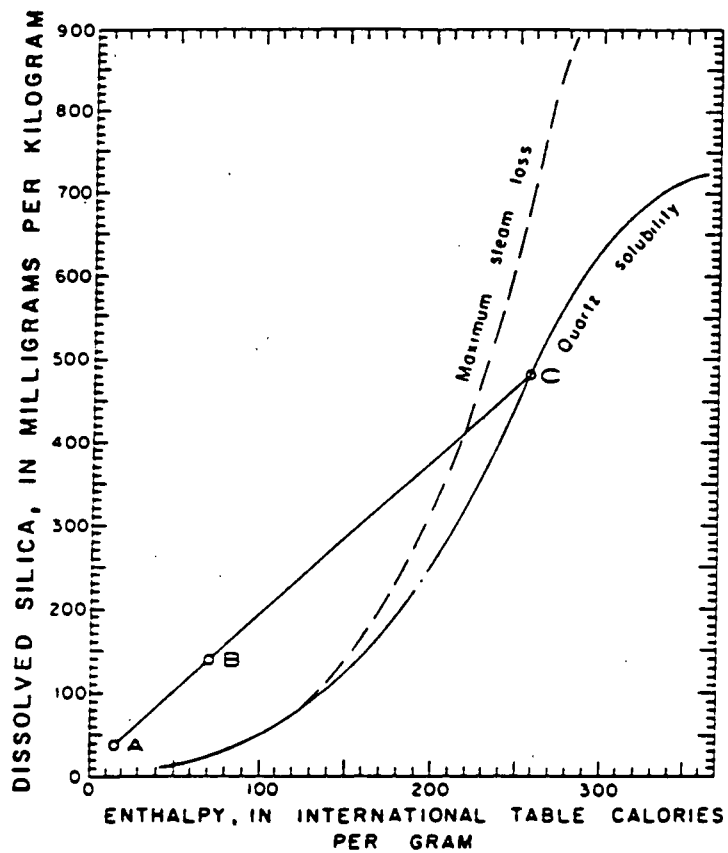
- Assuming no loss of steam or heat before mixing, then do the following:
1. Determine or estimate the temperature and silica content of nonthermal ground water in the region and plot as a point in Figure 5.2.18, the silica-versus-enthalpy graph. Plot temperatures in degrees Celsius as calories. This is shown as point A in Figure 5.2.19.



—Dissolved silica-enthalpy graph for determining temperature of a hot-water component mixed with cold water yielding warm spring water.

Figure 5.2.18

from Fournier and Truesdell (1977)



—Dissolved silica—enthalpy graph to be used when assumption is made that no steam or heat has been lost before mixing. See text for explanation.

Figure 5.2.19

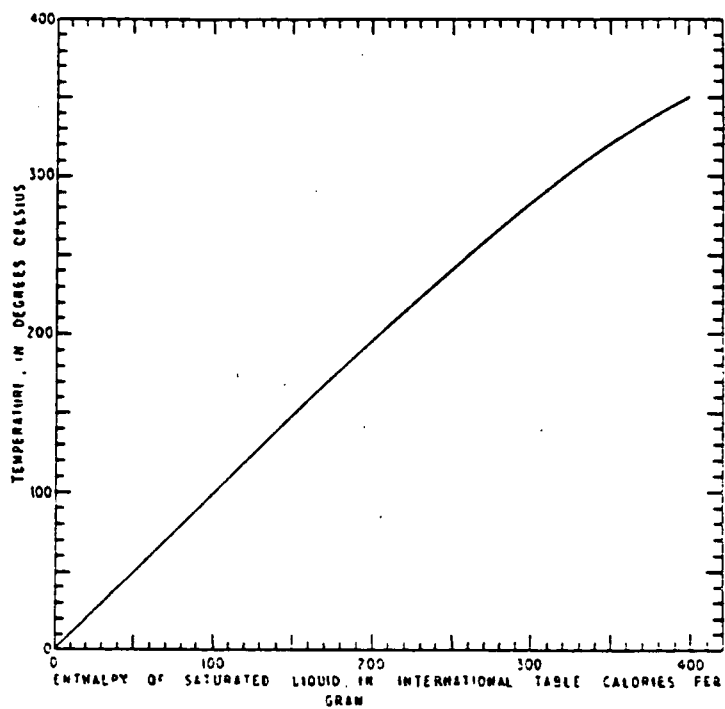
from Fournier and Truesdell (1977)

2. Plot the temperature and silica content of the warm spring water as another point on the graph, point B in Figure 5.2.19 (again plotting temperature as calories).
3. Draw a straight line through the two points and extend that line to intersect the quartz solubility curve, point C in Figure 5.2.19. Point C is the enthalpy and silica content of the deep hot-water component.
4. Obtain the temperature of the hot-water component from its enthalpy by using steam tables (Keenan and others, 1969) or Figure 5.2.20.
5. Determine the fraction of hot water in the warm spring by dividing the distance AB by AC.

It is possible that point B may plot at too high a silica value for the extension of line AB to intersect the quartz solubility curve. This may be due to the assumption of too low a value for the silica content of the nonthermal water, and this value may be increased if it seems reasonable. Alternately, the hot-water component may have lost heat, but not silica, before mixing. If heat was lost by separation of steam, it is possible to evaluate the situation.

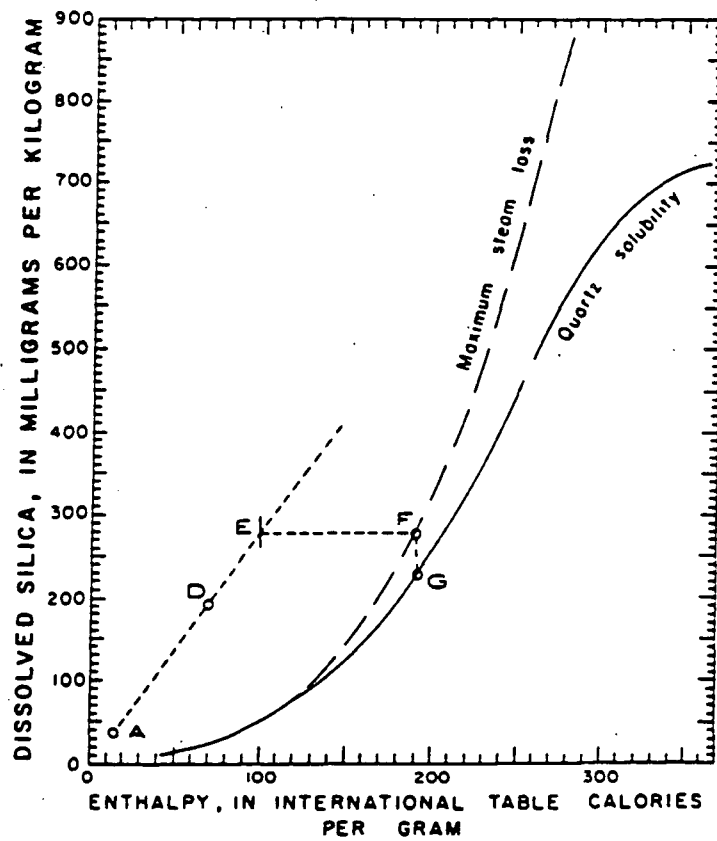
Assuming steam loss from an adiabatically cooled liquid before mixing with cold water, then do the following:

1. Plot the temperature and silica contents of the warm and cold waters as in the above procedure (Fig. 5.2.21, points A and D).
2. Draw a straight line between those points (A and D) and extend that line to the liquid-water enthalpy equivalent of the temperature at which steam is assumed to have escaped before mixing (point E for 100°C in Figure 5.2.21).
3. Move horizontally across the diagram parallel to the abscissa until the maximum steam-loss curve is intersected (point F in Fig. 5.2.21). Point



—Temperature-enthalpy relations for liquid water in equilibrium with steam.

Figure 5.2.20
from Fournier and Truesdell (1977)



—Dissolved silica—enthalpy graph to be used when assumption is made that steam separated at 100°C from the hot-water component before mixing. See text for explanation.

Figure 5.2.21

from Fournier and Truesdell (1977)

F gives the enthalpy of the hot-water component before the onset of boiling, and point G gives the original silica content before loss of steam occurred.

4. Determine the fraction of hot water (after steam loss) in the warm spring by dividing the distance AD by AE. The weight fraction of original hot water lost as steam before mixing, x , is given by the formula

$$x = 1 - \frac{\text{silica value at point G}}{\text{silica value at point F}} \quad (5.2.13)$$

If steam is lost at temperatures above 100°C, point F will lie on an intermediate steam loss (ISL) curve between the 100°C maximum steam loss (MSL) curve and the quartz solubility (QS) curve. The relative distance of the ISL curve from the QS and MSL curves is in the proportion $(H_{QS} - H_{ISL}) / (H_{ISL} - H_{100})$ where H_{QS} is the enthalpy of liquid water at the quartz solubility curve at a given value of silica, H_{ISL} is the enthalpy of liquid water at the actual temperature of steam loss, and H_{100} is the enthalpy of liquid water at 100°C.

If steam separates at less than 1 atmospheric pressure, the enthalpy of the residual liquid water will be less than 100 cal_{IT}/g. Point F will then be positioned at a different maximum steam-loss curve located slightly to the left of the maximum steam-loss line shown in Figure 5.2.21. However, the change in position of the maximum steam loss curve as a function of the atmospheric pressure (altitude) is generally trivial.

The maximum enthalpy of the hot-water component that can be reliably determined is set by the point at which an extended line, such as AB (Fig. 5.2.19), would be tangent to the quartz solubility curve. For most reasonable silica contents of nonthermal water, this will be at about 300 cal_{IT}/g (~285°C). Higher initial enthalpies of the hot-water component would cause an extended line to intersect the quartz solubility curve at two points, and the

lower enthalpy point probably would be erroneously selected as the solution to the mixing problem. Although this presents a problem in interpretation, another problem inherent in dealing with very high enthalpy waters (above 275 to 300 cal_{IT}/g) is probably more serious. Quartz precipitates relatively quickly from such waters, and therefore, temperatures derived from any relation assuming no silica precipitation are likely to be in error.

This method does allow easy evaluation of the effects of variations in assumed silica content and temperature of nonthermal water. The method also allows results obtained assuming no steam loss to be compared quickly with results obtained assuming steam loss at various intermediate temperatures. Similar graphical methods can be used to accomodate other silica phases such as chalcedony and crisobalite."

5.3 QUALITATIVE FLUID GEOTHERMOMETERS

Qualitative fluid geothermometers are used extensively during the preliminary geochemical surveys to locate zones of upwelling, determine the distribution of the thermal waters, the directions of groundwater flow, and obtain information on the distribution of rock types in the reservoir. Fluid constituents that have proven to be particularly useful during these surveys include the soluble elements Cl, B, As, Cs and Br. Ellis and Mahon (1964, 1967) showed that the solubilities of these elements are controlled mainly by diffusion and extraction processes, and that once liberated they do not form stable secondary minerals. Changes in the concentrations of these elements as the fluids migrate from depth occur mainly from dilution or boiling. The use of atomic ratios (i.e., Cl/B) can be used to study these effects.

Other fluid constituents that are frequently used as qualitative geothermometers include Li, trace metals (Sb, Zn, Cu, U, Hg), NH_4 , H_2S , and the ratios Cl/F, Cl/ SO_4 , Na/Ca, Na/Mg and Cl/ $\text{HCO}_3 + \text{CO}_3$. In general, the concentrations and ratios increase with increasing temperature reflecting changes in constituent concentrations as a result of interaction between the fluids and rock at depth (Mahon, 1970).

Maps of the distribution of chloride and boron in waters in the region surrounding Roosevelt Hot Springs, Utah, are presented in Figures 5.3.1 and 5.3.2 and illustrate the use of two of these qualitative geothermometers. The data was compiled from published analyses of well and spring waters. This distribution of Cl and B suggested that the Roosevelt Hot Springs area is indeed a major center of upwelling thermal fluids and that exploration activities should be concentrated in this area. Changes in the concentrations of Cl and B occur as the thermal fluids are diluted with local groundwaters. Movement of the fluids appears to be first westward and then northward. The

plume of westward-migrating thermal waters provides an explanation both for the relatively high thermal gradients encountered in the shallow wells and for anomalous concentrations of soil Hg which extends westward from the thermal area.

A second source of thermal fluids located at Thermo Hot Springs can be identified from the distribution of B (southwestern portion of Figure 5.3.1), but is indistinct on the Cl map, as a result of the variable and locally high Cl contents found in non-thermal waters throughout the area. These variations in Cl are believed to indicate the presence of shallow evaporite sequences related to Lake Bonneville within the basin.

The ratios of gases discharged from fumaroles have also been used as qualitative geothermometers. Mahon (1970) showed that fumaroles with the lowest ratios of $\text{CO}_2/\text{H}_2\text{S}$, CO_2/NH_3 , and CO_2/H^+ were the most directly connected to the deep aquifers. The concentrations of these constituents are controlled by steam-rock reactions which can rapidly deplete the contents of H_2S , NH_3 , and H^+ in the steam. The longer the steam path to the surface is, the greater these depletions are likely to be.

5.4 GEOTHERMOMETERS BASED ON MINERAL SATURATIONS

The relationship between the fluid chemistry and the mineralogy of the reservoir rocks can, at least, in theory also be used to establish possible subsurface temperatures through the application of various equilibrium models. During the past several years, several different equilibrium models have been proposed (among the better known models are PATH, PHREEQE, WATEQ, and WATEQF). While the actual calculations used in each of the models vary to some extent, the models share several common features. Each requires complete and accurate chemical analyses of the fluids, estimated or calculated fluid parameters for the temperatures of interest, such as pH, and the partial pressure of the gases in solution, thermodynamic data at temperature for the phase of interest (the available data is of variable quality), and knowledge about the phases present in the reservoir including their compositions and structural states (generally unknown). In practice it is often necessary to treat minerals of variable composition as pure end member phases. Finally, it must be assumed that equilibrium between the fluids and rocks has been reached (a fact that has proven almost impossible to demonstrate) and that the effects of dilution or boiling have been adequately accounted for. Indeed at temperatures below about 200°C, there is abundant evidence that indicates equilibrium between the fluids and rocks is generally not achieved.

Despite the difficulties involved in the use of equilibria models, useful and complementary data can be obtained. Capuano and Cole (1982) applied thermodynamic models to the Roosevelt Hot Springs system in Utah. In their study, equilibrium models were used to calculate the distribution of alteration minerals at different temperatures. The composition of the fluid used for this study was calculated from analyses of the brine, steam and non-condensable gases sampled at the well head. Mineral assemblages were

predicted for temperatures of 150, 200, 250 and 300°C (Fig. 5.4.1). The reservoir has a maximum measured temperature of about 270°C. The predicted relationships are generally in close agreement with the observed alteration phases and thus suggest that equilibrium has been achieved. Several of the minerals present in the reservoir rocks, which texturally appear to be related to the active geothermal system, including calcite and anhydrite, however, did not exhibit equilibrium with the cooling fluid. Capuano and Cole (1982) conclude that the precipitation of these minerals may be related to other factors such as boiling or mixing, or, that the calculations are in error as a result of inadequate thermochemical data.

Bogie (1983) and Ware (personal communication), in contrast, have used of anhydrite as a geothermometer. Anhydrite is one of several minerals exhibiting "retrograde" solubility; that is, its solubility increases with decreasing temperature. Consequently anhydrite is likely to be undersaturated in well and spring waters. Equilibrium models can be applied to calculate the saturation temperature of anhydrite. Because of its solubility relationships, this temperature should be very nearly the same as the maximum temperature "seen" by the geothermal fluids. While the method holds promise in geothermal systems which do contain anhydrite, the application of the equilibrium models requires input data that must be calculated or estimated (for example pH, f_{O_2}).

WATEQ and its updated Fortran version WATEQF (Truesdell and Jones, 1974; Plummer et al., 1976) are comparatively easy to use, and are well-suited to applications in moderate- to low-temperature resources, such as those occurring in Spain. The original papers describing these models and their application, and a listing of the computer program are included in Appendix 5.B.

5.5 INTERPRETATION OF GEOTHERMOMETER TEMPERATURES

Interpretation of geothermometer-calculated temperatures should not begin until the quality of the analysis has been evaluated, ion ratios have been computed, and the chemical characteristics of the waters plotted on a Piper diagram. Further analysis at this point will be different for each water type (refer to Fig. 4.1.2 for the characteristics of each fluid type).

NaCl FLUIDS

The NaCl fluids may be of geothermal, oceanic, connate, or oilfield origin. Thus the origin of the fluid should immediately be established by comparing the ion ratios and TDS of these fluids to the fluids sampled.

If the sampled fluids resemble seawater, and the Mg and SO_4 contents are close to that of seawater, then the geothermometer equations on Table 5.2.2 should be used. In particular, the K/Mg geothermometer should be used. Silica geothermometers should also be useful. Where the measured temperatures are below $100^\circ C$ (hot springs are below boiling), the chalcedony polymorph should be considered. The quartz polymorph should be applied where temperatures greater than $100-150^\circ C$ are indicated. Where temperatures less than $50^\circ C$ are indicated, the silica geothermometer may give spurious results.

If the sampled fluids resemble seawater, but have low Mg and SO_4 (i.e., Reykjanes brine, Table 5.2.3), the Na-K-Ca-Mg, quartz, Na/K, and the $\Delta^{18}O$ (SO_4-H_2O) geothermometers (Table 5.2.1) may be applied.

All samples resembling seawater should be examined with mixing diagrams of chemical elements vs. enthalpy prior to geothermometer interpretation to determine mixing. This is important because the waters with seawater-normal Mg and SO_4 may have been mixed after heating. If the chemical element-enthalpy relationships are consistent with a pre-heating seawater component,

the geothermometers may be used as an aid to the chemical element-enthalpy mixing calculations.

A connate fluid or oilfield brine component is generally indicated by a TDS greater than 40,000 ppm. In this case the K/Mg and Li/Mg geothermometers (Table 5.2.2) are most useful. Silica geothermometers (Table 5.2.1) may be used but the temperatures calculated may only be useful in a qualitative sense, especially at low to moderate temperatures and high or variable salinities. As with seawater, mixing should be examined with respect to enthalpy prior to geothermometer interpretation.

Where the NaCl fluids sampled do not appear to represent connate, oceanic, or oilfield brines, the geothermometers listed in Table 5.2.1 should be used. For these fluids with measured temperatures below 100°C, use of the chalcedony polymorph of silica should be considered. Those samples with RMg (Table 5.2.1) values greater than 45-50 should be treated as never having attained temperatures higher than those measured at the time of sample collection.

If geothermometer temperatures are inconsistent with each other and the measured temperature of the NaCl fluid is below 100°C, the Na-K-Ca-Mg is generally the best indicator of subsurface temperature. On the other hand, if the geothermometer temperatures are inconsistent and the measured temperatures are greater than 100°C, conductive cooling, boiling, or mixing should be suspected and chemical element-enthalpy diagrams used to resolve the disagreements.

NaHCO₃ FLUIDS

NaHCO₃ fluids are found in many geothermal environments. In volcanic terrains these fluids may represent steam-heated groundwaters. In contrast, NaHCO₃ may also develop through ion exchange reactions with clays in

sedimentary basins.

Fluids with NaHCO_3 character due to clay cation exchange should be treated with the geothermometers listed in Table 5.2.1. As with NaCl fluids, mixing should be examined prior to interpretation of the geothermometers and measured temperature should be a consideration in the choice of geothermometers. The cation geothermometers are likely to give misleading or erroneous information when applied to steam-heated waters for two reasons. First, these waters often only represent a shallow cap over a deeper high-temperature brine. Secondly, such waters may not be in equilibrium with the reservoir rocks because of the continued influx of acid gases.

MIXED CHARACTER FLUIDS

Fluids of "mixed type" (Fig. 4.1.2) should be evaluated in a manner similar to that used for NaCl fluids. The most likely origin of these fluids will be either a mixture of NaCl geothermal and meteoric waters or conductively heated near-surface meteoric waters. The Na-K-Ca-Mg , Na/Li and chalcedony geothermometers should be applied to these waters.

Ca-Mg HCO_3 FLUIDS

Ca-Mg HCO_3 fluids are typically cold groundwaters. Cation geothermometers should not be applied unless their measured temperatures exceed 30°C . Even then the RMg values are likely to be high. If RMg is $> 45-50$, then the measured temperatures should be considered as the most reasonable.

5.6 SUMMARY OF THE USE, ASSUMPTIONS, AND LIMITATIONS OF CATION GEOTHERMOMETERS

Chemical geothermometers provide a powerful tool for estimating the reservoir temperatures during exploration and assessing changes in the temperatures during production.

Despite the importance and widespread use of chemical geothermometers a great deal of care must be taken in their interpretation and application. Too often the geothermometers are used to "prove" a hypothesis rather than provide an additional piece of data that must be integrated with other geological, geochemical and hydrologic information.

There are several basic assumptions inherent in the use of these geothermometers. Fournier et al. (1974) list five main assumptions. These are:

1. Temperature-dependent reactions occur at depth.
2. All constituents involved in a temperature-dependent reaction are sufficiently abundant.
3. Water-rock equilibrium occurs at the reservoir temperature.
4. Reequilibration or changes in composition are minimal as the water cools during flow to the surface.
5. The hot water does not mix with cooler, shallow groundwater.

In most geothermal systems, all of the assumptions will not be fulfilled, and corrections must be made to the geothermometers. They further suggest that for boiling springs with small flow rates (< 200 l/min, for a single isolated spring and < 20 l/min for single springs of larger groups) conductive cooling without steam loss should be assumed. For large flow rate boiling springs assume adiabatic cooling and maximum steam loss. For the geochemistry of non-boiling springs with low flow rates, geothermometers will generally yield

ambiguous results. However, geothermometers that assume conductive cooling are likely to yield minimum temperatures. For non-boiling springs with large flow rates do not assume conductive cooling. If temperatures are higher than the background water temperature ($> 25^{\circ}\text{C}$) apply mixing models.

Most geothermal waters display some evidence of mixing and reequilibration. Thus different geothermometers will give different results. Insofar as possible these results should be integrated to evaluate the history of the fluid.

Models of fluid-mineral equilibria (mineral saturation models) provide an alternative, although at present a limited approach to geothermometry. These models require accurate thermochemical and chemical data that often must be approximated. An interesting example of the effects of choosing different structural states of feldspar on the equilibrium models is given by Fournier (1980). He shows that at 100°C $\log [\text{Na}/\text{K}]$ for the assemblage low albite + microcline is .2 units lower than for low albite + andularia and .7 units lower than for high albite + sanidine. These differences could have large effects on the temperature estimates.

Further difficulties arise in determining the concentrations and pressures of all aqueous and gaseous species. Because of gas loss the partial pressures of O, S, CO_2 and the pH will differ in the sampled and reservoir fluid. Various assumptions about the fluid-mineral relationships at depth often must be made to calculate the compositions of these species in the reservoir (for example, whether calcite is in equilibrium with the reservoir fluids). Many hydrothermal minerals are alumino-silicates of varying composition. The solubility of aluminum is so low that special care must be used to detect it. In addition, its low concentration is easily overpowered by dissolution during analysis of microscopic clay colloids that may escape

through the sample filter.

Several investigators have used assumptions to bypass this problem. Some use the solubility of Al in kaolinite (Hammerstrom and Brown, 1977) or albite (Merino and Ransom, 1982), and some simply use non-geothermal non-aluminous minerals to determine saturation (Reed, 1984).

The effects of composition on the results of the equilibrium models may also be significant. Good thermodynamic data is generally available for only a few end member compositions and methods to correct the thermochemical values for intermediate compositions are still very approximate. This problem is particularly significant in the case of the sheet silicates.

Finally, fluid-mineral equilibrium must be demonstrated if equilibrium models are to be used as geothermometers. While the fluids appear to be in equilibrium with the hydrothermal minerals in many high temperature systems above about 200°C, equilibrium does not appear to be achieved in lower temperature fields. Because of anhydrite's retrograde solubility it holds particular promise as a potential geothermometer in some geothermal systems. Its use, however, is dependent on its presence in the deep reservoir.

CHAPTER 5 REFERENCES

- Allen, E. T., and Day, A. L., 1935, Hot springs of the Yellowstone National Park: Carnegie Inst. Washington Pub. 466, 525 p.
- Arnorsson, S., 1975, Application of the silica geothermometer in low temperature hydrothermal areas in Iceland: *Am. J. Sci.*, v. 275, p. 763-784.
- Arnorsson, S., 1978, Major element chemistry of the geothermal sea-water at Reykjanes and Svartsevgi, Iceland: *Miner. Mag.*, v. 42, p. 209-220.
- Bischoff, J. L., and Seyfried, W. E., 1978, Hydrothermal chemistry of seawater from 25° to 350°C: *Am. J. Sci.*, v. 278, p. 838-860.
- Bodvarsson, G., 1950, Geophysical methods in prospecting for hot water in Iceland: *J. Eng. Assoc. Iceland*, v. 35, p. 49-59.
- Capuano, R. M., and Cole, D. R., 1982, Fluid-mineral equilibria in a hydrothermal system, Roosevelt Hot Springs, Utah: *Geochim. Cosmochim. Acta*, v. 46, p. 1353-1364.
- Christiansen, R. L., and Blank, H. R., Jr., 1972, Volcanic stratigraphy of the Quaternary rhyolite plateau in Yellowstone National Park: *U.S. Geol. Survey Prof. Paper 729-B*, 18 p.
- Eaton, G. P., Christiansen, R. L., Iyer, H. M., Pitt, A. M., Mabey, D. R., Blank, H. R., Jr., Zeitz, I., and Gettings, M. E., 1975, Magma beneath Yellowstone National Park: *Science*, v. 188, p. 787-796.
- Ellis, A. J., 1966, Volcanic hydrothermal areas and the interpretation of thermal water compositions: *Bull. Volcanol.*, v. 29, p. 575-584.
- Ellis, A. J., 1970, Quantitative interpretation of chemical characteristics of hydrothermal systems, in *United Nations Symposium on the Development and Utilization of Geothermal Resources*, Pisa 1970, v. 2, pt.: *Geothermics*, Spec. Issue 2, p. 516-528.
- Ellis, A. J., and Mahon, W. A. J., 1964, Natural hydrothermal systems and experimental hot water/rock interaction: *Geochim. Cosmochim. Acta*, v. 28, p. 1323.
- Ellis, A. J., and Mahon, W. A. J., 1967, Natural hydrothermal systems and experimental hot-water/rock interactions (Part 2): *Geochim. Cosmochim. Acta*, v. 31, p. 519-539.
- Ellis, A. J., and Mahon, W. A. J., 1977, *Chemistry and geothermal systems*: Academic Press, New York, 392 p.
- Fenner, C. N., 1936, Borehole investigations in Yellowstone Park: *Jour. Geology*, v. 44, p. 225-315.

Fouillac, C., and Michard, G., 1981, Sodium/lithium ratio in water applied to the geothermometry of geothermal waters: *Geothermics*, v. 10, p. 55-70.

Fournier, R. O., 1973, Silica in thermal waters: Laboratory and field investigations, in *Proceedings of the International Symposium on Hydrogeochemistry and Biogeochemistry*, Japan, 1970, Washington, D.C., p. 122-139.

Fournier, R. O., 1977, Chemical geothermometers and mixing models for geothermal systems, in *Proceedings of the International Atomic Energy Agency Advisory Group on the Application of Nuclear Techniques to Geothermal Studies*, Pisa, 1975: *Geothermics*, Spec. Issue, v. 5, p. 41-50.

Fournier, R. O., 1979a, A revised equation for the Na/K geothermometer: *Geothermal Resources Council, Transactions*, v. 3, p. 221-224.

Fournier, R. O., 1979b, Geochemical and hydrologic considerations and the use of enthalpy-chloride diagrams in the prediction of underground conditions in hot spring systems: *J. Volcanol. Geotherm. Res.*, v. 5, p. 1-16.

Fournier, R. O., 1981, Application of water geochemistry to geothermal exploration and reservoir engineering; Chapt. 4 in *Geothermal Systems: Principles and Case Histories*, L. Ryback and L. J. P. Muffler, eds., Wiley New York, p. 109-143.

Fournier, R. O., and Rowe, J. J., 1966, Estimation of underground temperatures from the silica content of water from hot springs and wet-steam wells: *Am. J. Sci.*, v. 264, p. 685-697.

Fournier, R. O., and Truesdell, A. H., 1970, Chemical indicators of subsurface temperature applied to hot spring waters of Yellowstone National Park, Wyoming U.S.A., in *United Nations Symposium on Development and Utilization of Geothermal Resources*, Pisa 1970, Proc. v. 2, pt. 1: *Geothermics*, Spec. Issue 2, p. 529-535.

Fournier, R. O., and Truesdell, A. H., 1973, An empirical Na-K-Ca geothermometer for natural waters: *Geochim. Cosmochim. Acta*, v. 37, p. 1255-1275.

Fournier, R. O., and Truesdell, A. H., 1974, Geochemical indicators of subsurface temperature, 2. Estimation of temperature and fraction of hot water mixed with cold water: *U.S. Geol. Survey. J. Res.*, v. 2, p. 263-270.

Fournier, R. O., White, D. E., and Truesdell, A. H., 1974, Geochemical indicators of subsurface temperature-Part 1, Basic assumptions: *U.S. Geol. Survey Jour. Research*, v. 2, no. 3, p. 259-262.

Fournier, R. O., White, D. E., and Truesdell, A. H., 1976a, Convective heat flow in Yellowstone National Park, in *Proceedings of the 2nd United Nations Symposium on the Development and Use of Geothermal Resources*, San Francisco, 1975, vol. 1: U.S. Government Printing Office, Washington, D.C., p. 731-739.

- Fournier, R. O., Sorey, M. L., Mariner, R. H., and Truesdell, A. H., 1976b, Geochemical prediction of aquifer temperatures in the geothermal system at Long Valley, California: U.S. Geol. Surv. Open-file Rep., 76-469, 35 p.
- Fournier, R. O., and Potter, R. W. II, 1979, Magnesium correction to the Na-K-Ca chemical geothermometer: Geochim. Cosmochim. Acta, v. 43, p. 1543-1550.
- Giggenbach, W. F., Gonfiantini, R., Jangi, B. L., and Truesdell, A. H., 1983, Isotopic and chemical composition of Parbati Valley geothermal discharges, NW Himalaya, India: Geothermics, v. 12, p. 199-222.
- Goff, F. E., and Donnelly, J. M., 1978, The influence of PCO_2 , salinity, and bedrock type on the Na-K-Ca geothermometer as applied to the Clear Lake geothermal region, California: Geothermal Resources Council, Transactions, v. 2, p. 211-213.
- Hammerstrom, C. T., and Brown, T. H., 1977, The geochemistry of thermal waters from the Mount Meager hot springs area: B.C. Geol. Surv. of Canada, Open-File Rept. 532, 34 p.
- Henley, R. W., Truesdell, A. H., Barton, P. B., Jr., and Whitney, J. A., 1984, Fluid-mineral equilibria in hydrothermal systems: Reviews in Economic Geology, v. 1, 252 p.
- Honda, S., and Muffler, L. J. P., 1970, Hydrothermal alteration in core from research drill hole Y-1, Upper Geyser Basin, Yellowstone National Park, Wyoming: Am. Mineralogist, v. 55, p. 1714-1737.
- Keefer, W. R., 1971, The geologic story of Yellowstone National Park: U.S. Geol. Survey Bull. 1347, 92 p., 1 plate.
- Keenan, J. H., Keyes, F. G., Hill, P. G., and Moore, J. G., 1969, Steam Tables (International Edition - Metric Units): Wiley, New York, NY.
- Kharaka, Y. K., Specht, D. J., and Carothers, W. W., 1985, Low to intermediate subsurface temperatures calculated by chemical geothermometers: AAPG, v. 60, no. 2, p. 273.
- Lloyd, E. F., 1972, Geology and hot springs of Orakeikorako, New Zealand: Geol. Surv. Bull., 85: 164 p.
- Mahon, W. A. J., 1966, Silica in hot water discharged from drillholes at Wairakei, New Zealand: New Zealand Jour. Sci., v. 9, p. 135-144.
- Mahon, W. A. J., 1970, Chemistry in the exploration and exploitation of hydrothermal systems: Geothermics Spec. Issue No. 2, p. 1310-1325.
- Mercado, G. S., 1968, Localizacion de zonas de maxima actividad hidrotermal por medio de proporciones quimicas, Campo geotermico Cerro Prieto, Baja California, Mexico: Work presented at the III Congreso Mexicano de Quimica Pura y Aplicada, Comision Federal de Electricidad, Comision de Energia Geotermica, 32 p.

- Merino, E., and Ransom, B., 1982, Free energies of formation of illite solid solutions and their compositional dependence: *Clays and Clay Minerals*, v. 30, p. 29-39.
- Mizukami, M., and Ohmoto, H., 1983, Controlling mechanisms for the major element chemistry of aqueous solutions in tuff-rich environments: *Econ. Geol. Mono*, 5, p. 559-569.
- Morey, C. W., Fournier, R. O., and Rowe, J. J., 1962, The solubility of quartz in water in the temperature interval from 29° to 300°C: *Geochim. et Cosmochim. Acta*, v. 26, p. 1029-1043.
- Mottl, M. J., and Holland, H. D., 1978, Chemical exchange during hydrothermal alteration of basalt by seawater - I. Experimental results for major and minor components of seawater: *Geochim. Cosmochim. Acta*, v. 42, p. 1103-1115.
- Paces, T., 1975, A systematic derivation from Na-K-Ca geothermometer below 75°C and above 10^{-4} atm P_{CO_2} : *Geochim. Cosmochim. Acta*, v. 39, p. 541-544.
- Plummer, L. N., Jones, B. F., and Truesdell, A. H., 1976, WATEQF - a Fortran version of WATEQ, a computer program for calculating chemical equilibrium of natural waters: *U.S. Geol. Survey, Water Res. Inv.*, 76-13.
- Reed, M. H., 1982, Calculation of multicomponent chemical equilibria and reaction processes in systems involving minerals, gases and an aqueous phase: *Geochim. Cosmochim. Acta*, v. 46, p. 513-528.
- Reed, M. J., 1976, Geology and hydrothermal metamorphism in the Cerro Prieto geothermal field, Mexico, in *Proceedings of the 2nd United Nations Symposium on the Development and Use of Geothermal Resources*, San Francisco, 1975, Vol. 1, U.S. Government Printing Office, Washington, D.C., p. 539-547.
- Seyfried, W. E., and Bischoff, J. L., 1979, Low temperature basalt alteration by seawater: an experimental study at 70°C and 150°C: *Geochim. Cosmochim. Acta*, v. 43, p. 1937-1947.
- Truesdell, A. H., 1976, Summary of section III-geochemical techniques in exploration: *Second United Nations Symposium on the Development and Use of Geothermal Resources*, San Francisco, May, 1975, v. 1, p. liii-lxiii.
- Truesdell, A. H., and Jones, B. F., 1974, WATEQ, a computer program for calculating chemical equilibria of natural waters: *Jour. Res., U.S. Geol. Survey*, v. 2., p. 233-248.
- Truesdell, A. H., and Fournier, R. O., 1976, Calculation of deep temperatures in geothermal systems from the chemistry of boiling spring waters of mixed origin, in *Proceedings of the 2nd United Nations Symposium on the Development and Use of Geothermal Resources*, San Francisco, 1975, Vol. 1, U.S. Government Printing Office, Washington, D.C., p. 837-844.

Truesdell, A. H., Nathenson, M., and Rye, R. O., 1977, The effects of subsurface boiling and dilution on the isotope compositions of Yellowstone thermal waters: *Journal of Geophysical Research*, v. 82, p. 3694-3704.

Truesdell, A. H., and Fournier, R. O., 1977, Procedure for estimating the temperature of a hot-water component in a mixed water using a plot of dissolved silica vs. enthalpy: *U.S. Geol. Surv., J. Res.*, v. 5, p. 49-52.

Truesdell, A. H., and Hulston, J. R., 1980, Isotopic evidence on environments of geothermal systems, in Fritz, P., and Fontes, J. C., Eds., *Handbook of environmental isotope geochemistry, Volume 1: The terrestrial environment*: Elsevier Press, Amsterdam, p. 170-225.

Weissberg, B. G., and Wilson, P. T., 1977, Montmorillonites and the Na/K geothermometer: *New Zealand J. Sci.*, v. 20, p. 31-34.

White, D. E., 1974, Geochemistry applied to the discovery, evaluation, and exploitation of geothermal energy resources, in *United Nations Symposium on Development and Utilization of Geothermal Resources, Pisa 1970*, v. 1, pt. 2: Geothermics, Spec. Issue 2.

White, D. E., Muffler, L. J. P., Truesdell, A. H., and Fournier, R. O., 1968, Preliminary results of research drilling in Yellowstone thermal areas [abs.]: *Am. Geophys. Union Trans.*, v. 49, p. 358.

White, D. E., Fournier, R. O., Muffler, L. J. P., and Truesdell, A. H., 1975, Physical results of research drilling in thermal areas of Yellowstone National Park, Wyoming: *U.S. Geol. Surv., Prof. Paper*, p. 892.